



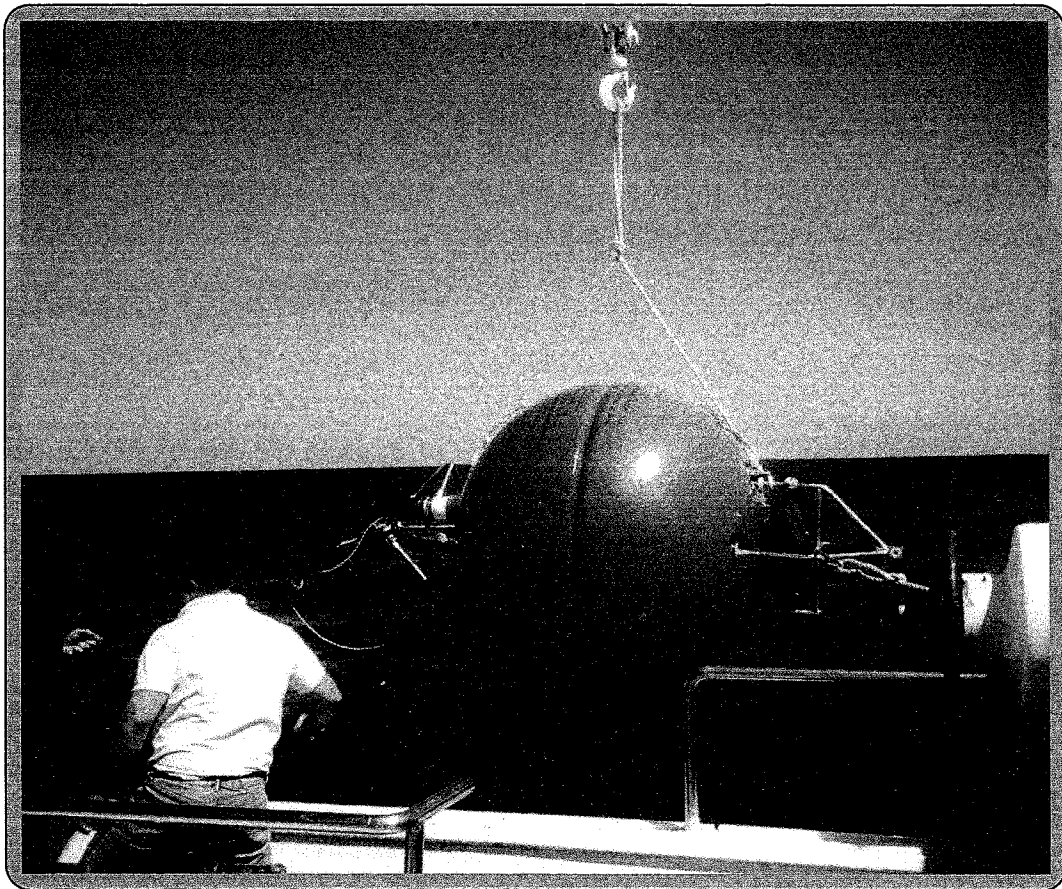
Institut Mediterrani d'Estudis Avançats (IMEDEA, CSIC)

Institut de Ciències del Mar (ICM, CSIC)

Centro Oceanográfico de Baleares (IEO)

**ADCP Technical Report:
"CANALES_97" FIELD EXPERIMENT**

January 1997 - January 1998



**Emilio García Ladona, Jordi Font
Institut de Ciències del Mar
CSIC**

**Jean Michel Pinot, Margalida Riera, Joaquin Tintoré
Institut Mediterrani d'Estudis Avançats
CSIC/UIB**

**Jose Luis López Jurado
Centro Oceanográfico de Baleares
IEO**

Contents

- 1 Introduction** 4
- 2 Description of the ADCP Device and Design of the Mooring Line** 6
 - 2.1 The ADCP Device 6
 - 2.2 Mooring design 6
- 3 History of the Experiment** 6
- 4 Data Conversion and Calibration** 8
 - 4.1 Instrument configuration 8
 - 4.2 Conversion of raw data to physical units 8
 - 4.3 Calibration 9
- 5 Pre-processing** 10
 - 5.1 Introduction 10
 - 5.2 Methodology 11
 - 5.3 Pulishing step by step 13
 - 5.4 Data Interpolation 17
 - 5.5 Filtering 17
- 6 Results** 19
 - 6.1 Data Set: Odon_1 20
 - 6.2 Data Set: Odon_2 42
 - 6.3 Data Set: Odon_3 56
 - 6.4 Data Set: Odon_4 70
- Appendix I: Mooring Hydrodynamics** 84
- Appendix II: Instrument Configuration** 86

Appendix III: DATA files	87
Appendix IV: RDI mail	90
Appendix V: IDL procedures	91

Abstract

The "CANALES_97"¹ field experiment was carried out during 1997 with the aim to investigate the water exchanges through the Balearic channels. Exchanges that are therefore considered crucial to understand the dynamics of the western Mediterranean sea. As part of the experiment, an RDI ADCP was deployed from January 1997 to January 1998 in the Ibiza channel in order to monitor the time variability of the fluxes in the upper 250 m layer.

In this report we first describe the main objectives of the experiment, the ADCP device, its configuration and some technical aspects on the mooring design. Second, we present a detailed description of all the procedures adopted to post-process the raw data acquired during the experiment and finally we show some preliminary results.

Resumen

El experimento "CANALES_97" se desarrolló durante 1997 con el objetivo de investigar los intercambios de agua a través de los canales de las Islas Baleares. Dichos intercambios son considerados como cruciales para entender la dinámica del Mediterraneo occidental. Parte del experimento consistió en la colocación de un correntímetro Doppler (ADCP) entre Enero de 1997 y Enero de 1998 en el canal de Ibiza con el fin de observar la variabilidad de los flujos de la capa correspondiente a los primeros 250 metros.

En este informe se describen primero los principales objetivos del experimento, el correntímetro utilizado, su configuración y el diseño del anclaje. Posteriormente se hace una descripción detallada de la metodología utilizada en el post-procesado de los datos y finalmente se presenta el análisis preliminar de los mismos.

Acknowledgments

This data report is a contribution of the IMEDEA, ICM and IEO institutions to the INTERMESO and MATER/MTPII (WorkPackage 2) projects respectively funded by the Spanish CICYT (AMB95-0901-C02-01-CP) and by the **European Community (DG XII)** program MAST (MAS3-CT96-0051). The ADCP was purchased thanks to funding by the Spanish CICYT (IN94-0662). We acknowledge the assistance of the crews of R/V **Odón de Buen** and R/V **García del Cid**. Special thanks go to Miquel Moll (E.M.S.) and Agustí Julià (ICM) for their valuable help during most of the deployment and recovery cruises. We are also thankful to all the persons of the different institutions who took part in the cruises or provided their help for any aspect of the project. The hydrodynamics of the mooring line was studied with the MOUSTASH algorithm developed at the CMO (EPSHOM, Brest) whose support during all the CANALES experiment is gratefully acknowledged. Discussion with Yves Camus (CMO) was very helpful for the conception of the mooring line.

¹Cover illustration: Deployment of the RDI ADCP in the eastern Ibiza channel onboard R/V *Odón de Buen* on April, 5, 1997.

1 Introduction

The "CANALES_97" field experiment was designed as part of the INTERMESO and MATER projects to study the annual cycle and the scales of time variability of the circulation in the Balearic channels as a continuation to the previous "CANALES_96" experiment. For several years, the Balearic Sea has been considered as a key transition basin between the northern Gulf of Lion and the southern Algerian basin. The idea that the southward spreading of Mediterranean waters cooled in the north and the northward spreading of warmer waters from the south strongly interact in the Balearic basin on a seasonal scale has been reinforced by recent satellite and large scale modelling studies (López-García et al., 1994; Álvarez et al., 1994). In situ high resolution surveys have also highlighted that the circulation in this basin is characterized by a high mesoscale activity (e.g. Pinot et al., 1994) that substantially distorts the mean circulation pattern of along-slope density currents (Font et al., 1988). More recent studies have emphasized the role played by the Balearic channels in controlling (limiting and/or concentrating) the meridional fluxes (mass, heat and salt), hence, its relevance for the general circulation of the Western Mediterranean (López-Jurado et al., 1995; García-Ladona et al., 1996; Salat, 1995; Castellón et al., 1990). In particular, a few observations in areas close to the Balearic channels lead to some preliminary conclusions about likely strong effects of large mesoscale sub-surface eddies of Winter Intermediate Waters (WIW) on the mean seasonal exchange through the Ibiza channel (Pinot et al., 1995). However, all these observations were inferred from cruises of a few days duration which missed the time evolution of the flow. The few mooring experiments performed in the Balearic Sea focused on the northern continental slope (Font, 1990; Font et al., 1990) except a few months deployment of one mooring in the Ibiza channel in 1990-91 (García-Lafuente et al., 1995).

Hence, one of the aims of CANALES_97 was to deploy moored instruments in the Balearic channels on a yearly basis to monitor the fluxes, assess their time variability at sub-inertial scales and describe the interaction between the seasonal scale and the mesoscale. Figure 1.1 shows the area under study during CANALES_97, where as part of the experiment, 5 moorings were deployed in the Balearic channels including an RDI ADCP which was moored in the eastern Balearic channel at position A2. The choice for its deployment location was motivated by the fact that the significant inflows of Modified Atlantic Water which occur over the Ibiza slope are confined to the upper 100 m layer where no instrument can in practice be deployed at least above 80 m depth, because of the intense fishing activity (tunny fishing, drifting nets, etc.). A subsurface mooring equipped with an upward looking current profiler was considered as the only way to safely record fluxes in the surface layer. The mooring was deployed over the lower part of the Ibiza slope in 900 m water depth, where it is in principle safe from trawling.

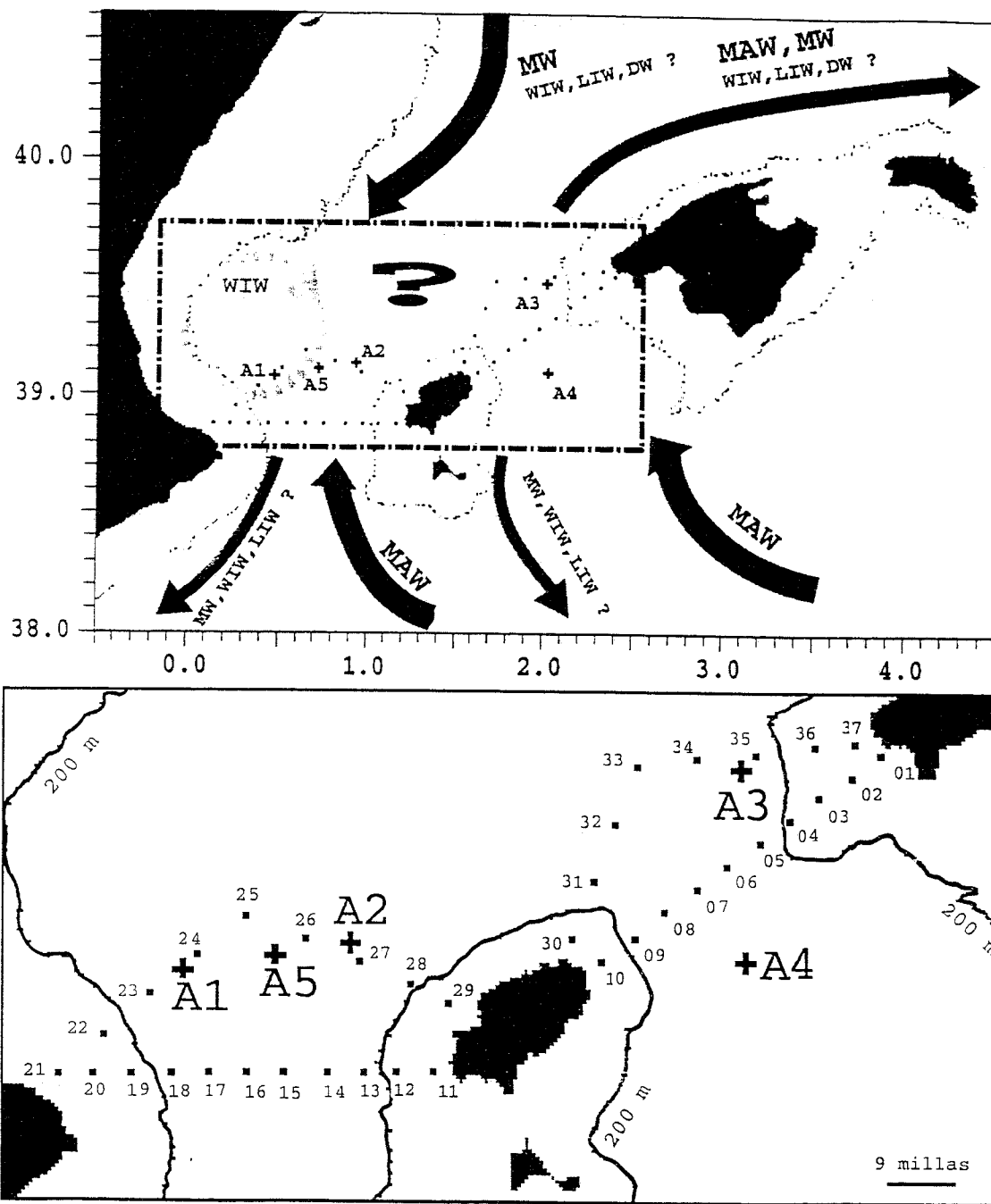


Figure 1.1: *Top*: The area under study during CANALES.97 experiment. *Bottom*: Detailed map with the hydrographic survey (37 stations) performed approximately every 2 months during 1997 in the Balearic channels. Crosses indicate mooring locations. The ADCP was moored at site A2.

2 Description of the ADCP Device and Design of the Mooring Line

2.1 The ADCP Device

The ADCP moored during the CANALES_97 experiment is an RDI BroadBand ADCP working at 150 kHz in its configuration Blue-Water (long-term deployment) and equipped with a High-Power module allowing a nominal profiling range of about 300 m. Transducers are mounted in a convex 20° configuration (4 transducers). Heading, pitch and roll sensors are included together with a temperature sensor.

2.2 Mooring design

The mooring line was designed in order to have the upward-looking ADCP moored at a nominal depth of 250 m in a water depth of 900 m (Figure 2.1). The ADCP was fitted into a 500 kg buoyancy float of syntactic foam (Flottation Technologies Inc.). On the opposite side to the transducers (which are the heaviest part of the device), an ARGOS beacon (ORCA Inc.) and a xenon flash beacon with pressure switch were mounted on the buoy (see cover picture). An 8 mm kevlar rope was used for the mooring line. An Aanderaa RCM-7 mechanical currentmeter was inserted in the mooring line at 625 m. A couple of acoustic releases (ORCA Inc.) was used for more safety. Both the Aanderaa currentmeter and the acoustic releases had their own floats right above them. Prior to deployment, the hydrodynamics of the mooring was analysed using the 'MOUSTASH' software developed at the Centre Militaire d'Océanographie (EPSHOM, Brest). Results for the cases of realistic low currents and for a particular strong event ('ocean storm') are described in Appendix I. They lead to the conclusion that a dead weight of 600 kg (2 train wheels in water) was enough to ensure mooring stability.

3 History of the Experiment

Deployments and recoveries were performed on the following dates:

- January, 31th, 1997, onboard R/V **Odón de Buen**. 1st deployment.
- April, 3rd and 5th, 1997, onboard R/V **Odón de Buen**. Recovery and 2nd deployment.
- July, 1st and 2nd, 1997. onboard R/V **García del Cid**. Recovery and 3rd deployment.
- October, 2th and 8th, 1997, onboard R/V **Odón de Buen**. Recovery and 4th deployment at location A2 (the mooring broke on September, 29th, due to corrosion

CANAL DE IBIZA - FONDEO ADCP 1997
A2
(39 _ 06.52 N, 0 _ 55.95 E)

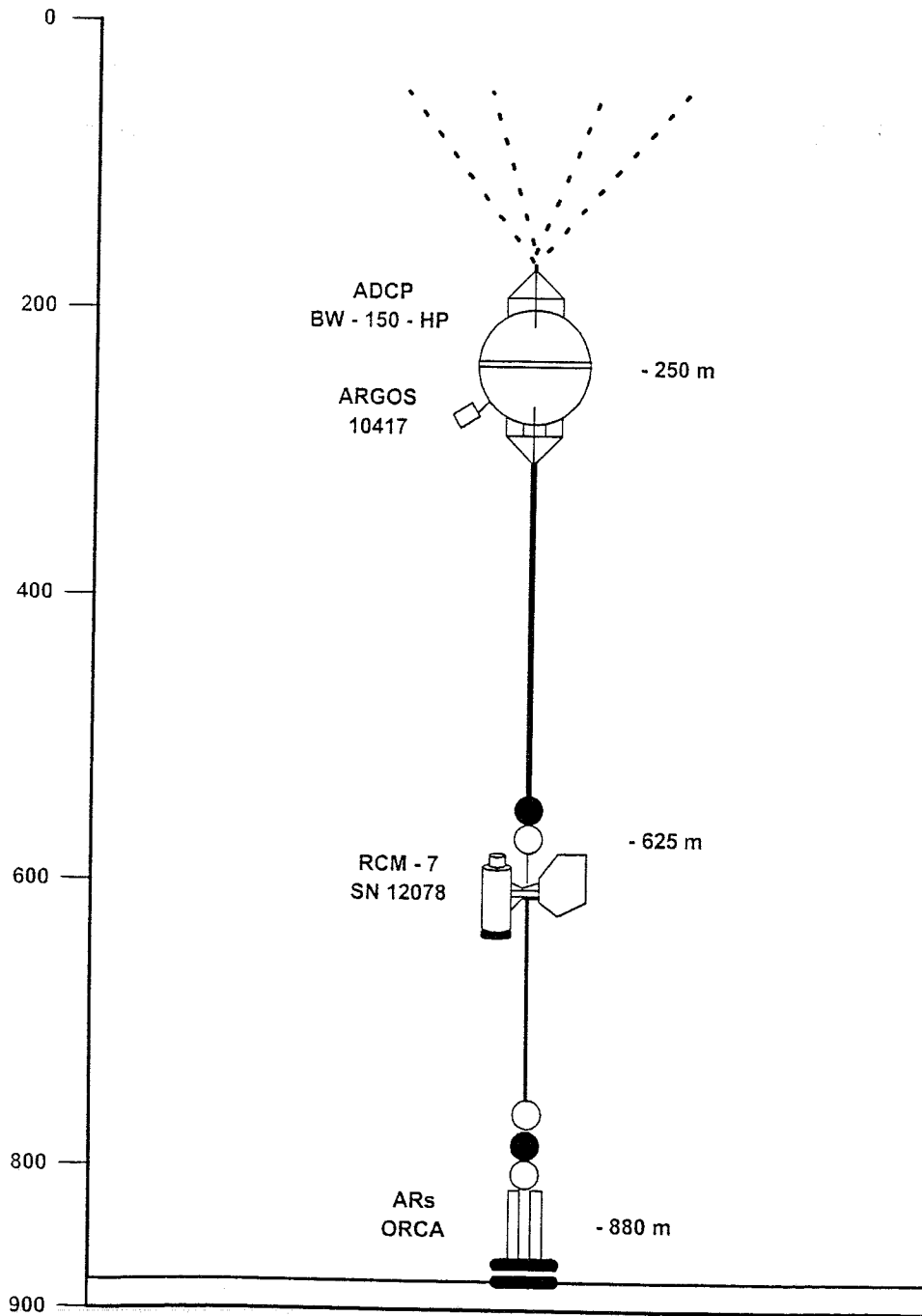


Figure 2.1: Schematic view of the mooring line including the ADCP.

of the acoustic release ring, and the whole mooring line came to the surface. Warning and mooring position were given by ARGOS).

- January 28th, 1998, onboard R/V **Odón de Buen**. Final recovery.

Deployment positions, obtained from the ship GPS as the dead weight was thrown from the deck, were almost the same for all 4 deployments:

Deployment	Latitude	Longitude	Depth (Ship Echo-Sounder)
1	39° 06.46' N	0° 55.69' E	885 m (OdB)
2	39° 06.38' N	0° 55.54' E	884 m (OdB)
3	39° 06.52' N	0° 55.95' E	899 m (GdC)
4	39° 06.86' N	0° 56.07' E	900 m (OdB)

Then, the collected time series can be assigned to a single mean position at:

$$39^{\circ} 06.55 \text{ N}, 0^{\circ} 55.81' \text{ E}$$

with a standard deviation error about 300 m. Deployment depths were taken from ship echo sounder.

4 Data Conversion and Calibration

4.1 Instrument configuration

The number of depth cells (or bins) was 33, with a depth cell size of 8 m. The sampling interval was of 0.5 h during the first period (from 31/01/97 to 03/04/97) while on the others the sampling interval was fixed to 1 h with 10 pings per ensemble (one ping every 6 min). An example of the command file with the settings used for data acquisition is listed in Appendix II.

4.2 Conversion of raw data to physical units

Sampled data are automatically converted to physical units and stored in binary format in the ADCP internal memory. During our experiment, the earth velocity components (east and north components) were internally computed using the ADCP compass (heading data) and systematically stored. Parameter settings were defined so that the following time series of data profiles were stored :

- east, north, vertical velocity components and error velocity in earth coordinates,
- percent good, intensity, correlation and rms velocity for all 4 beams

together with scalar time series of:

- date, GMT time, temperature, heading, pitch, roll and rms values for the latter 3 parameters.

All velocity calculations were performed using the 'ADCP reference', that is, final velocity characterizes the motion of the water relative to the moored ADCP. Hence, interpreting the data as the absolute current relies on the assumption that the mooring line has negligible motions. ASCII conversion was done using RDI software 'BBCONV'. In Appendix III we show detailed examples of report files describing the parameter settings and small examples of characteristic data files provided by BBCONV.EXE.

4.3 Calibration

The time drift of the internal ADCP clock was checked after each recovery cruise. No time drift larger than 1 min over 3 months was detected and no correction was applied to the data.

Temperature data were calibrated on the basis of several CTD casts performed in the vicinity of mooring A2 location (stations #27 and #28, see figure 1.1). Temperature values for both instruments are listed below.

Date	T_{CTD}	T_{ADCP}	δT
01/02/97	13.18	13.06	0.12
03/04/97	13.11	13.04	0.07
28/05/97	13.15	13.06	0.09
01/07/97	13.19	13.06	0.13
03/08/97	13.18	13.06	0.12
28/01/98	13.21	13.06	0.15

For the first deployment, temperature comes from a CTD profile obtained at the same place of the mooring location (A2). The others values come from an average made at 240 m depth between temperatures from two consecutive CTD casts (26 and 27) weighted by their distance to ADCP mooring site. Differences are always positive and around 0.1 °C, so the error is satisfactorily characterized and corrected by an offset of 0.1 +/- 0.02 °C.

Finally, a comparative analysis between ADCP velocity data and the geostrophic velocity computed from CTD data of station pair #27-28 (repeated several times during 1997) will be carried out to check the consistency between the fluxes calculated by both methods.

5 Pre-processing

5.1 Introduction

In this section, we report the methodology used in preprocessing data and some preliminary results. The methodology consists in performing a data 'cleaning' to obtain a reliable dataset on which finer analysis can be carried out. The experiment was divided in 4 temporal segments covering the period from January 1997 to January 1998 (see fig. 5.1). For convenience, the 4 data sets (generically labeled as Odon_1, Odon_2, Odon_3 and Odon_4) have been treated separately. The ADCP, configured with 33 bins of 8 m,

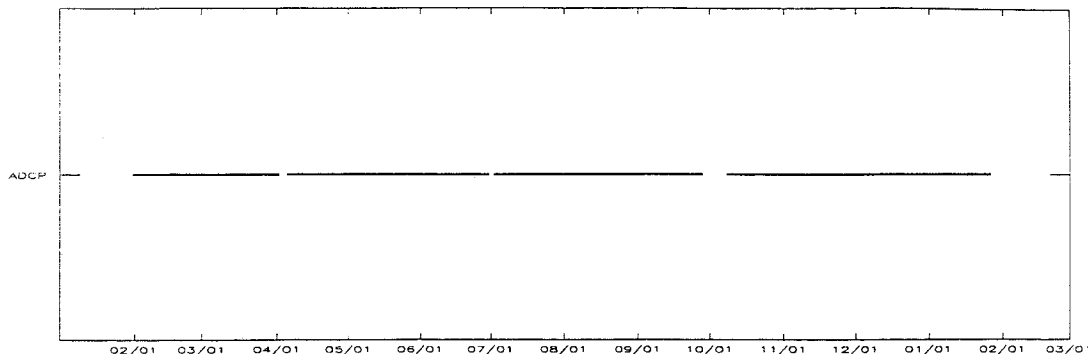


Figure 5.1: Time coverage during CANALES_97 experiment

was moored looking upward in a water depth of 900 m. The targeted depth for the ADCP device was 250 m but it was later established that the actual depth of the ADCP was 238 m in average. Thus, in order to get the bins depth, z , we must compute,

$$z \text{ (meters)} = 238 - \text{Bin_Range}$$

BN	BR	z	BN	BR	z	BN	BR	z	BN	BR	z	BN	BR	z
7	222	16	13	174	64	19	126	112	25	78	160	31	30	208
8	214	24	14	166	72	20	118	120	26	70	168	32	22	216
9	206	32	15	158	80	21	110	128	27	62	176	33	14	224
10	198	40	16	150	88	22	102	136	28	54	184			
11	190	48	17	142	96	23	94	144	29	46	192			
12	182	56	18	134	104	24	86	152	30	38	200			

Table 5.1: Equivalence between Bin_Number (BN) (counted downward), Bin_Range (BR, in meters, counted from the transducers) and Bin_depth (real depth, in meters).

In table 5.1 we list the equivalence between depth in meters, bin number and bin range in the bin interval (7-33). Data outside this range are not available for several reasons as it is later explained.

After converting data into physical units several files were created (short examples of the these data files are listed in Appendix III).

- filename.asc: ASCII file with the scalar time series (date, temperature, etc.)
- filename.rpt: 2 ASCII files reporting data conversion.
- filename_000.rms: ASCII file with rms values of data.
- filename_00*.asc: ASCII files with velocity measurements and related time series.

5.2 Methodology

Here we describe in detail the procedure we have followed to pre-process the data. The work has been completely undertaken interactively by means of IDL language, but some routines and procedures have been implemented to perform particular tasks. The data set was read in a multidimensional array and we combined interactive procedures to pre-process data together with the CORRENT² tool to perform some drawings. In the future the methodology described in this report and part of such procedures will be implemented through GUI tools.

In general, we have several sources of bad bin values. They can be divided in two classes, those detected by the internal instrument algorithms (echo intensity under the threshold, for example) which are rejected by automatic flagging (9999 value) and those that apparently are good measurements, but do not seem physically meaningful. Thus, we must distinguish several cases:

- **Out-of-the-water data:** Values that are obtained during deployment or recovery operations are located at the beginning and at the end of the time series. The time of the deployment and recovery operations and a look at the ASCII temperature records allow to easily drop out such data (see fig. 5.2).

- **Surface reflexions and flagged (9999) values:** Usually, near-surface bins can be affected by surface reflexions producing side-lobe effects. Theoretically, 6% of the ADCP depth values plus 1 bin are affected (see comments by an RDI engineer in Appendix IV), which would correspond to the upper 22 m (14+8) in our experiment. A close look to data show that bins 1 to 5 are clearly beyond the surface and bin 6 is systematically within the region of side-lobe influence. Though bin 7 lied within the region of theoretical surface effects, most of data can be considered as good. In table 5.2 we have listed the percentage of bad (flagged) records for bins 4 to 21. The percentage of bad bin values are lower than 1% below bin 7 except in the Odon_4 data set, where the percentage is about 10% up to bin 15. These bad values are isolated or grouped in several consecutive records. In the first case we decided to perform a linear interpolation and in the second case we applied a procedure based on fitting an autoregressive model. In general, the percentage of bad bin values is mainly located in records at the end of the interval.

²CORRENT.PRO is a GUI tool to visualize and preprocess time series.
(see <http://www.icm.csic.es/cgi-bin/lista-cgi?idl/GUI-tools/corrent/>)

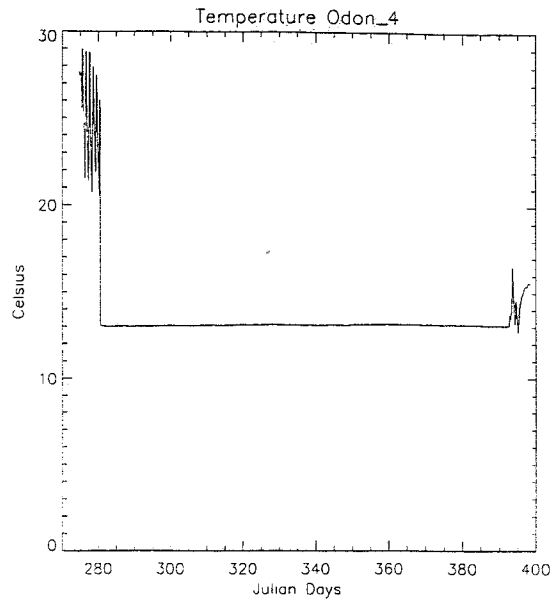


Figure 5.2: Example of a complete temperature record (Odon_4 data set)

Bin	Odon_1	Odon_2	Odon_3	Odon_4
4	64.5	35	65	79
5	15	53	54	69
6	55	55	39	22.5
7	< 1	< 1	< 1	15
8	.	.	.	14
9	.	.	.	12.5
10	.	.	.	11.5
11	.	.	.	11
12	.	.	.	11
13	.	.	.	12
14	.	.	.	12
15	.	.	.	10
16	.	.	.	6
17	.	.	.	3
18	.	.	.	1.5
19	.	.	.	1
20	.	.	.	1
21	.	.	.	< 1

Table 5.2: Percentage of bad values in bins 4-21 for each data set.

The case of Odon_4 data set is particularly complicated because the percentage of bad bin values is high. However, most of them are found at the end of the sampling period. In this case, in order to avoid too many data interpolations, we decided to discard the end of the data file and keep the records between 144 to 1400 which represent 46% of the total sampling.³

- **Physically unrealistic values:** Some records are considered as bad to the extent that velocity values lie outside a meaningful physical range (for example, $v \gg 100$ cm/s). Other records present unrealistic abrupt changes in the velocity (spikes). Such records are not detected by the internal rejection algorithm and may appear either in one velocity component or in all three components simultaneously. In the first case, a bad component may contaminate the calculation of the other components producing isolated peaks but within the expected physical range. This case must be treated with particular attention. As we can see in figure 5.3, U (or V) exhibits spikes while the other component also is anomalous but within the realistic physical range. This kind of errors are present mostly as individual records and we have corrected them by a simple linear interpolation.

A general algorithm to detect these data may be based on looking the error velocity (5th column). This parameter, which must be small in normal conditions, also present spikes coinciding with bad records (fig. 5.3). We also have observed, at least in the first two data sets (Odon_1 and Odon_2), that spikes are present through the whole profile (see fig. 5.4).

5.3 Polishing step by step

To clarify the strategy followed to correct the problems before mentioned, here we explain step by step the procedures applied to polish the data sets. From the computing point of view most part of the procedures may be easily vectorized by using IDL commands in an interactive way. In Appendix V we show some detailed IDL interactive procedures and routines used in preparing the CANALES-97 data sets.

1. Out-of-the-water data can easily be eliminated manually editing the temperature data *filename.asc* file. Good data were considered once the temperature is stabilized after deployment and before recovery operation when temperature rapidly increases.
2. Data affected by surface reflexions (bins 1 to 6) were replaced by zero for drawing purposes.

³Bin 6 does not seem to be contaminated by surface effects in Odon_4 data set. The mooring line was deployed slightly to the north of previous locations so that the water depth likely was greater, hence, the ADCP deeper. However, it does not affect the procedure here explained

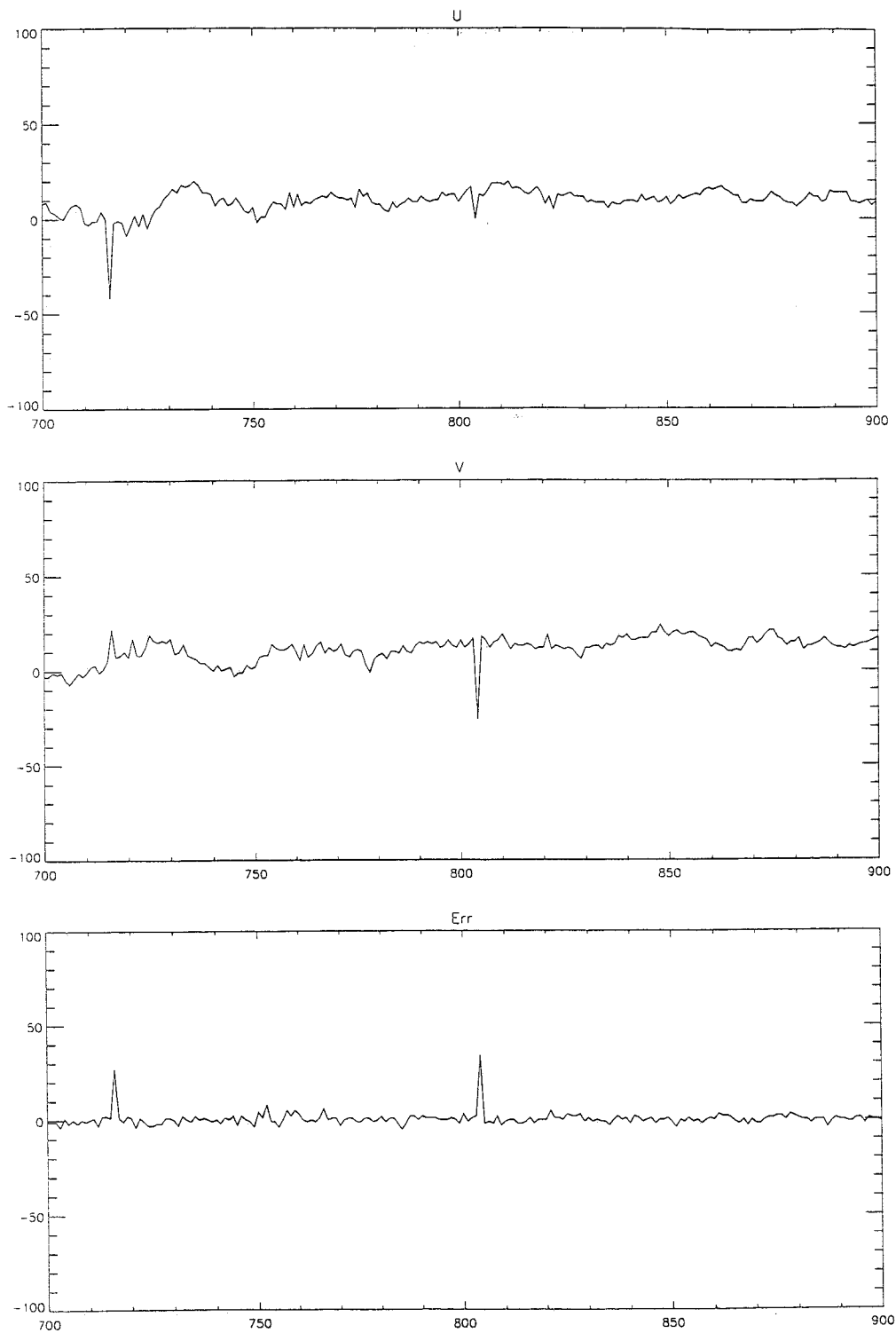


Figure 5.3: U, V, and error velocity (in cm/s) versus record number to illustrate how a spike in one component can affect the other components. In this case, the problem can be detected by the error velocity.

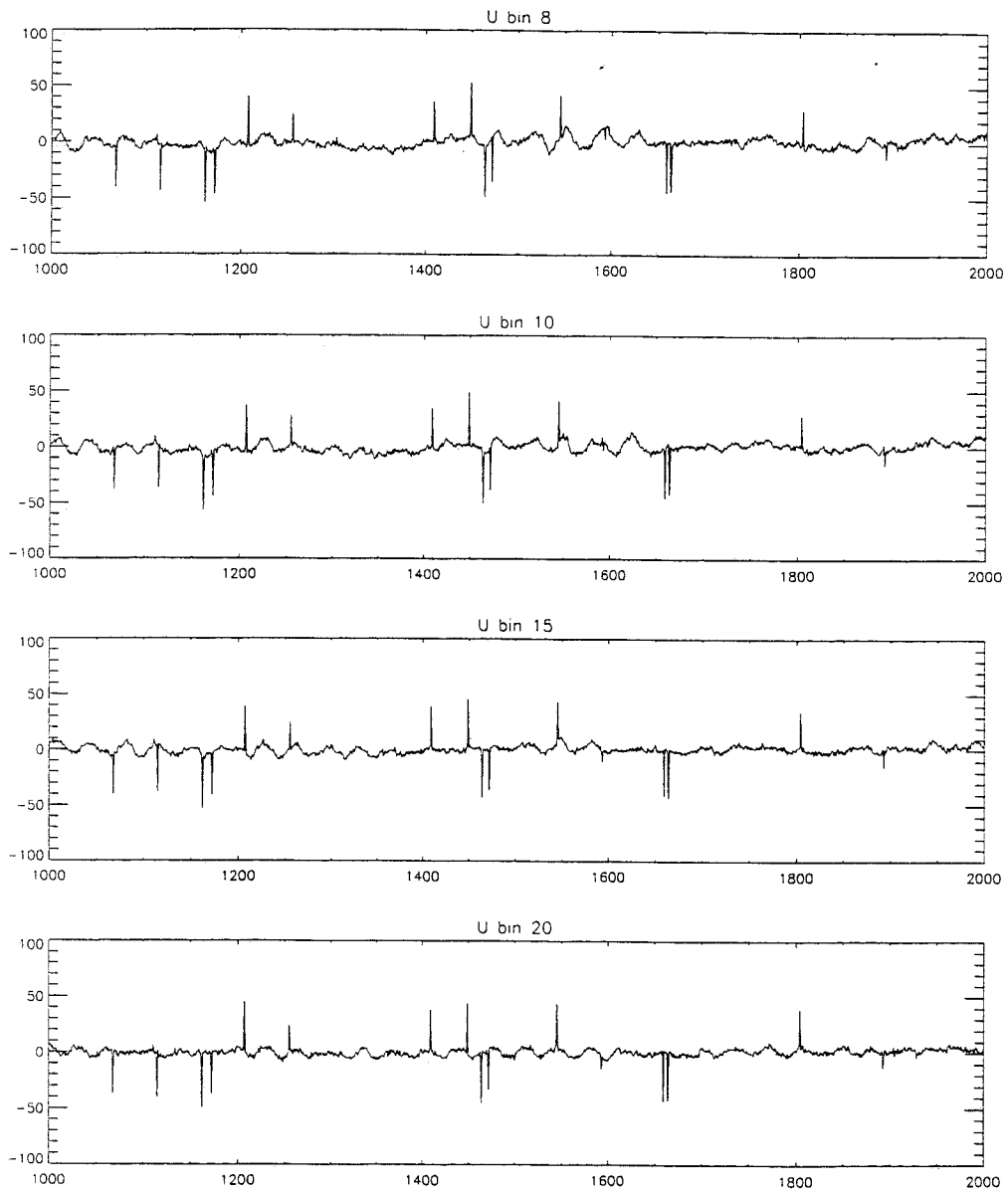


Figure 5.4: U component for bins 8, 10, 15 and 20 (Odon-1 data set)

3. Bins flagged as 9999 were listed and when an isolated value was found, a linear interpolation was performed on the three velocity components. This is the most frequent situation, however bin 7 in Odon_1 and several bins in Odon_4 data sets contained interval of 5 to 10 consecutive records flagged as 9999. They were individually analyzed by means of an autoregressive model described below.
4. Correcting anomalous values (*spikes*). For each bin we plotted the error velocity versus record number and searched for 9999 flags in the error column. The corresponding error velocity values were set systematically to 0.0 to avoid a biasing of the statistics. Next, the statistics of the error velocity was computed to estimate the mean $\langle Err \rangle$ and the standard deviation σ_t . Then, a rejecting criterium was applied which consisted in detecting values lying outside the interval $[\langle Err \rangle - 3\sigma_t, \langle Err \rangle + 3\sigma_t]$ (fig. 5.5). Then, a linear interpolation of the three velocity components was performed as a first guess estimation. Note that this criterium is rather tolerant in order to preserve some extreme but physically relevant and consistent values.

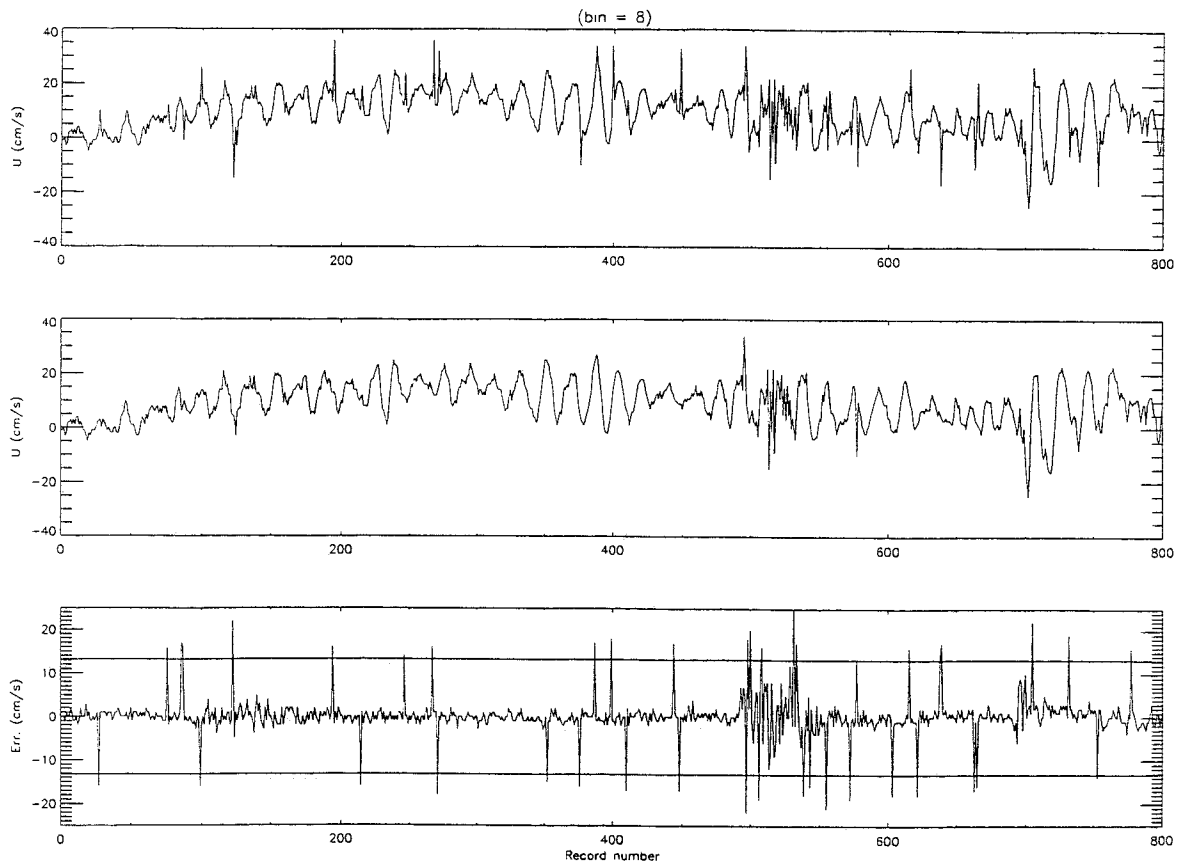


Figure 5.5: *Top*: U component for bin 8 (Odon_4 data set) showing characteristic spikes. *Middle*: U component after correction. *Bottom*: Error velocity series. Solid lines represent the limits of the interval $[\langle Err \rangle - 3\sigma_t, \langle Err \rangle + 3\sigma_t]$.

5. Finally the temperature data also has been corrected by a systematic offset of 0.10 ± 0.02 °C estimated from comparison with CTD data.

5.4 Data Interpolation

In general, as we pointed before, most part of bad values appear isolated but sometimes they are grouped in intervals of consecutive bad records. Bin 7 in Odon_1 and bins 9 to 16 in Odon_4 contained an important percentage of bad bin values, most of them grouped in several but small finite intervals. In Odon_1, the longest bad interval contained 28 consecutive records while the most frequent ones included 2 consecutive values. In Odon_4, the interval goes between 2 and 8 consecutive bad bin values. In such cases, to reconstruct the time series we adjusted an autoregressive (AR) model. An AR model of order p means that a forecast value is a linear combination of p consecutive previous values plus a random error,

$$x_t = a_1 x_{t-1} + a_2 x_{t-2} + a_3 x_{t-3} + \dots + a_p x_{t-p} + \epsilon_t$$

where ϵ_t is an uncorrelated random error, and a_i are unknown coefficients to be determined in such a way that they minimize ϵ_t (Priestley, 1981). The main problem is to fix the order of the AR model to be used. Here we have adopted the Akaike's information criterion (Akaike, 1973, 1974). The procedure consist on fitting successive AR models where the error variance σ_ϵ^2 is estimated. Then p is chosen as the value that minimizes

$$AIC(q) = n \ln(\sigma_\epsilon^2) + 2q$$

where n is the total number of observations. In figure 5.6 we have represented an exemple of the AIC function. It can be appreciate that as p increases the AIC function decreases for small values of p . Then a minimum is reached and the AIC function starts to grow as p increases. Nevertheless, given that in some cases it has been produced a forecasting of relatively long intervals where the model could fail, we consider that such time series had to be looked with caution.

5.5 Filtering

In this section we focus on exploratory and preliminar analyses that basically consist on visualization and filtering of the data sets. Temperature records have been low-pass filtered with a 5-day Gaussian filter. Velocity records have been low-pass filtered by applying a 120 h low pass filter. This filter is based on a variational technique described in Thompson (1983) which eliminates the local inertial frequency band and several tidal components. Very briefly, given a symmetric filter

$$y_t = \sum_{k=-n}^n w_k x_{t+k} \quad w_{-k} = w_k$$

Thompson's approach consists in finding the w_k as the result of minimizing the filter response error in comparison to an ideal filter response. We search for a low frequency

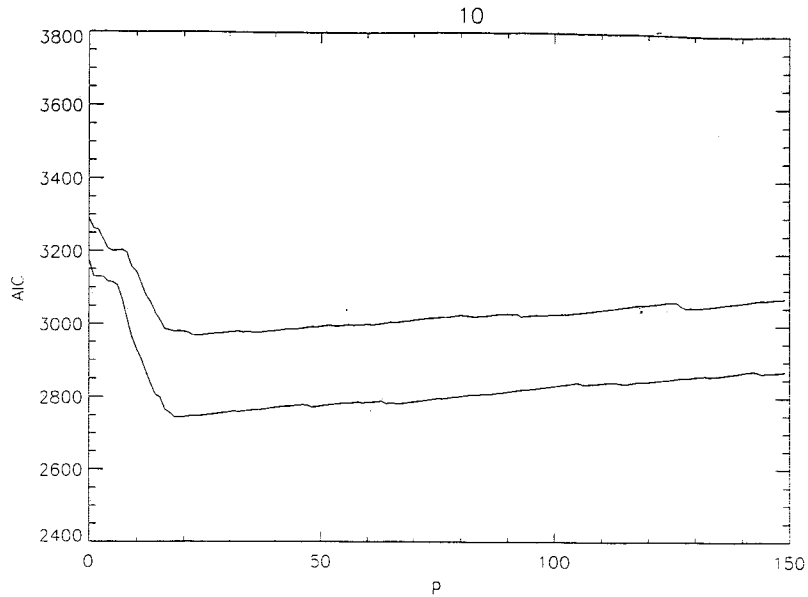


Figure 5.6: The AIC function of U and V components for bin 10 (Odon_4 data set). The minimum is around 18.

response near unity, a small response at high frequencies and exactly zero response at fixed frequencies (inertial and tidal). Then, an error function is built as the difference between the filter response function $R(\omega)$ and a desired shaped filter function $L(\omega)$.

$$E = \frac{1}{2\pi} \int_0^\pi [R(\omega) - L(\omega)]^2 d\omega$$

$L(\omega)$ is defined as

$$L(\omega) = \begin{cases} 1 & \text{for } \omega < \Omega_1. \\ \frac{1}{2} \left[1 + \cos \left(\frac{\pi(\omega - \Omega_1)}{(\Omega_2 - \Omega_1)} \right) \right] & \text{for } \Omega_1 < \omega < \Omega_2 \\ 0 & \text{for } \Omega_2 < \omega \end{cases}$$

where Ω_i are chosen to have a smooth decay from Ω_1 to Ω_2 . The problem is completed by the constraints that no power should pass at the frequencies ω_j in such a way that

$$R(\omega_j) = \omega_j + 2 \sum_{k=1}^n \omega_j \cos(\omega_j k) = 0$$

In our case⁴ we have applied this filter to suppress the O_1 , K_1 , Q_1 , P_1 , M_2 , S_2 , N_2 components and the inertial frequency at $39^\circ 6.55' \text{ N}$ ($T_m = 19.0 \text{ h}$).

⁴This filter has been implemented in IDL by E. Del Rio.

(see <http://www.icm.csic.es/cgi-bin/lista.cgi?idl/GUI-tools/filter/>)

6 Results

This section reports the preliminary results corresponding to data sets for each sampling period. The section is thus divided in four parts where we show

1. The temperature (unfiltered and low-pass filtered), the heading and its standard deviation. Julian days are referred to January 1 of 1997.
2. Vector progressive plots (unfiltered velocity data)
3. Stick plots (unfiltered data)
4. Colored contouring of low-pass U and V components.

The final data sets are composed of the following files that will be available through a web site accessible under permission. The available list of files is (asterisc means the four periods)

1. Tar file `od*_tar` containing
 - `od*_pl.dat`: pulished data set
 - `od*_asc.dat`: scalar data set
 - `od*_fl.dat`: filtered data set
2. Tar file: `odon*_tar`, original and report data files.
3. Compressed tar file `report.tar.gz` including this documentation in Postscript format and all the graphics.

6.1 Data Set: Odon_1

This deployment contains pulsed data in the period

14:18:17 of 31/01/97 (record 14) to 11:18:17 of 03/04/97 (record 2984)

Remember that the time sampling in this data set was of 0.5 hours.

BIN	$ \vec{v} _{max}$	$\langle \vec{v} \rangle$	u_{max}	$\langle u \rangle$	σ_u	v_{max}	$\langle v \rangle$	σ_v
6	40.4	9.9	40.0	4.7	6.2	36.0	-1.9	8.2
7	40.3	14.1	31.0	7.6	7.9	37.0	-3.0	11.5
8	38.1	14.2	29.0	7.7	7.7	35.0	-2.9	11.7
9	38.1	14.1	32.0	7.7	7.8	36.0	-3.0	11.6
10	38.3	13.8	29.0	7.6	7.7	36.0	-3.0	11.4
11	38.0	13.4	29.0	7.4	7.5	35.0	-2.9	11.1
12	36.7	13.1	28.0	7.4	7.3	33.0	-2.8	10.8
13	37.3	12.7	28.0	7.2	7.1	35.0	-2.8	10.5
14	36.7	12.2	28.0	6.9	7.1	34.0	-2.8	10.1
15	36.7	11.7	28.0	6.7	6.9	33.0	-2.8	9.6
16	34.4	11.3	28.0	6.5	6.7	31.0	-2.6	9.3
17	34.4	10.8	25.0	6.1	6.5	31.0	-2.5	8.9
18	31.8	10.3	23.0	5.9	6.3	29.0	-2.4	8.3
19	31.4	9.7	22.0	5.5	6.0	27.0	-2.4	7.8
20	30.4	9.2	22.0	5.2	5.8	27.0	-2.1	7.4
21	28.8	8.7	21.0	5.0	5.4	24.0	-2.0	7.1
22	28.4	8.4	20.0	4.7	5.3	23.0	-1.8	6.8
23	30.2	8.0	20.0	4.4	5.2	25.0	-1.7	6.4
24	26.6	7.6	20.0	4.2	5.0	22.0	-1.6	6.1
25	23.3	7.3	20.0	4.0	4.9	21.0	-1.4	5.7
26	25.6	7.1	21.0	3.8	4.8	20.0	-1.2	5.5
27	27.6	6.8	19.0	3.6	4.6	21.0	-1.1	5.3
28	25.5	6.6	20.0	3.4	4.5	18.0	-1.0	5.1
29	23.4	6.4	16.0	3.3	4.4	22.0	-0.9	4.9
30	23.8	6.1	20.0	3.1	4.2	23.0	-0.6	4.8
31	24.4	5.7	18.0	2.8	4.1	20.0	-0.6	4.5
32	22.4	5.5	16.0	2.7	3.9	21.0	-0.5	4.2

Table 6.1.1: Statistics of Odon_1 data set

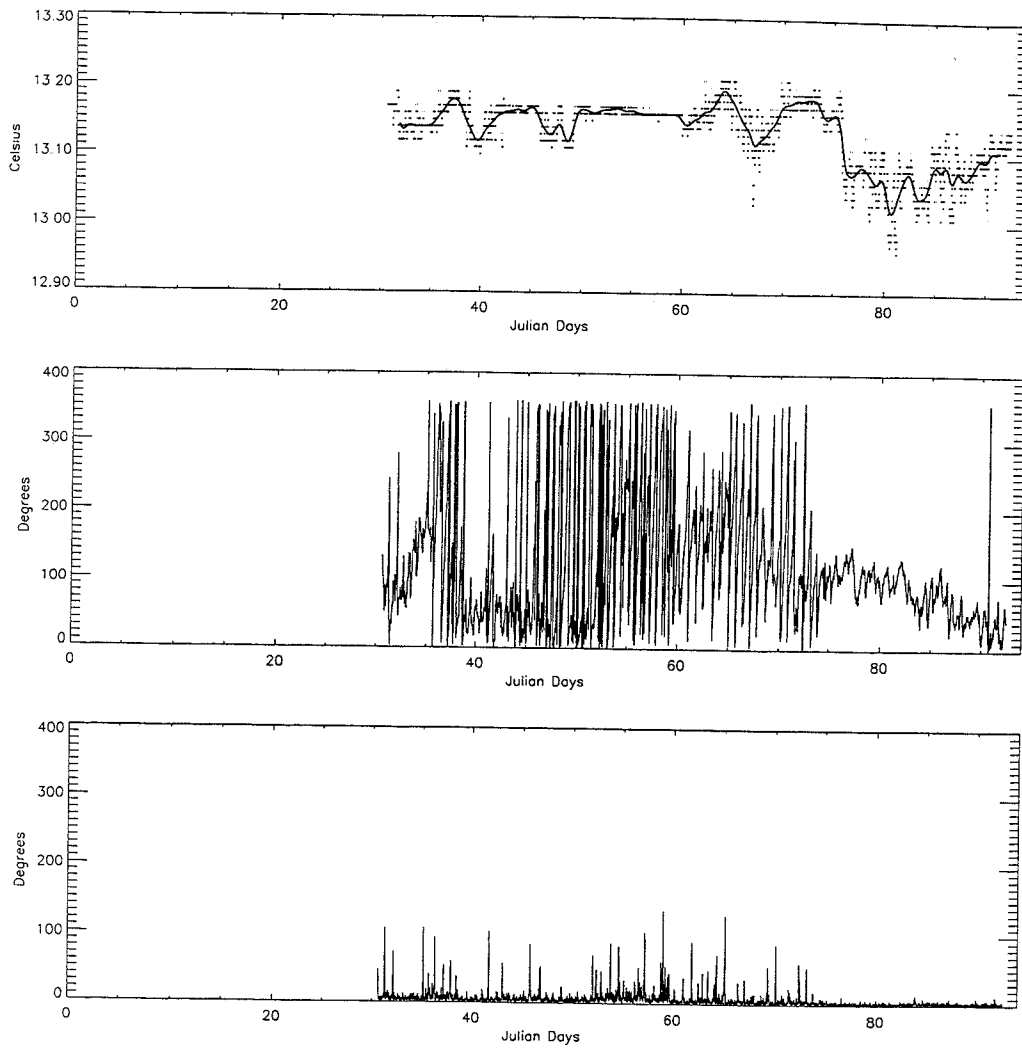


Figure 6.1.1: Temperature, Heading and Standard deviation of heading for Odon_1 data set

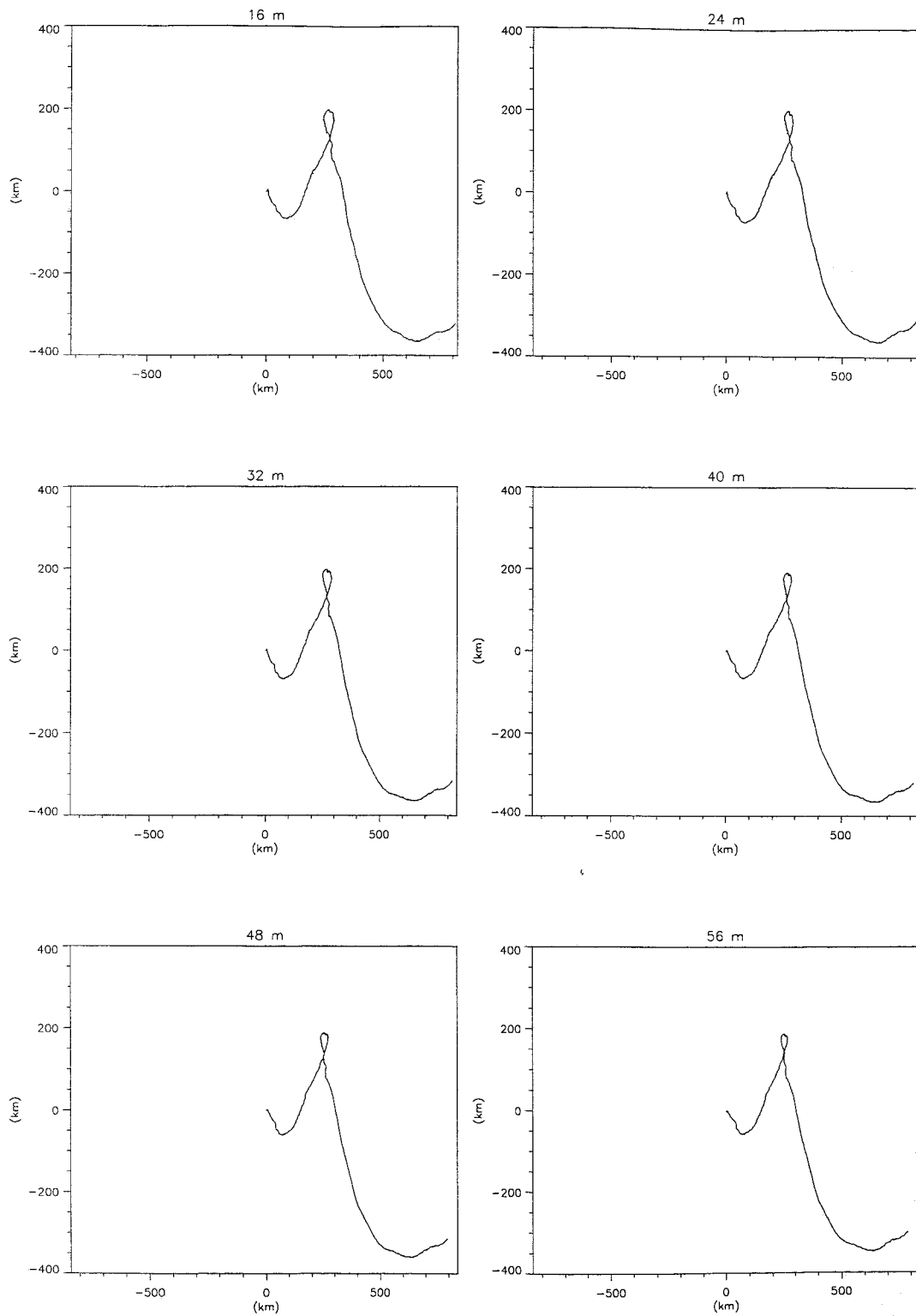


Figure 6.1.2: Progressive vectors plots at several depths recorded in Odon_1 data set. (Figs. 6.1.2-4)

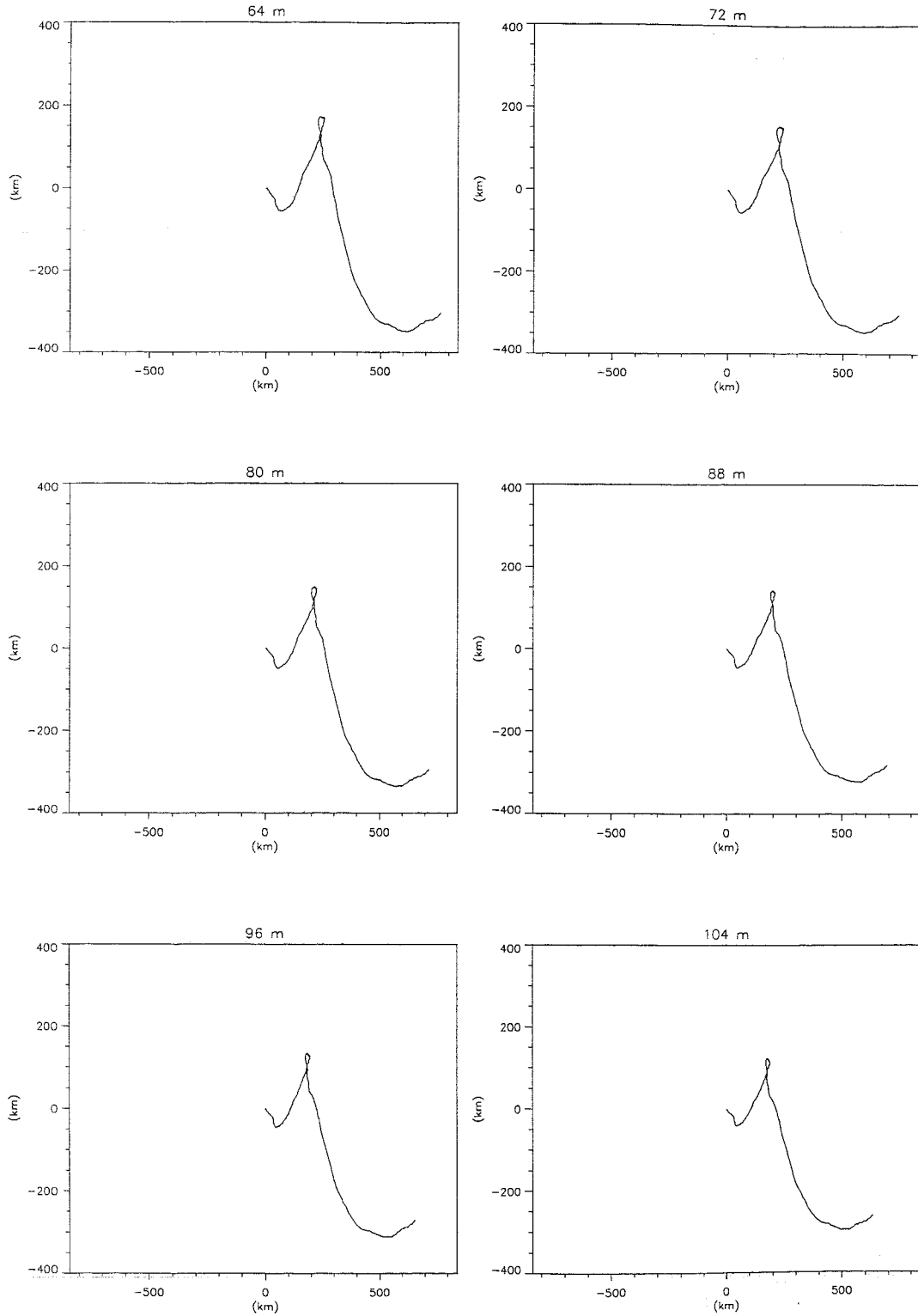


Fig.6.1.3: Odon.1: Progressive vectors (cont.)

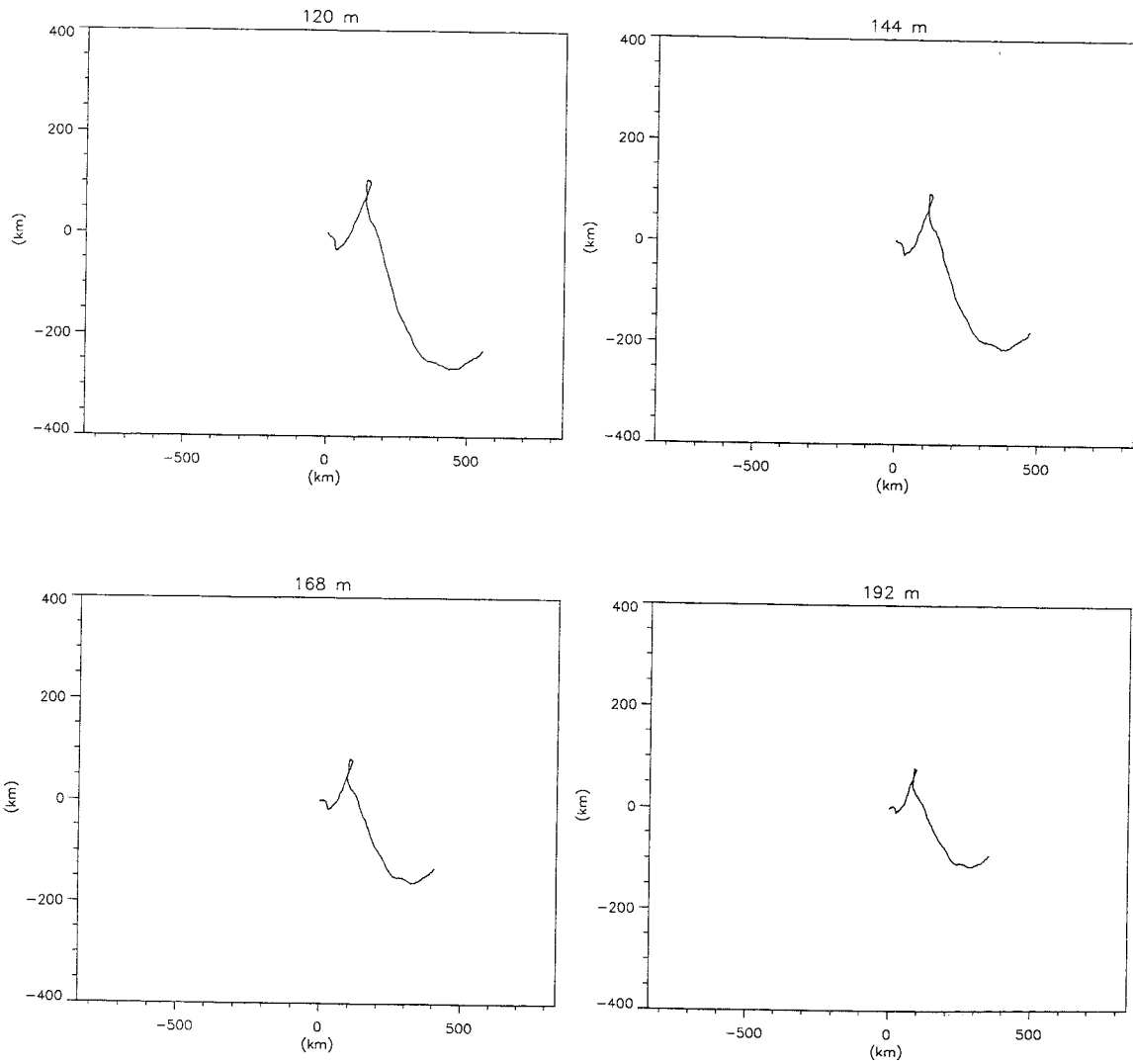


Fig.6.1.4: Odon_1: Progressive vectors (cont.)

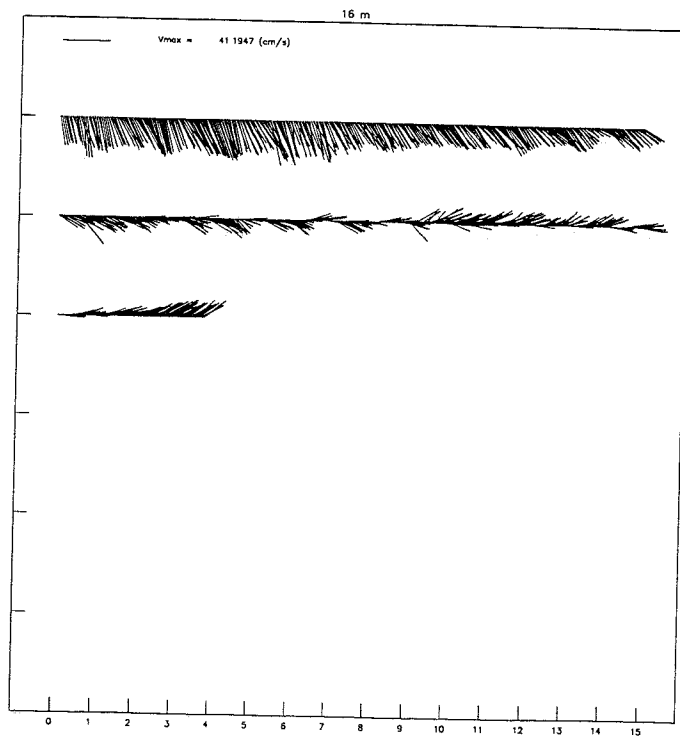
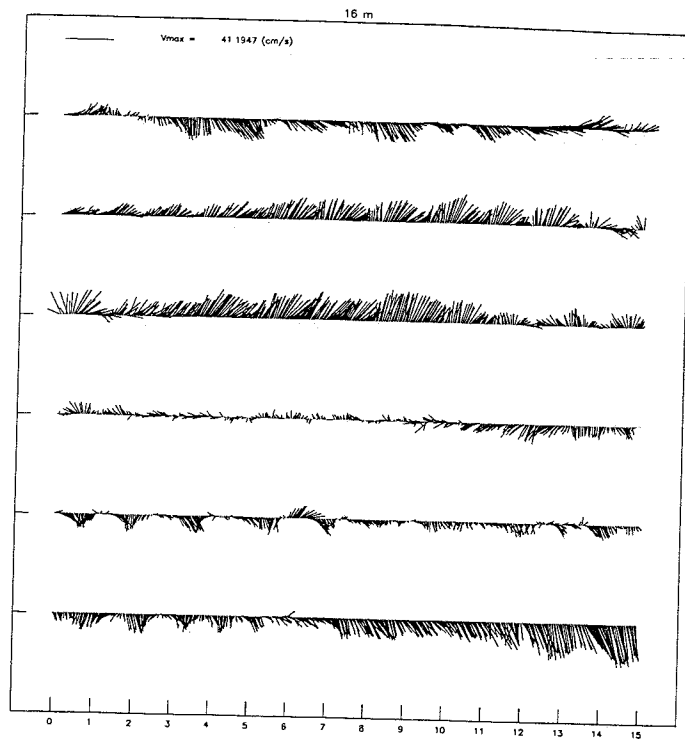


Figure 6.1.5: Stick plots at several depths recorded in Odon_1 data set. (Figs. 6.1.5-20)

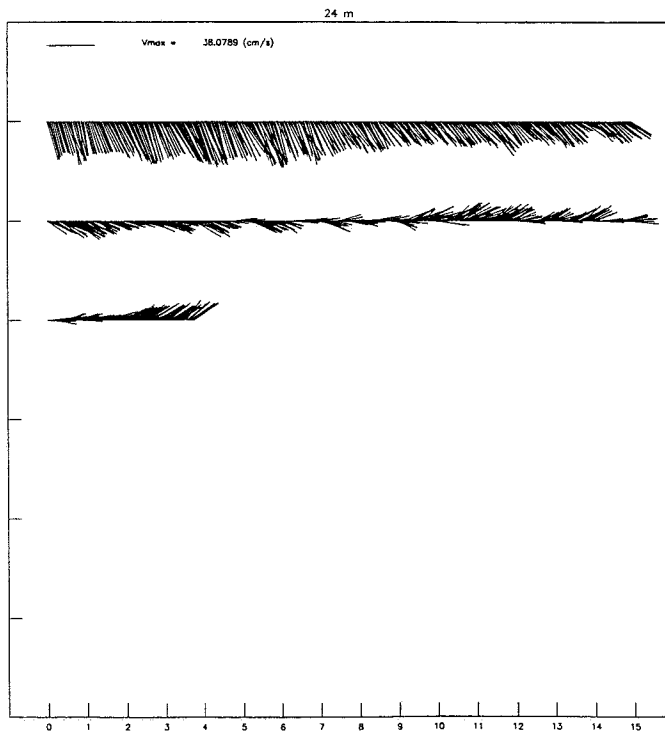
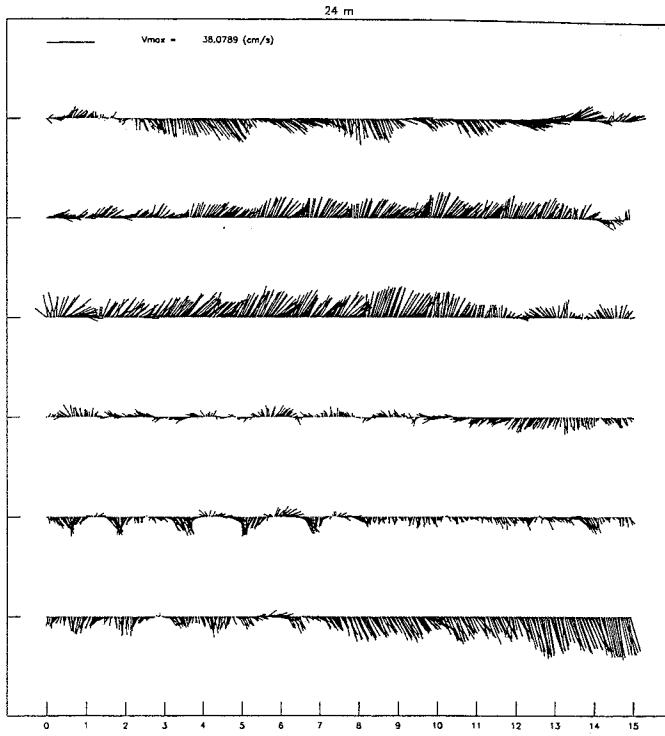


Fig.6.1.6: Odon-1: Stick plots (cont.)

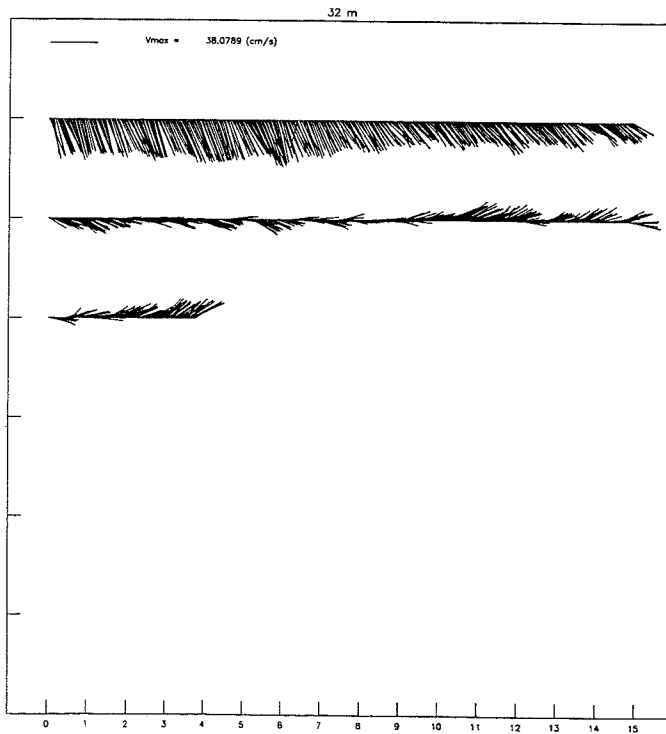
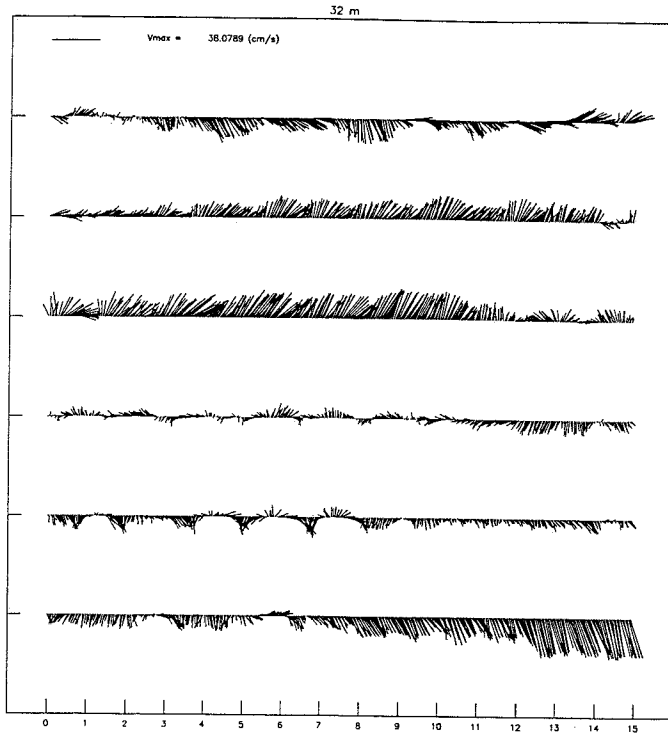


Fig.6.1.7: Odon_1: Stick plots (cont.)

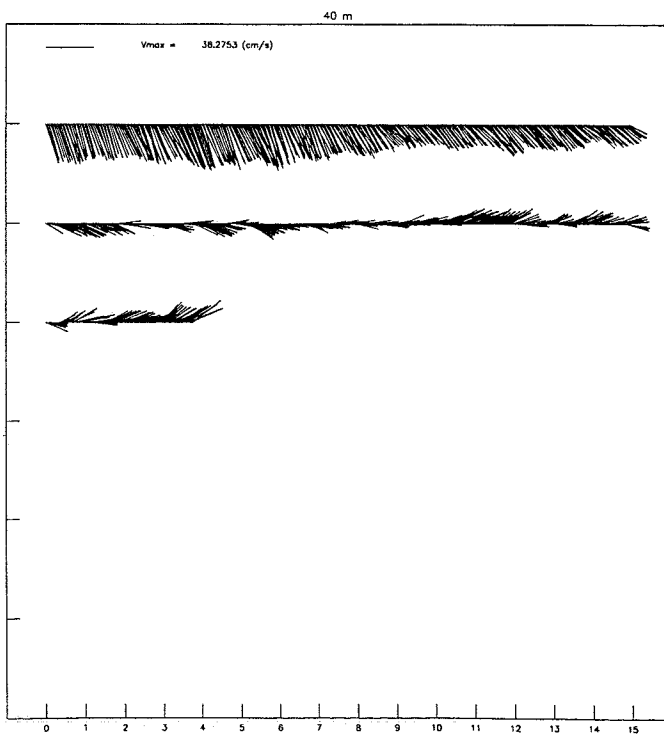
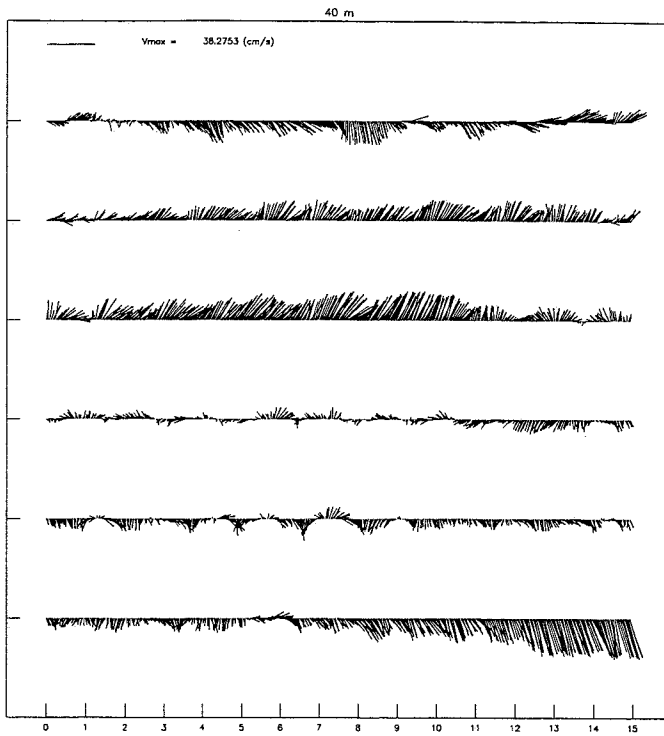


Fig.6.1.8: Odon_1: Stick plots (cont.)

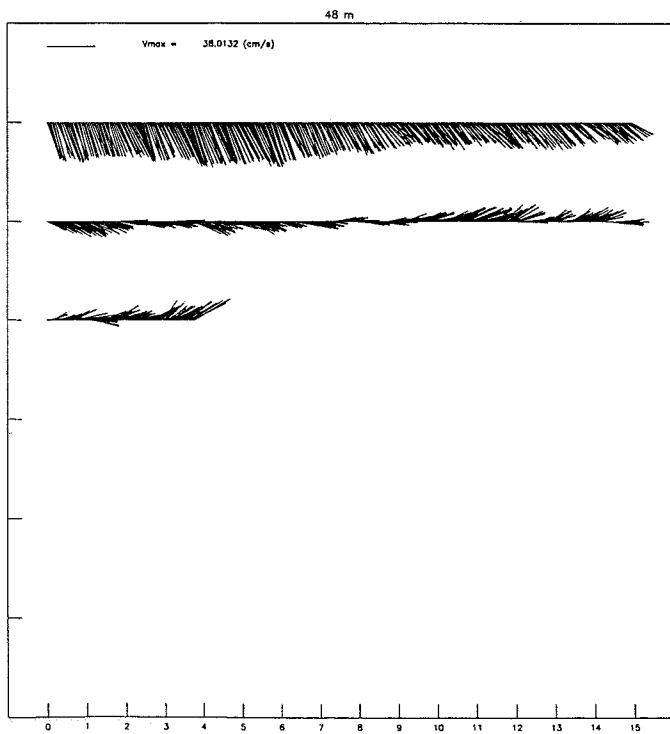
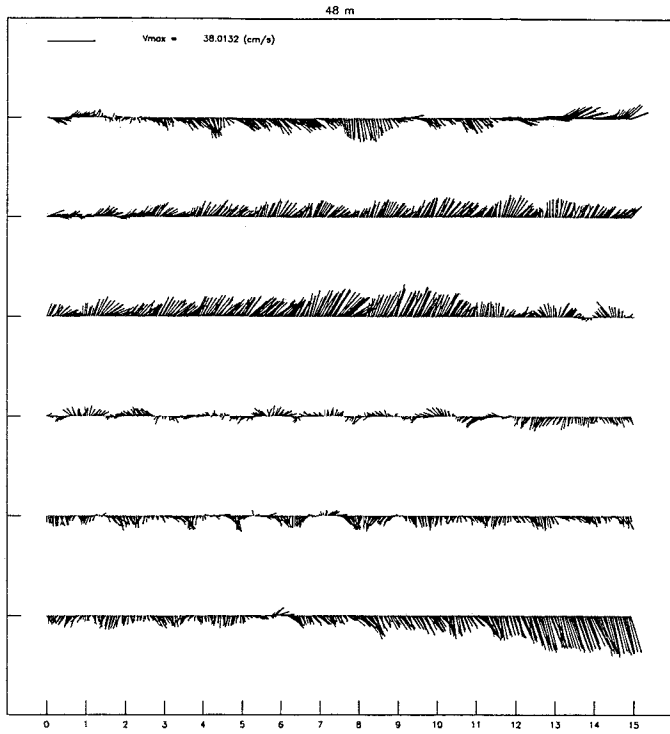


Fig.6.1.9: Odon_1: Stick plots (cont.)

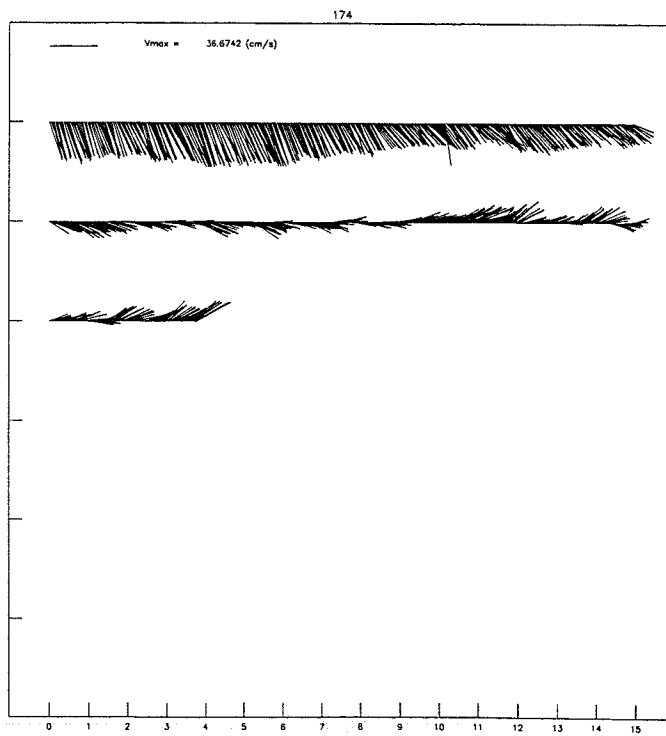
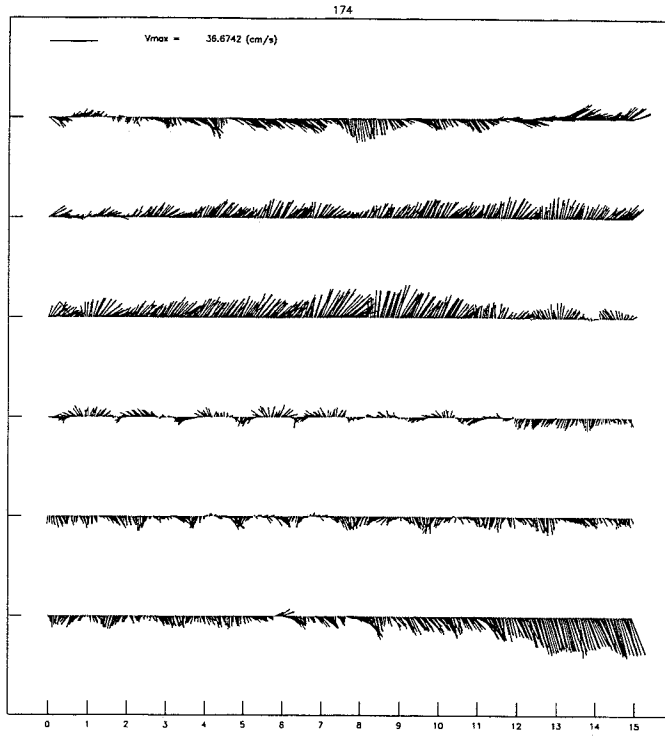


Fig.6.1.10: Odon_1: Stick plots (cont.)

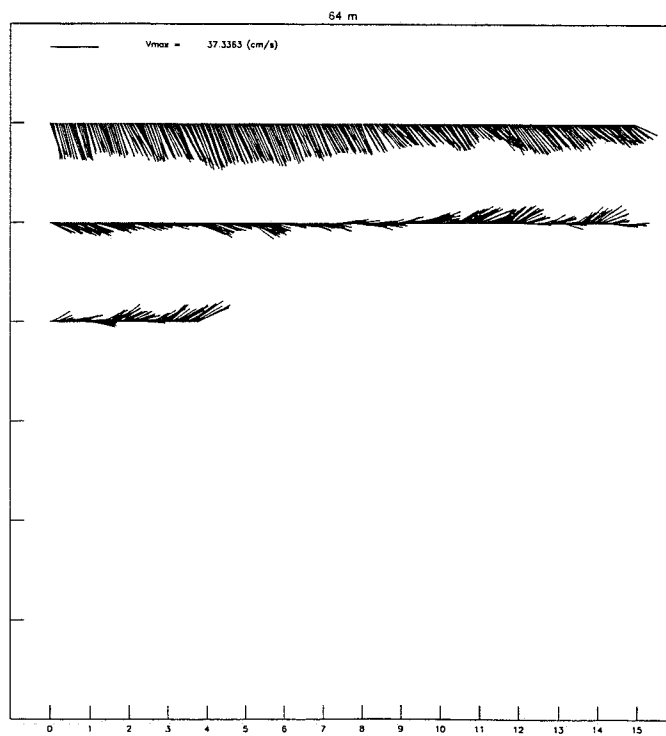
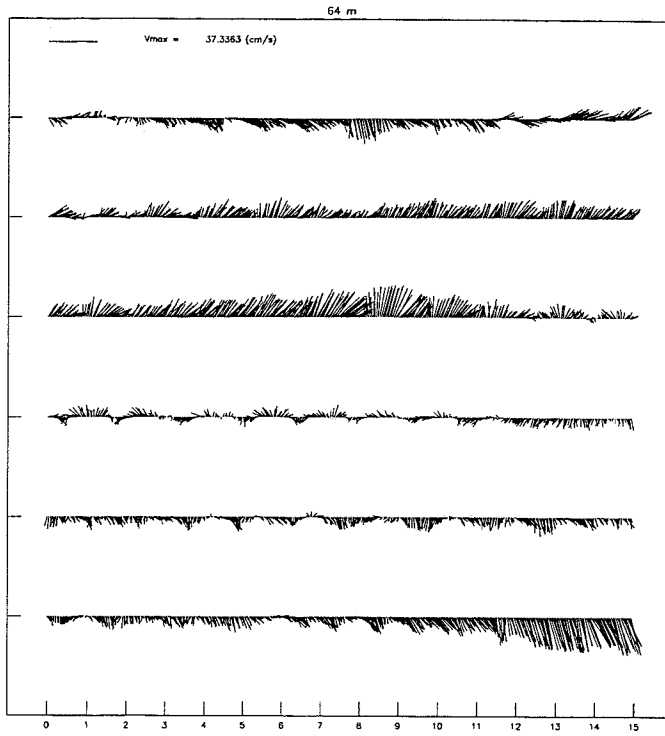


Fig.6.1.11: Odon.1: Stick plots (cont.)

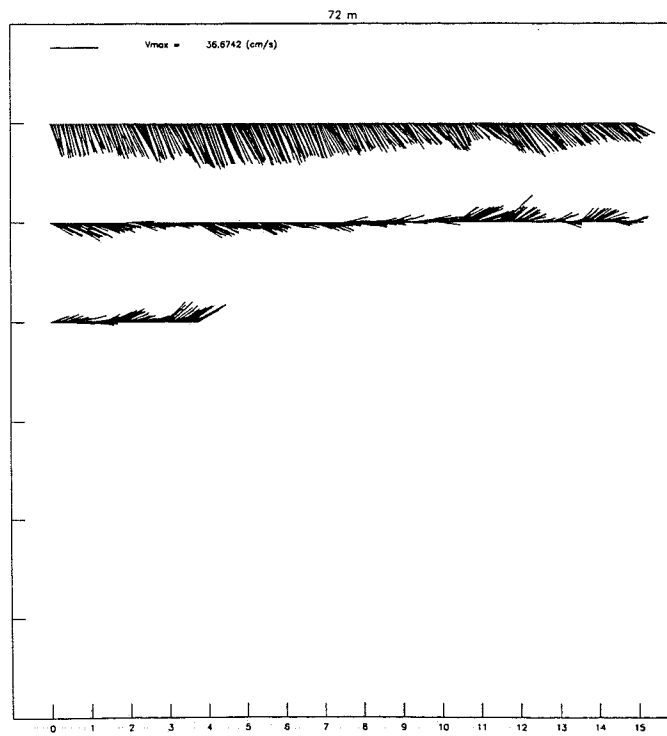
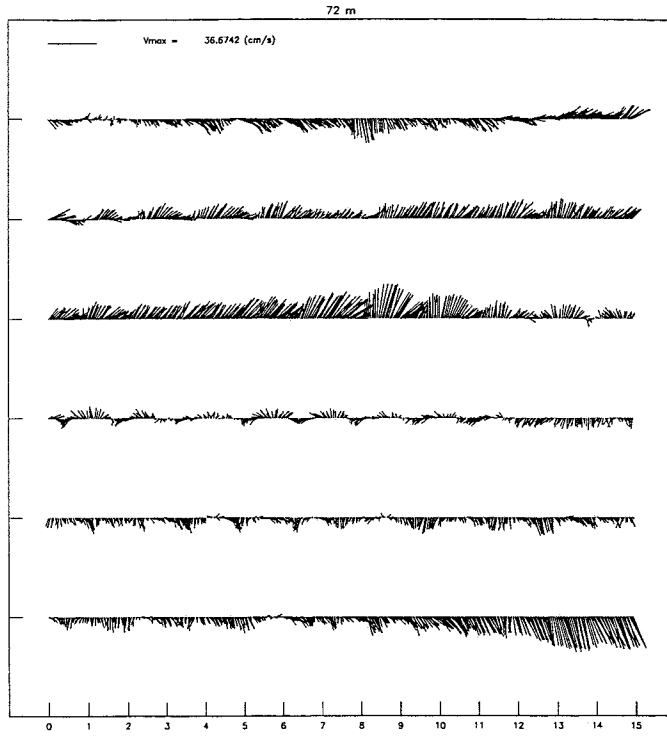


Fig.6.1.12: Odon_1: Stick plots (cont.)

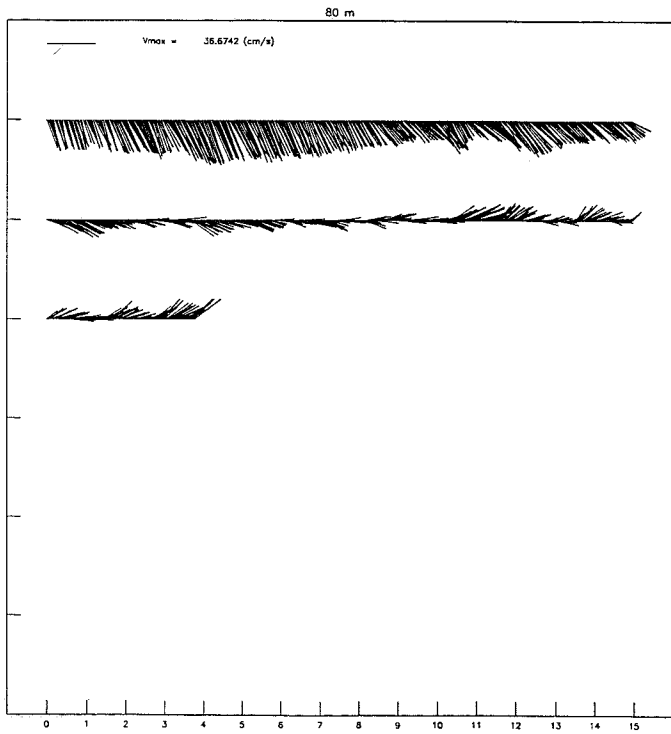
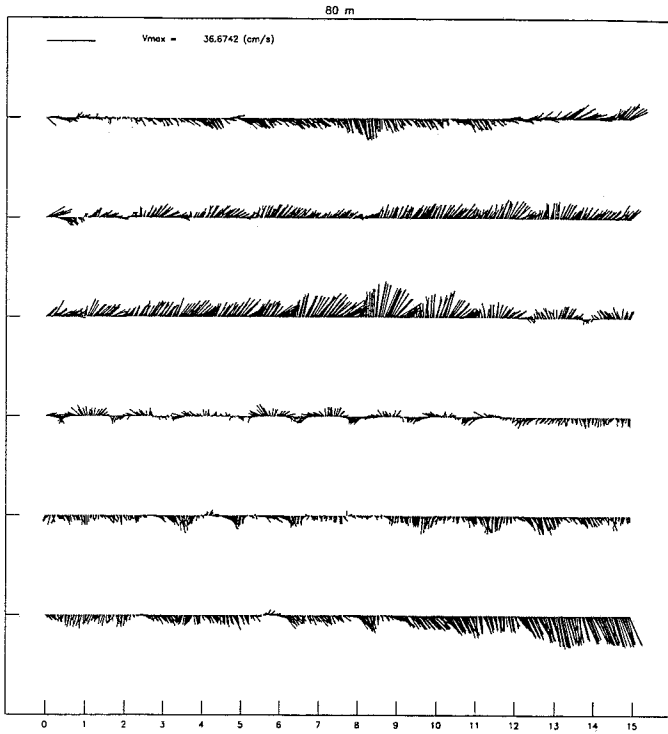


Fig.6.1.13: Odon_1: Stick plots (cont.)

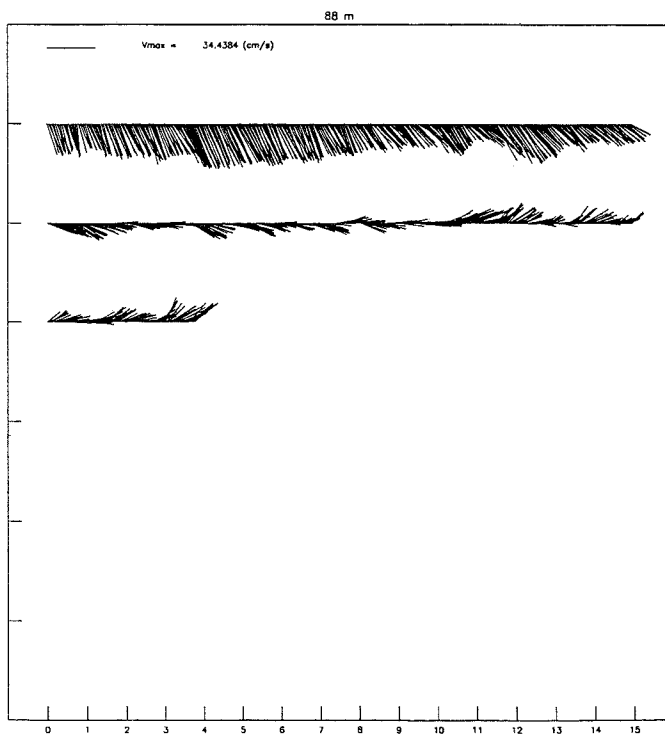
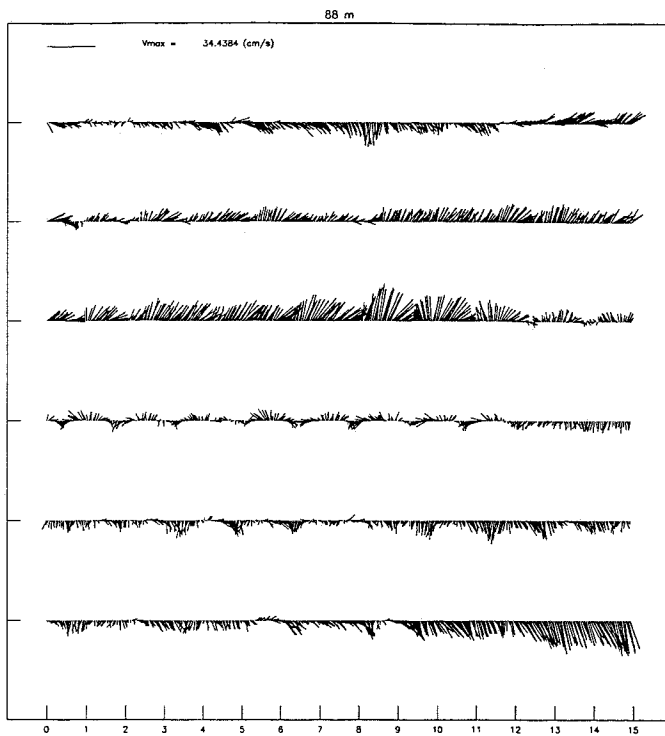


Fig.6.1.14: Odon_1: Stick plots (cont.)

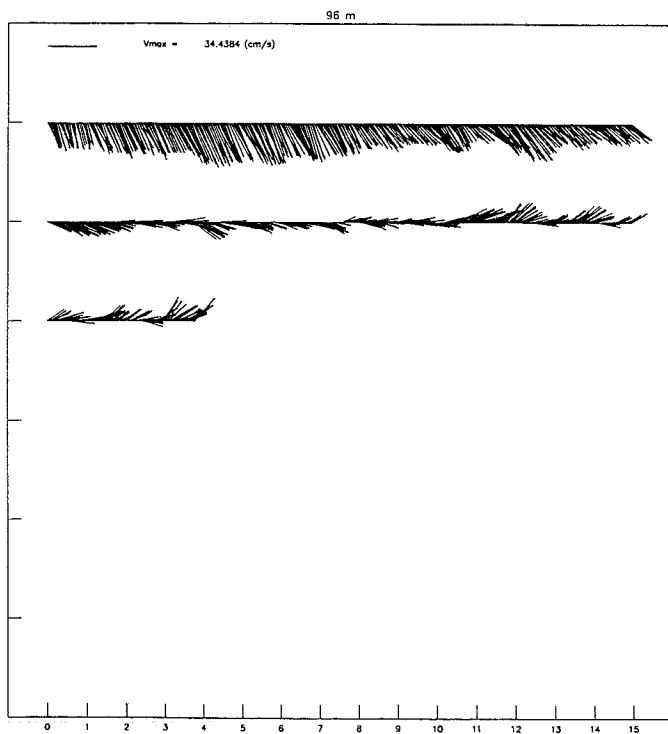
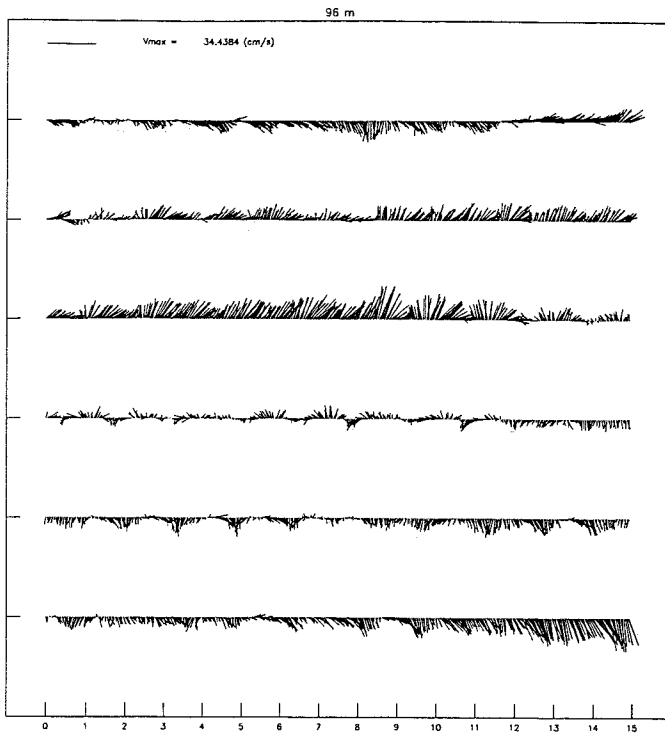


Fig.6.1.15: Odon_1: Stick plots (cont.)

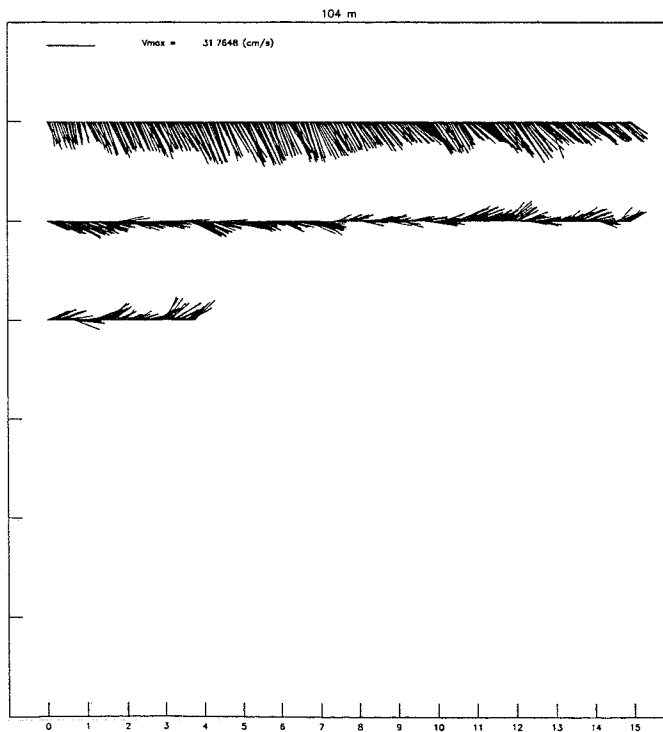
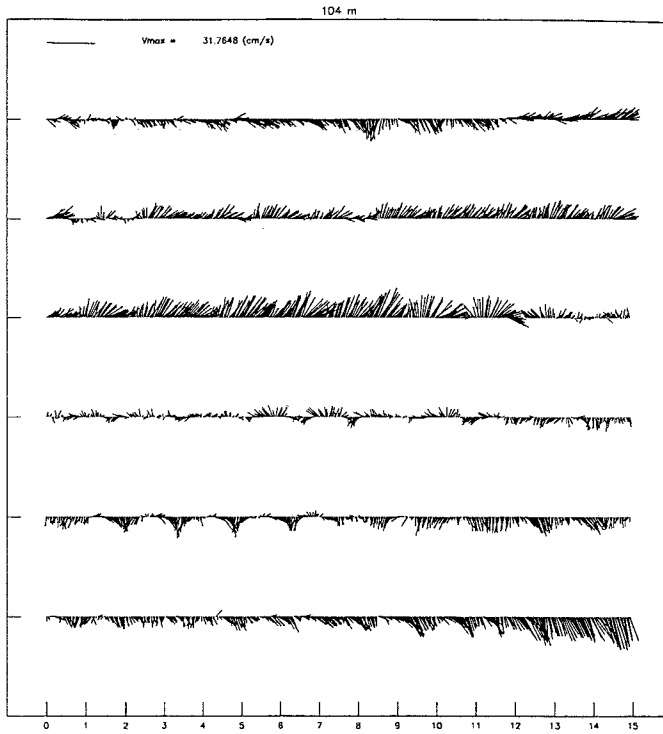


Fig.6.1.16: Odon_1: Stick plots (cont.)

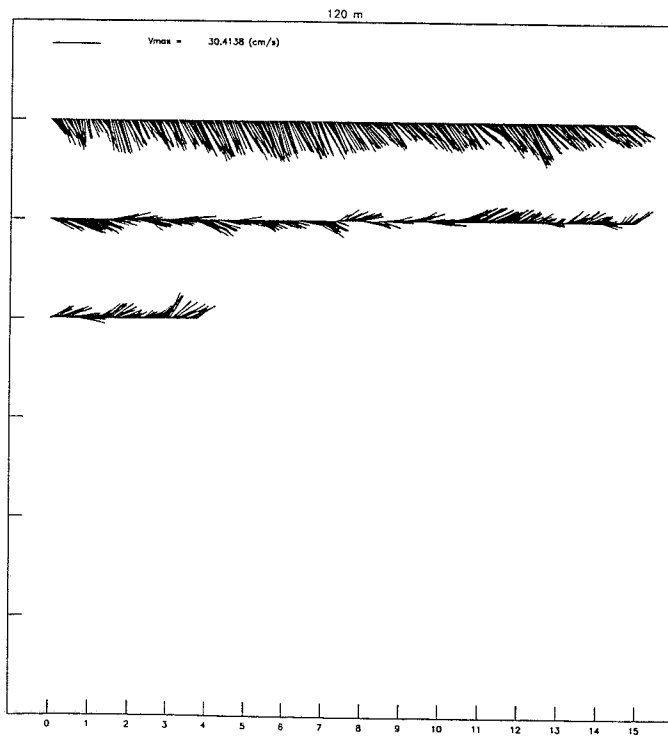
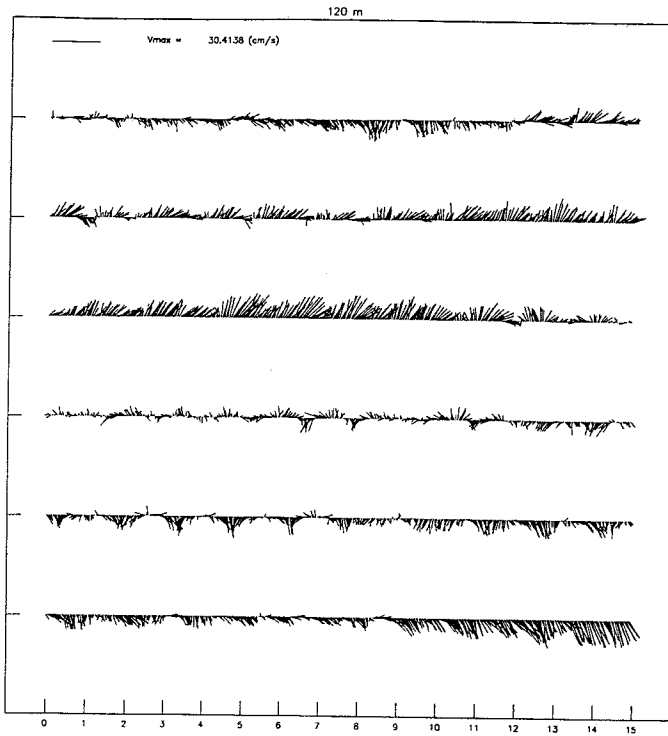


Fig.6.1.17: Odon_1: Stick plots (cont.)

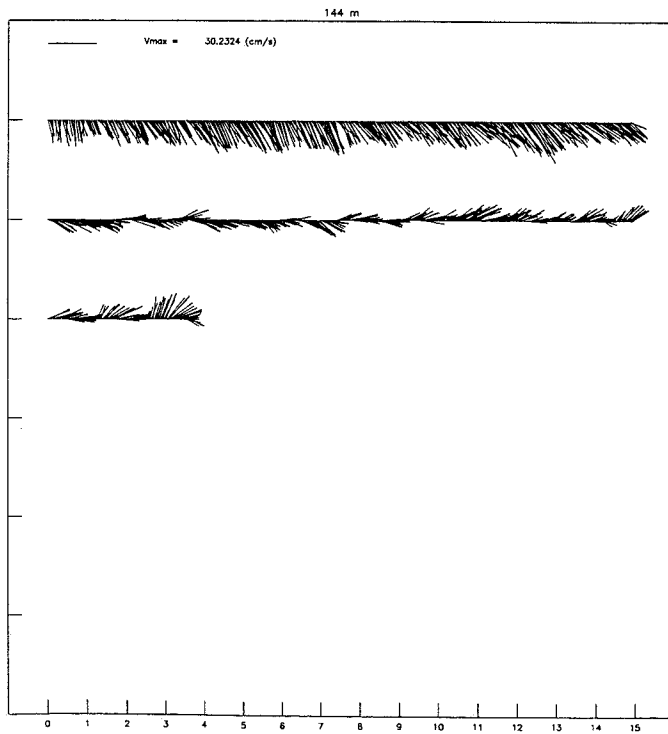
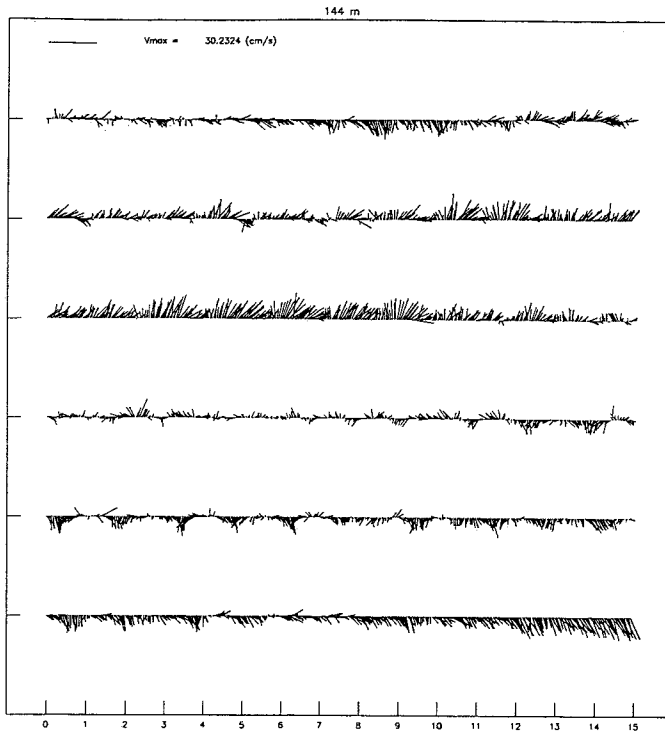


Fig.6.1.18: Odon_1: Stick plots (cont.)

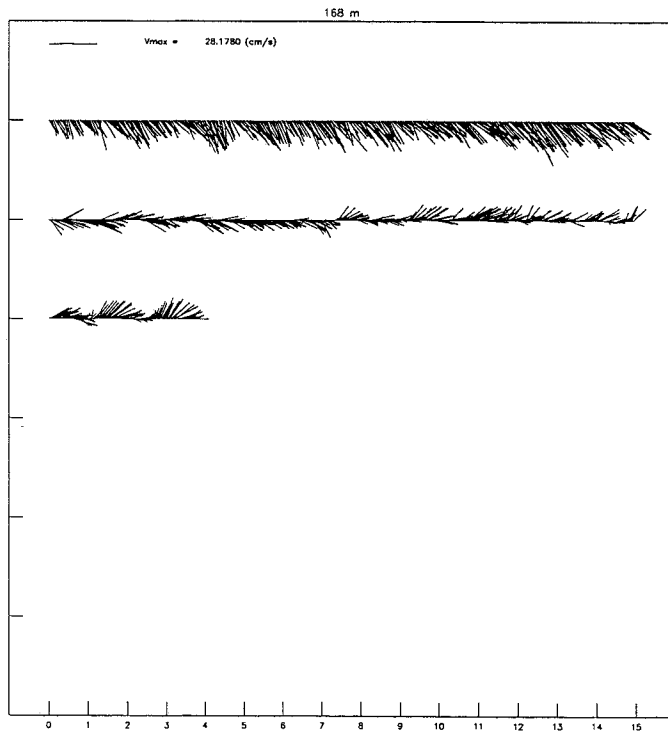
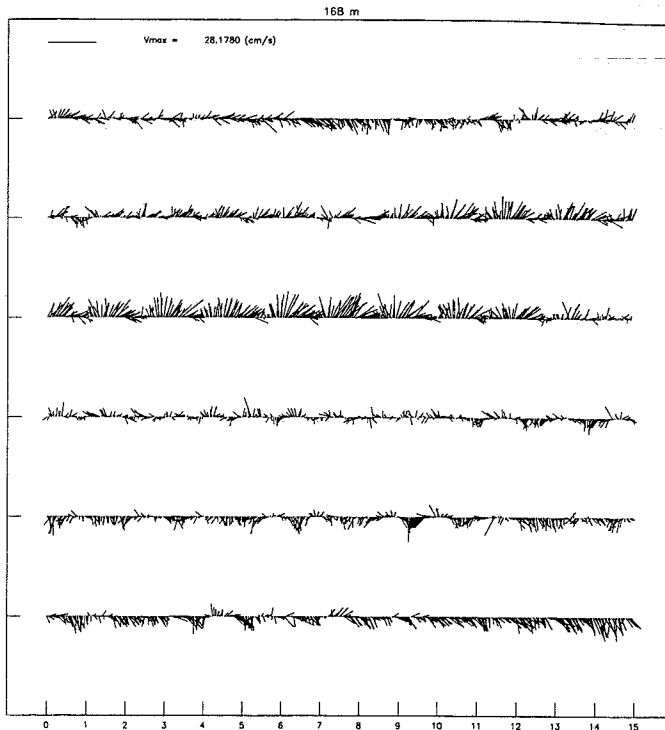


Fig.6.1.19: Odon_1: Stick plots (cont.)

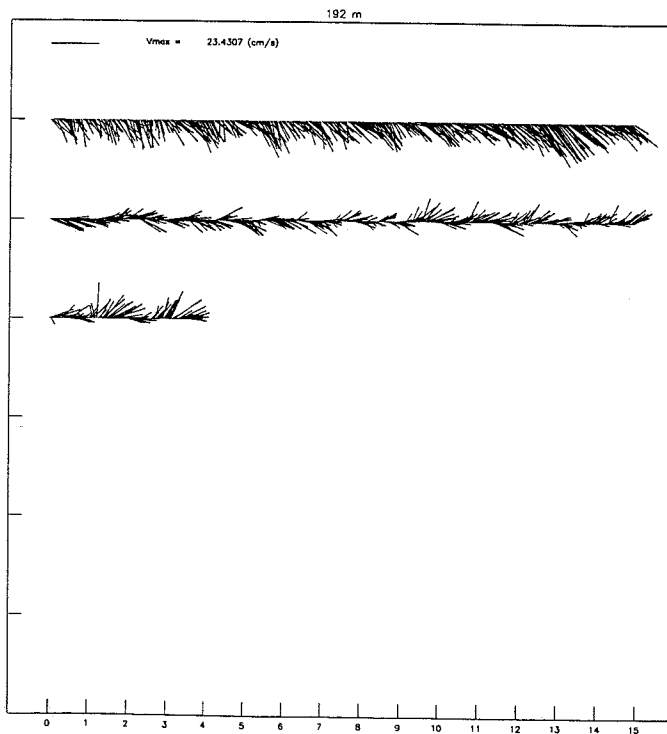
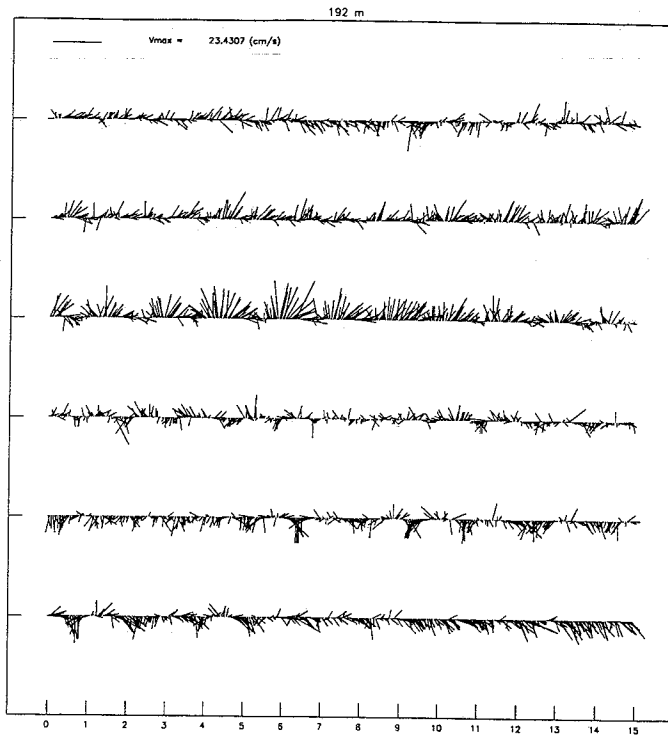


Fig.6.1.20: Odon_1: Stick plots (cont.)

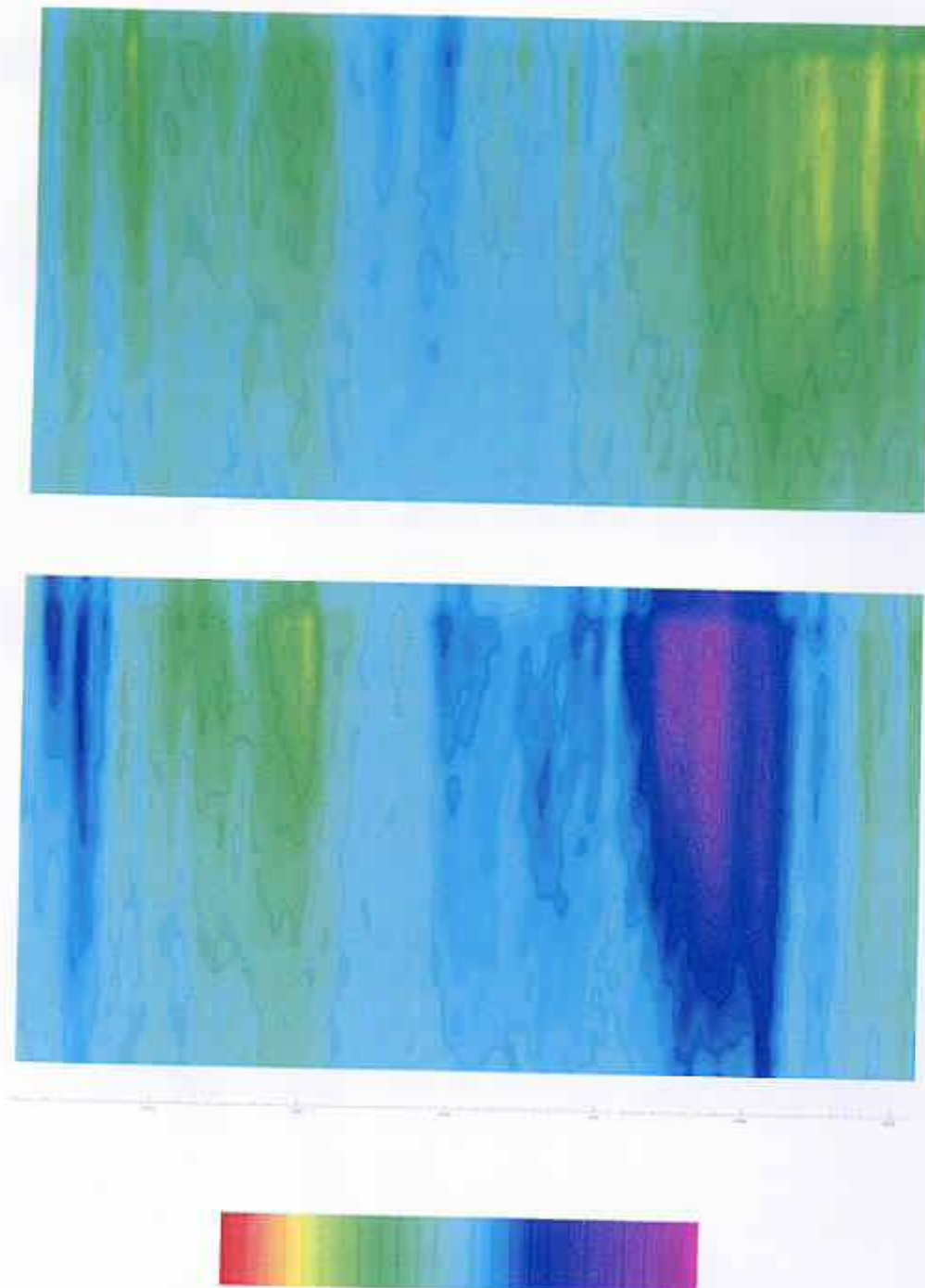


Figure 6.1.21: Filtered time series of U (upper) and V (lower) components in Odon_1. Time is Julian days and the color scale goes between -35.0 (blue tones) to 35.0 (red tones) cm/s.

6.2 Data Set: Odon_2

The series after deputation edge effects goes between

08:30:12 of 05/04/97 (record 14) to 05:30:12 of 01/07/97 (record 2099)

BIN	$ \vec{v} _{max}$	$\langle \vec{u} \rangle$	u_{max}	$\langle u \rangle$	σ_u	v_{max}	$\langle v \rangle$	σ_v
6	61.9	12.4	47.0	5.2	8.2	51.0	6.0	9.7
7	43.4	12.5	34.0	5.4	8.0	43.0	6.1	9.6
8	37.6	11.8	29.0	5.2	7.6	36.0	5.6	9.0
9	34.8	11.2	32.0	5.1	7.4	25.0	5.0	8.5
10	32.2	10.6	29.0	4.8	7.2	27.0	4.8	8.1
11	33.4	10.4	29.0	4.5	7.1	31.0	4.5	7.9
12	32.6	10.1	28.0	4.2	7.1	32.0	4.3	7.6
13	32.9	9.6	30.0	3.8	6.9	32.0	4.1	7.3
14	33.4	9.2	32.0	3.4	6.7	33.0	3.8	7.0
15	33.5	8.8	33.0	3.2	6.5	33.0	3.6	6.7
16	34.2	8.4	33.0	3.0	6.3	34.0	3.4	6.4
17	35.0	8.0	33.0	2.8	6.1	35.0	3.3	6.2
18	35.1	7.6	33.0	2.6	5.7	33.0	3.2	5.8
19	32.9	7.1	30.0	2.3	5.4	31.0	2.9	5.5
20	33.2	6.6	30.0	2.3	5.1	32.0	2.8	5.2
21	31.6	6.2	28.0	2.1	4.9	30.0	2.6	4.7
22	29.5	6.0	25.0	2.1	4.6	27.0	2.3	4.5
23	25.6	5.7	23.0	1.9	4.3	24.0	2.2	4.4
24	24.2	5.4	20.0	1.8	4.0	22.0	1.9	4.1
25	24.7	5.0	17.0	1.7	3.8	23.0	1.7	3.9
26	21.9	4.8	19.0	1.5	3.7	20.0	1.5	3.7
27	19.4	4.7	15.0	1.5	3.6	19.0	1.4	3.7
28	18.0	4.6	14.0	1.3	3.5	17.0	1.3	3.6
29	19.2	4.5	16.0	1.1	3.5	17.0	1.1	3.5
30	18.4	4.4	15.0	1.1	3.5	17.0	1.1	3.5
31	16.6	4.3	14.0	1.0	3.3	15.0	0.9	3.4
32	14.9	4.1	14.0	0.9	3.2	14.0	0.7	3.2

Table 6.2.2: Statistics of Odon_2 data set

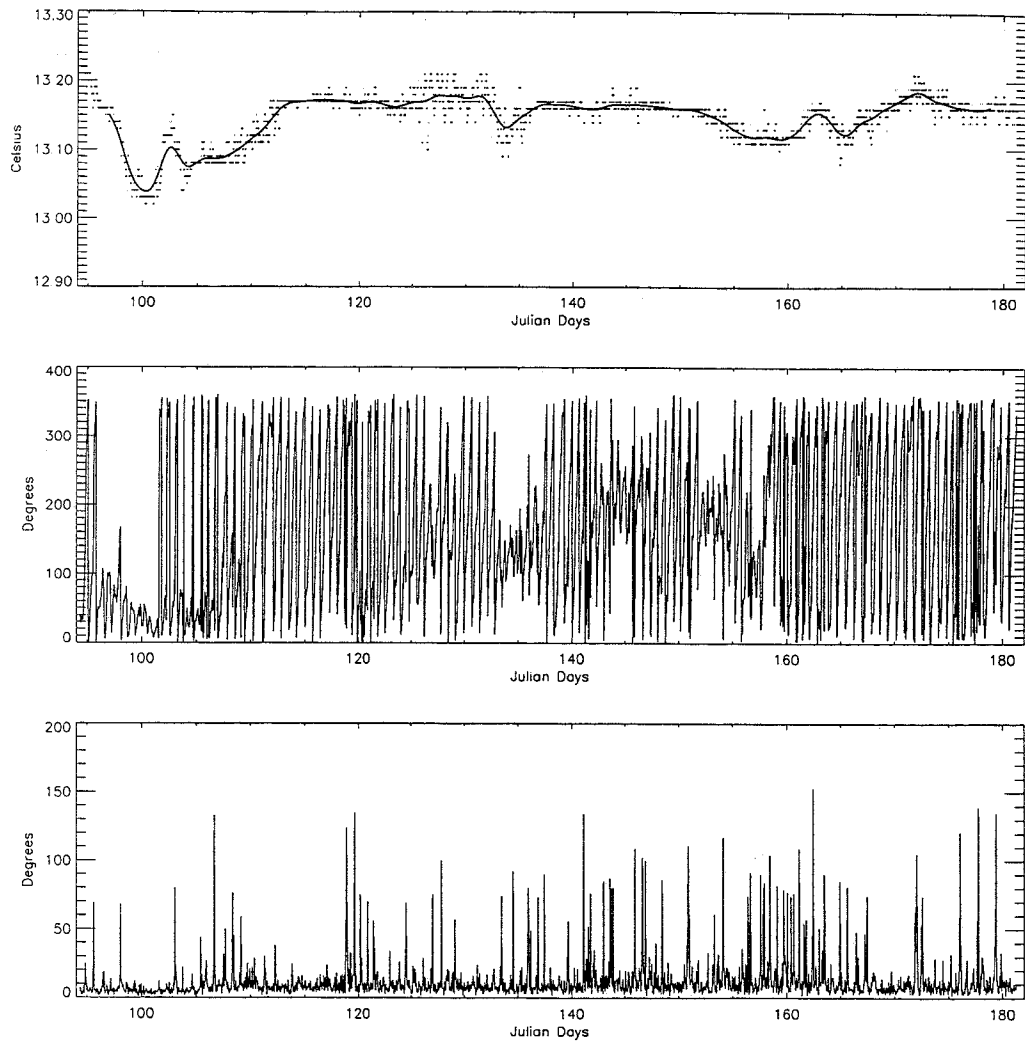


Figure 6.2.1: Temperature, Heading and Standard deviation of heading for Odon_2 data set

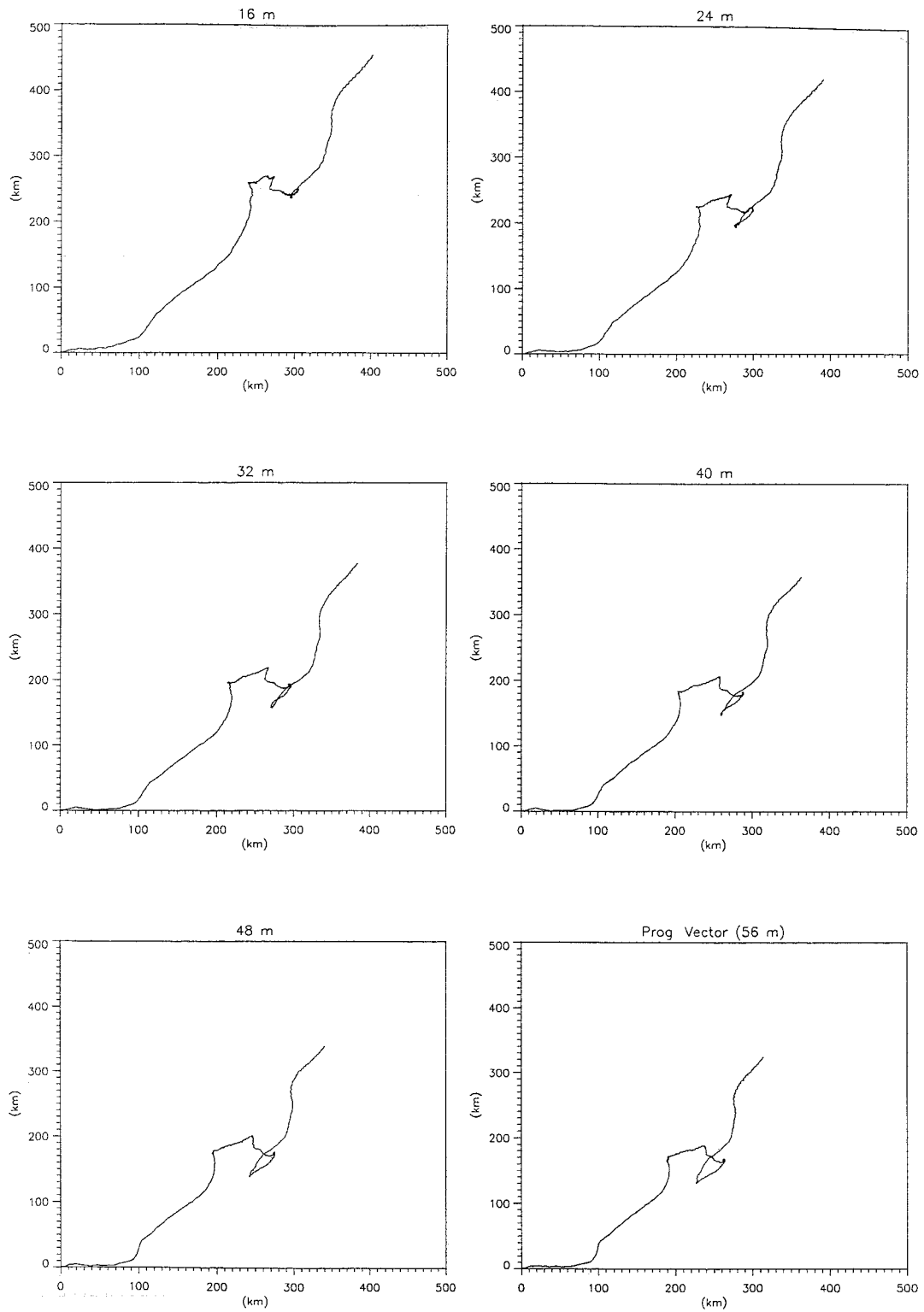


Figure 6.2.2: Progressive vectors plots at several depths recorded in Odon_2 data set. (Figs. 6.2.2-4)

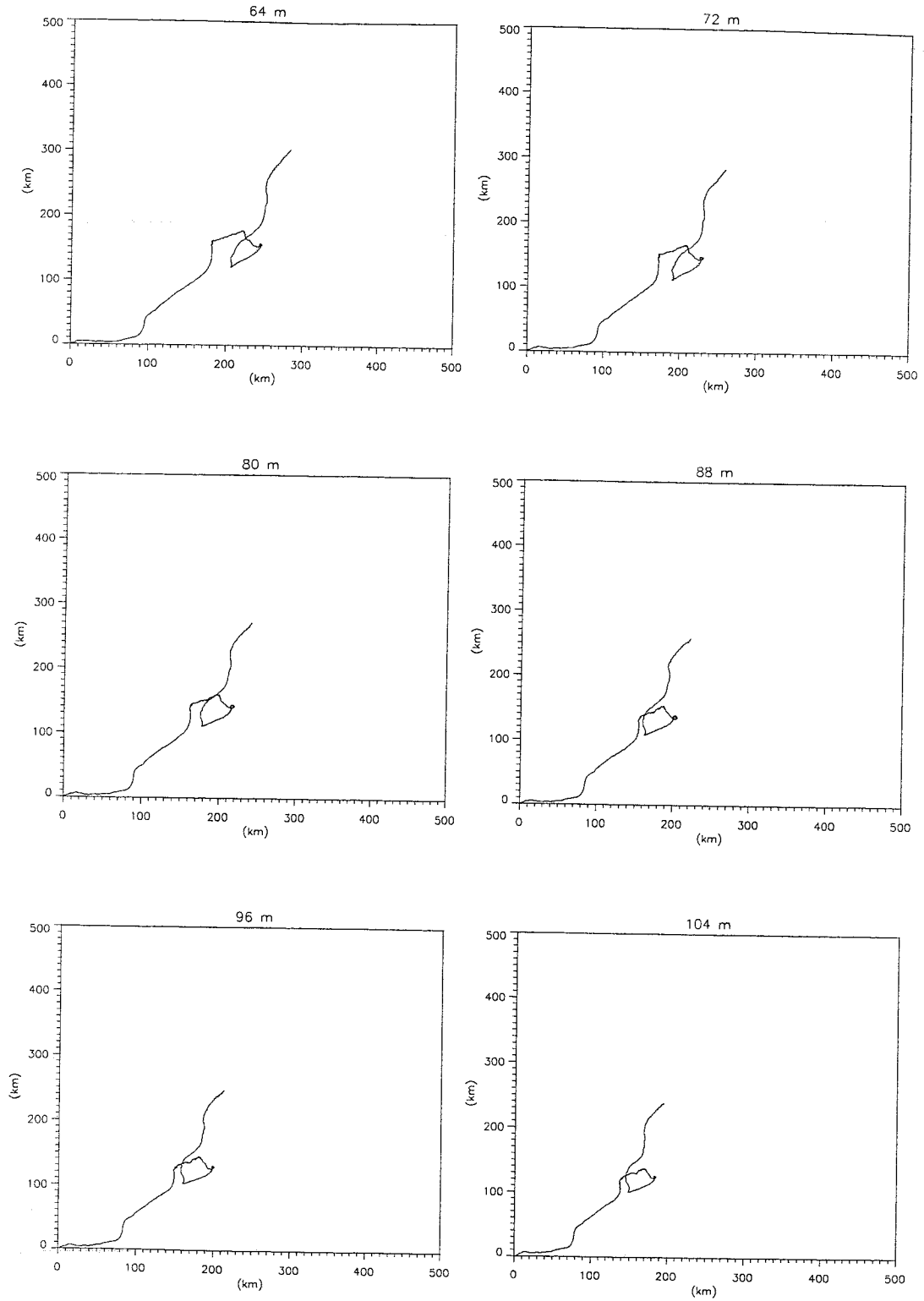


Fig.6.2.3: Odon_2: Progressive vectors (cont.)

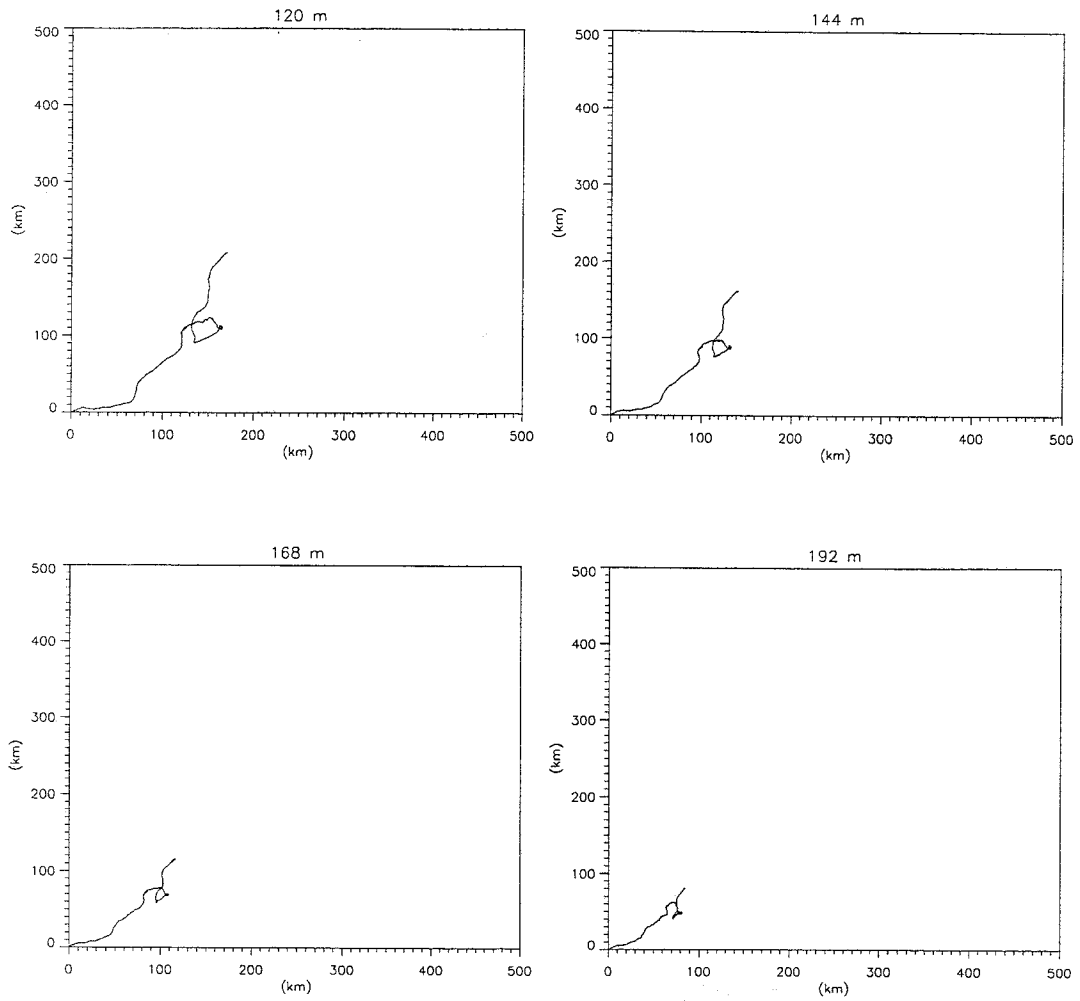


Fig.6.2.4: Odon_2. Progressive vectors (cont.)

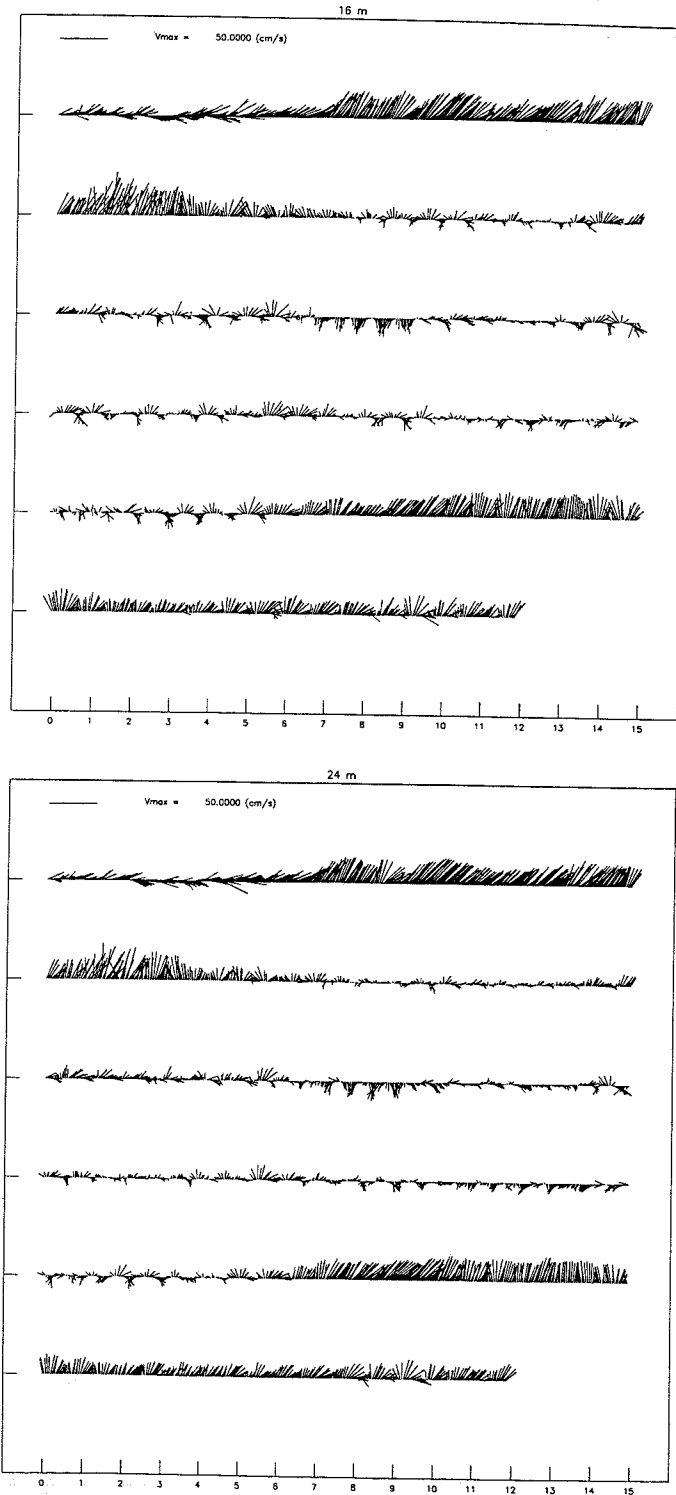


Figure 6.2.5: Stick plots at several depths recorded in Odon.2 data set. (Figs. 6.2.5-12)

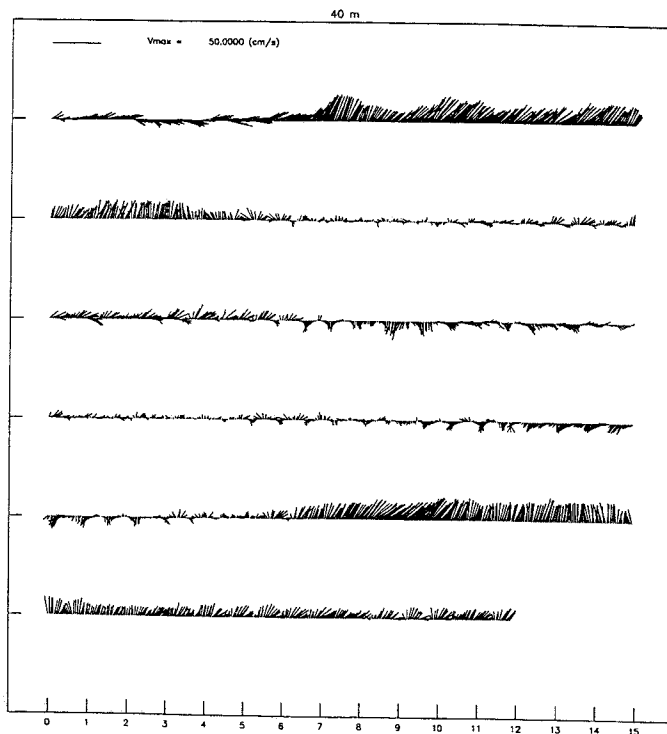
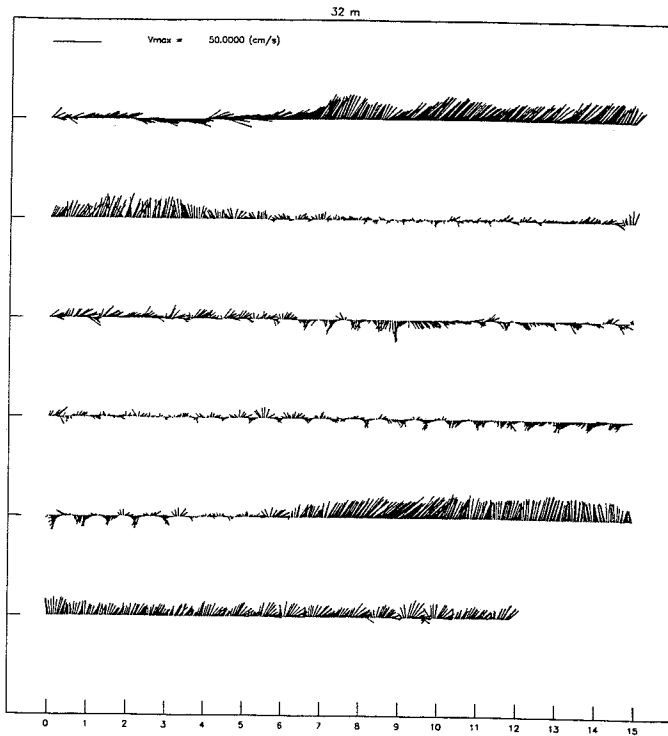


Fig.6.2.6: Odon_2. Stick plots (cont.)

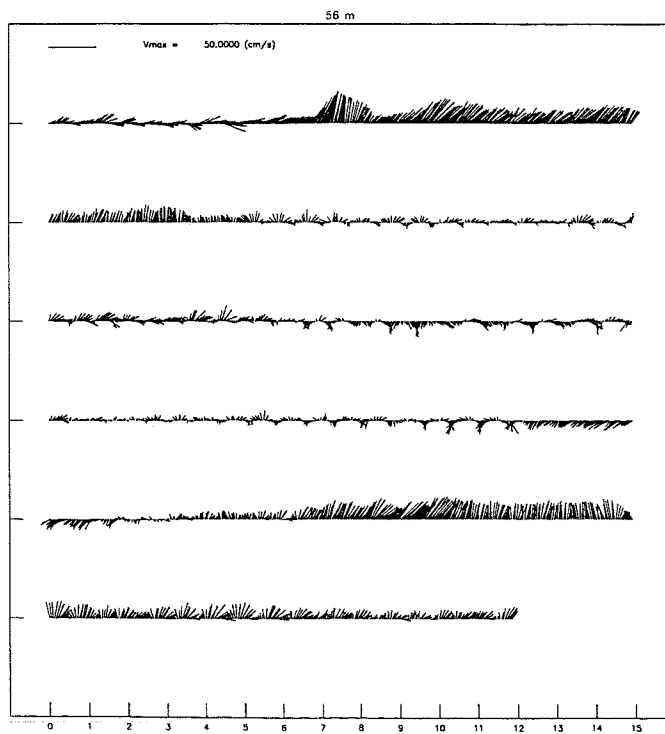
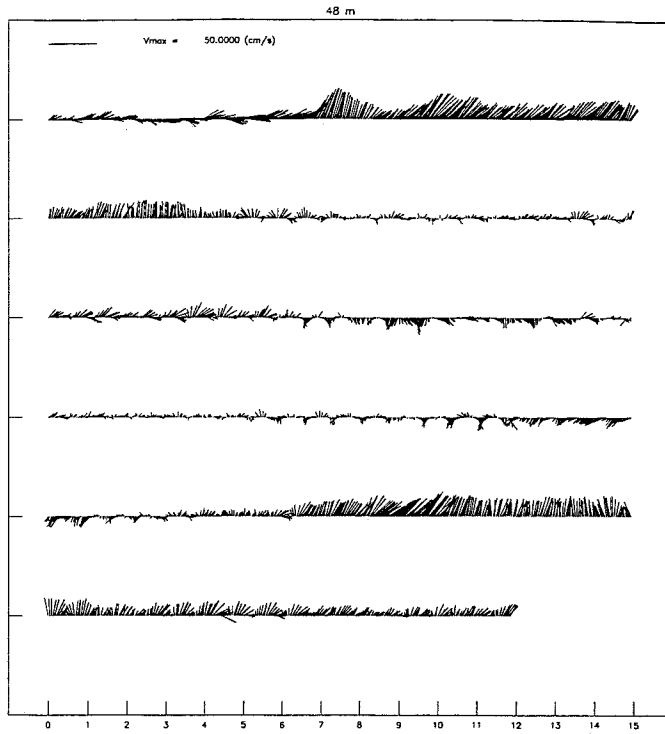


Fig.6.2.7: Odon_2. Stick plots (cont.)

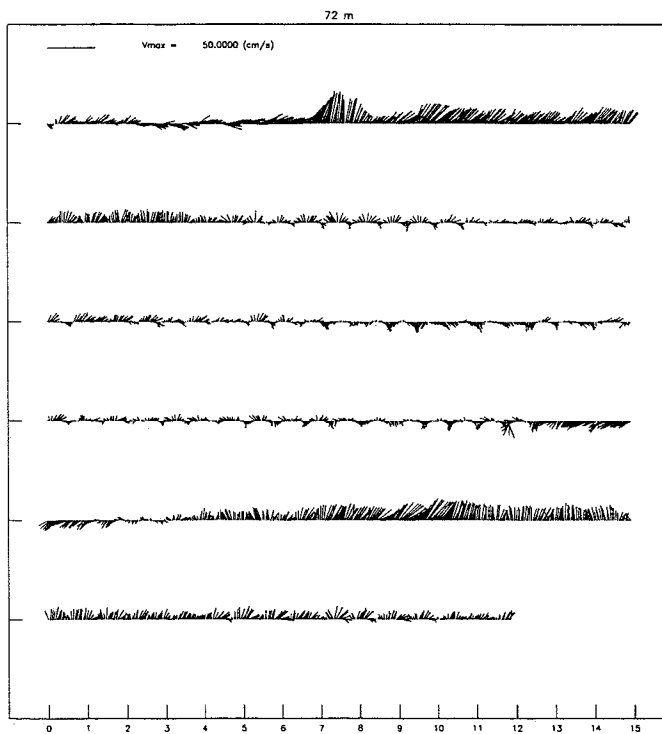
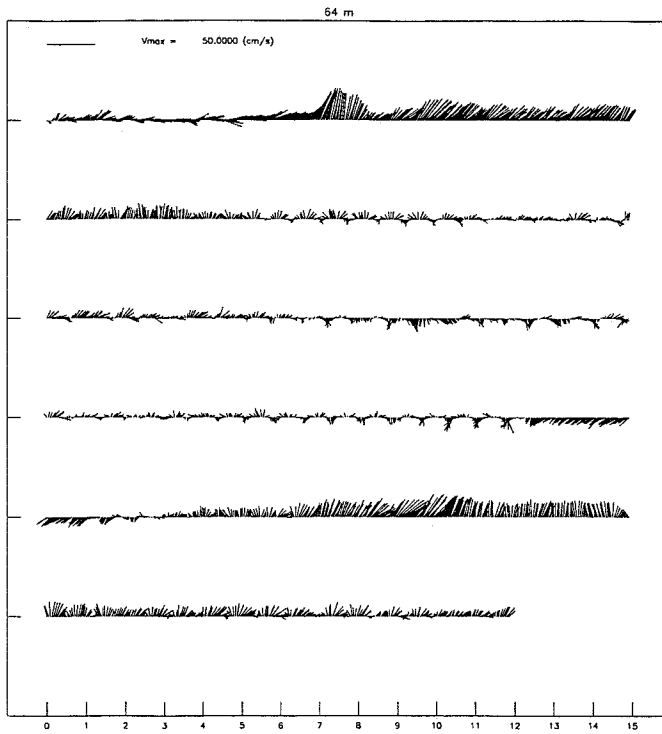


Fig.6.2.8: Odon_2. Stick plots (cont.)

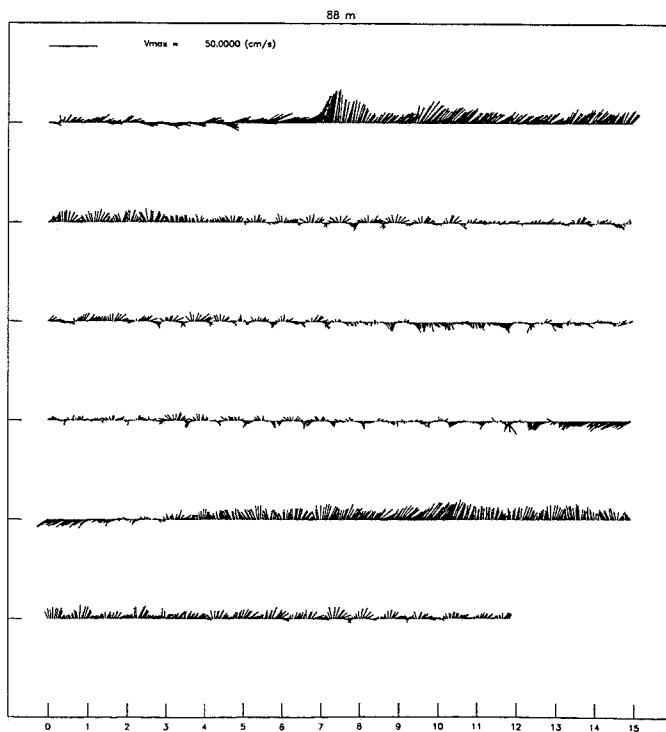
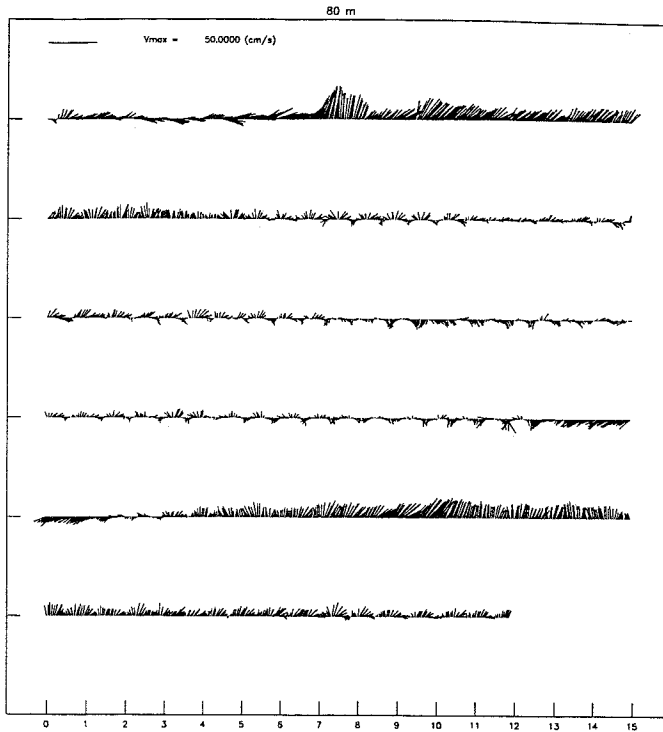


Fig.6.2.9: Odon.2. Stick plots (cont.)

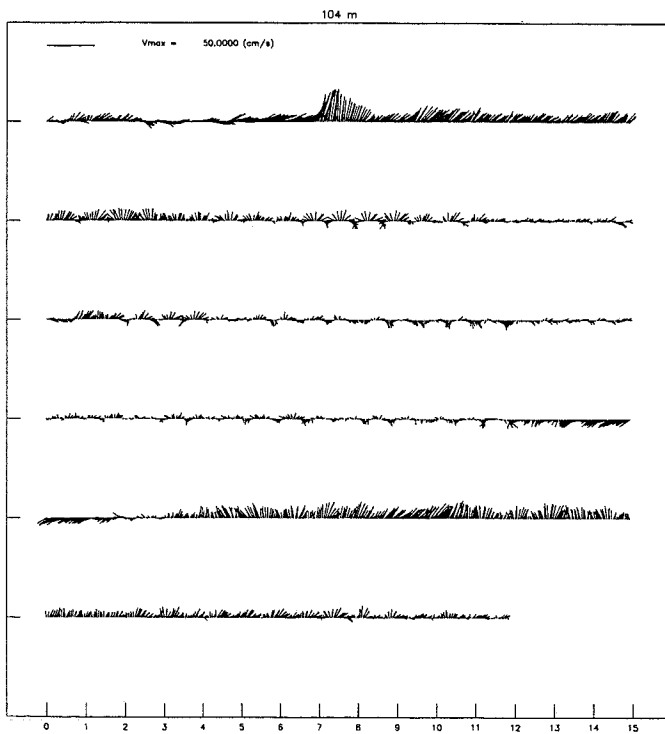
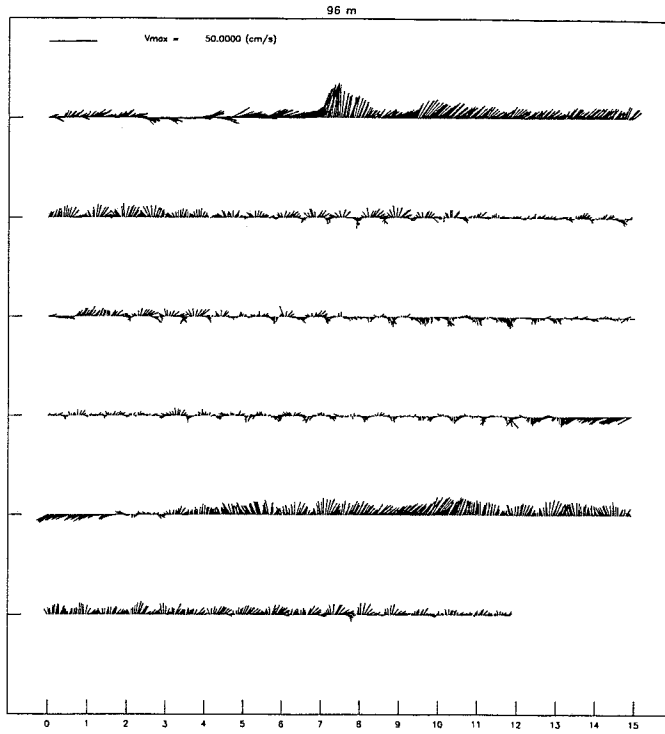


Fig.6.2.10: Odon_2. Stick plots (cont.)

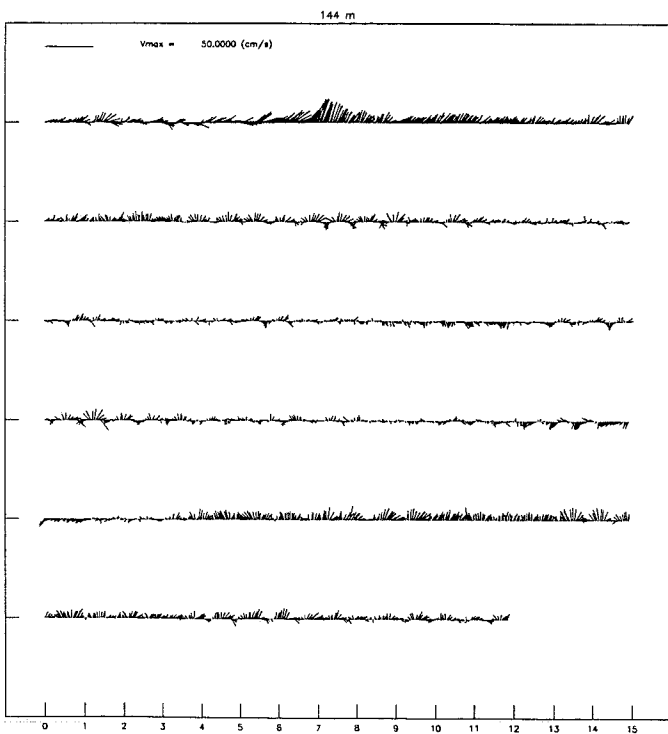
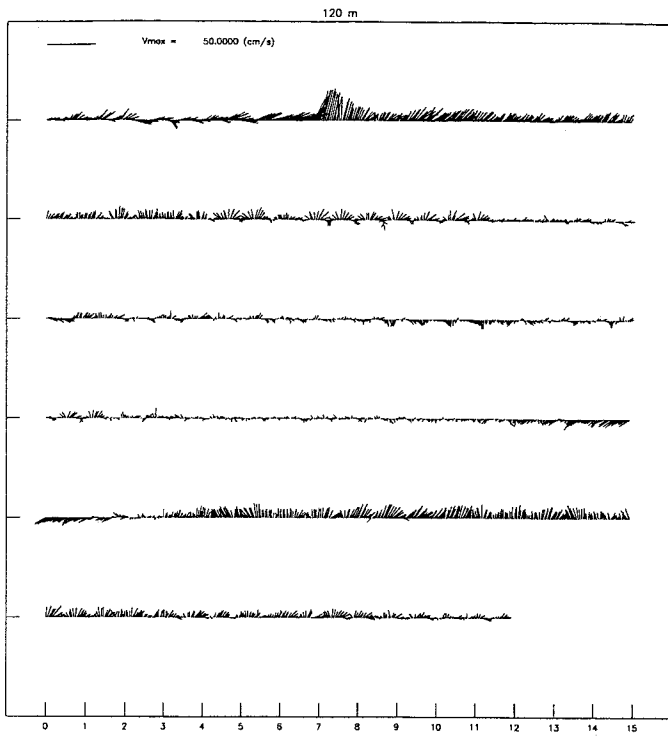


Fig.6.2.11: Odon_2. Stick plots (cont.)

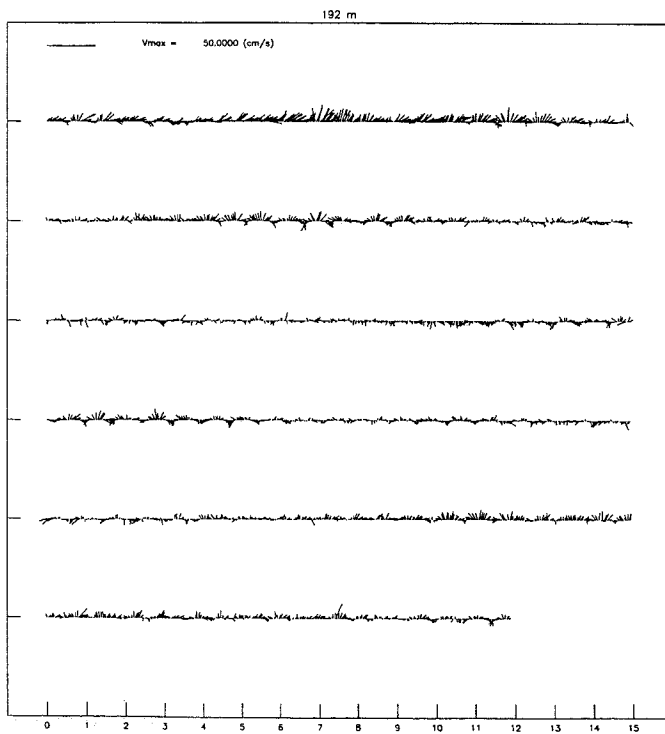
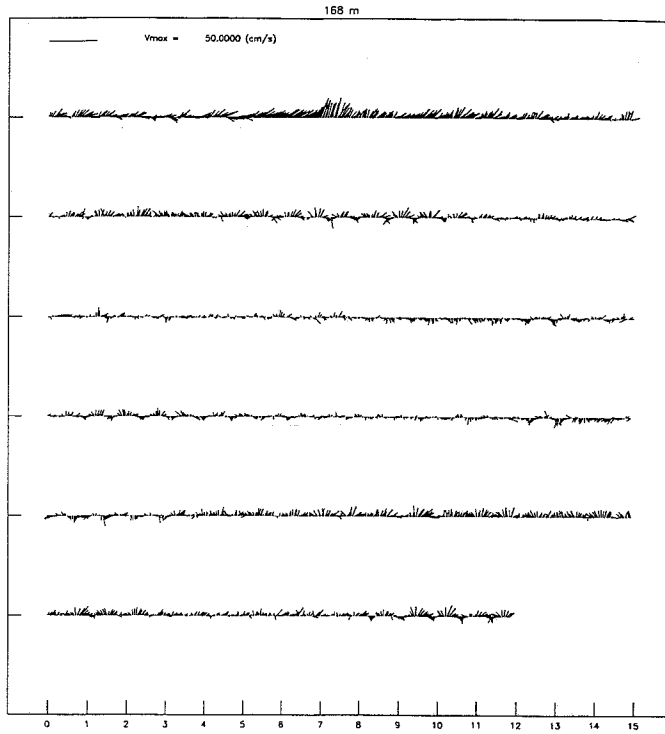


Fig.6.2.12: Odon_2. Stick plots (cont.)

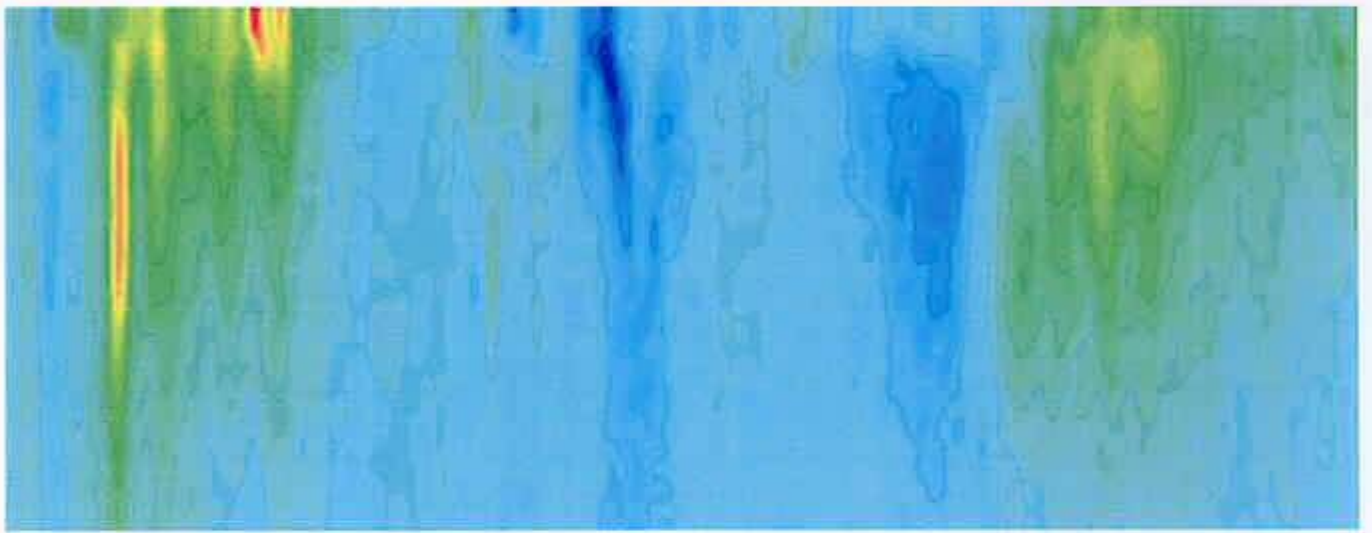
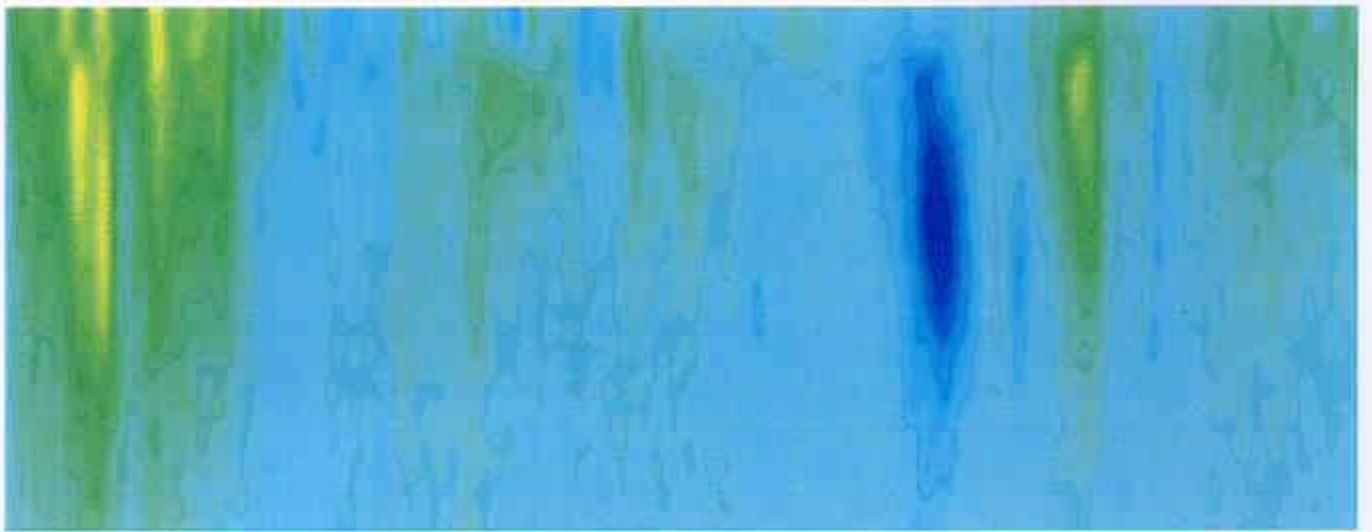


Figure 6.2.13: Filtered time series of U (upper) and V (lower) components in `Odon_2`. Time is Julian days and the color scale goes between -35.0 (blue tones) to 35.0 (red tones) cm/s.

6.3 Data Set: Odon_3

The series after deuration edge effects goes between

18:00:57 of 02/07/97 (record 32) to 11:00:57 of 29/09/97 (record 2161)

BIN	$ \vec{v} _{max}$	$\langle \vec{u} \rangle$	u_{max}	$\langle u \rangle$	σ_u	v_{max}	$\langle v \rangle$	σ_v
6	25.9	9.8	25.0	5.0	6.2	24.0	4.1	6.3
7	28.9	9.9	28.0	5.0	6.6	25.0	4.0	6.4
8	29.6	10.3	29.0	5.3	7.1	22.0	3.8	6.5
9	32.1	10.4	32.0	5.3	7.2	21.0	3.6	6.7
10	31.6	9.9	31.0	5.0	7.0	21.0	3.5	6.4
11	33.2	9.6	33.0	4.8	7.0	23.0	3.4	6.3
12	33.2	9.3	33.0	4.6	6.8	22.0	3.2	6.1
13	32.8	8.8	32.0	4.4	6.6	20.0	3.1	5.7
14	31.4	8.5	31.0	4.2	6.3	18.0	2.9	5.5
15	31.4	8.0	31.0	3.8	6.0	17.0	2.8	5.2
16	27.2	7.6	27.0	3.5	5.7	16.0	2.6	5.0
17	27.3	7.2	27.0	3.3	5.5	16.0	2.3	4.8
18	27.0	7.0	27.0	3.1	5.2	15.0	2.2	4.8
19	23.2	6.7	23.0	2.9	5.0	18.0	2.0	4.7
20	22.4	6.2	22.0	2.7	4.7	14.0	1.8	4.3
21	20.1	5.8	19.0	2.4	4.3	15.0	1.6	4.1
22	21.4	5.3	21.0	2.2	4.1	13.0	1.5	3.8
23	21.8	5.1	21.0	2.1	3.8	18.0	1.4	3.7
24	21.4	4.8	21.0	1.9	3.7	13.0	1.3	3.5
25	16.1	4.5	16.0	1.8	3.4	14.0	1.2	3.4
26	14.3	4.3	14.0	1.5	3.2	12.0	1.1	3.3
27	14.1	4.1	14.0	1.4	3.1	11.0	1.0	3.1
28	11.7	3.9	11.0	1.3	3.0	10.0	1.0	3.0
29	12.4	3.8	12.0	1.2	2.8	11.0	0.9	2.9
30	12.2	3.6	12.0	1.2	2.7	10.0	0.8	2.9
31	11.2	3.5	10.0	1.1	2.6	11.0	0.8	2.8
32	11.2	3.5	11.0	1.0	2.6	10.0	0.6	2.8

Table 6.3.3: Statistics of Odon_3 data set

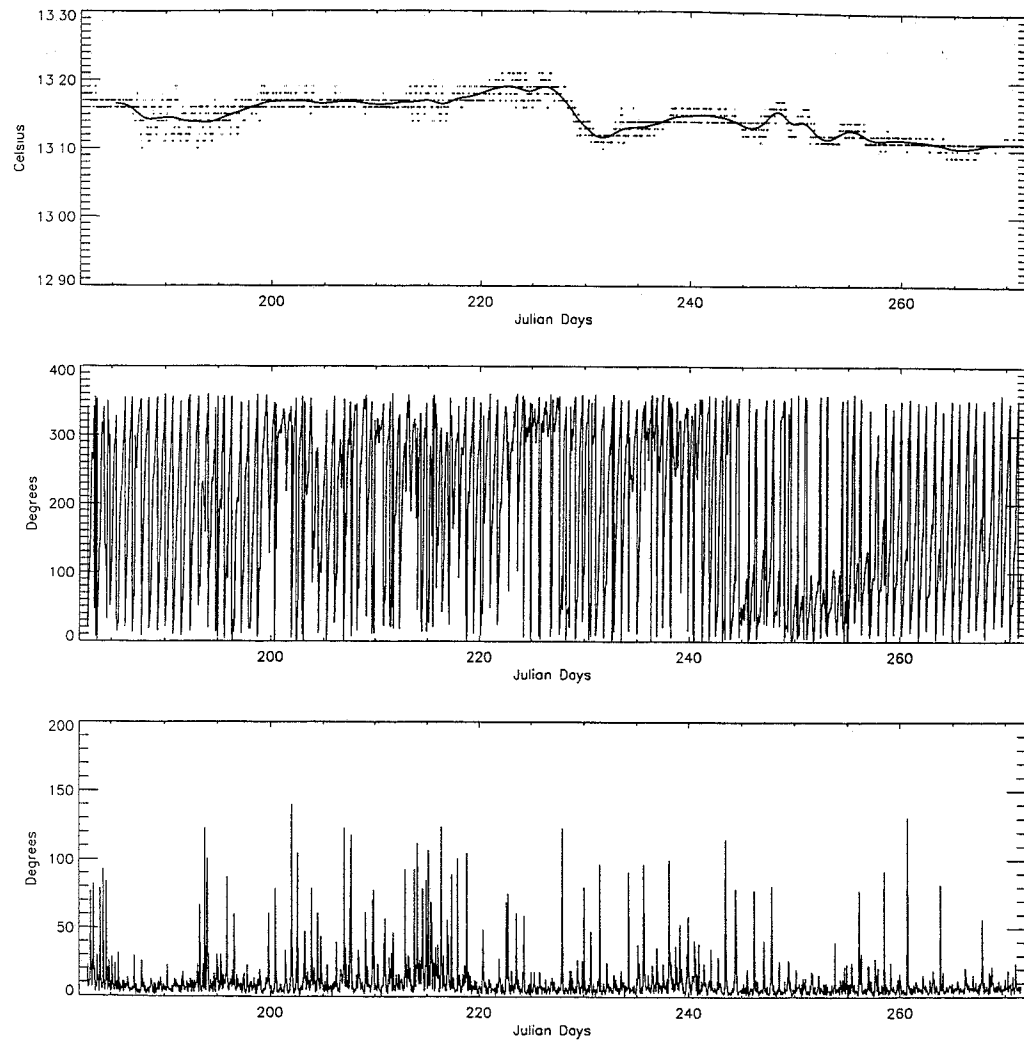


Figure 6.3.1: Temperature, Heading and Standard deviation of heading for Odon_3 data set

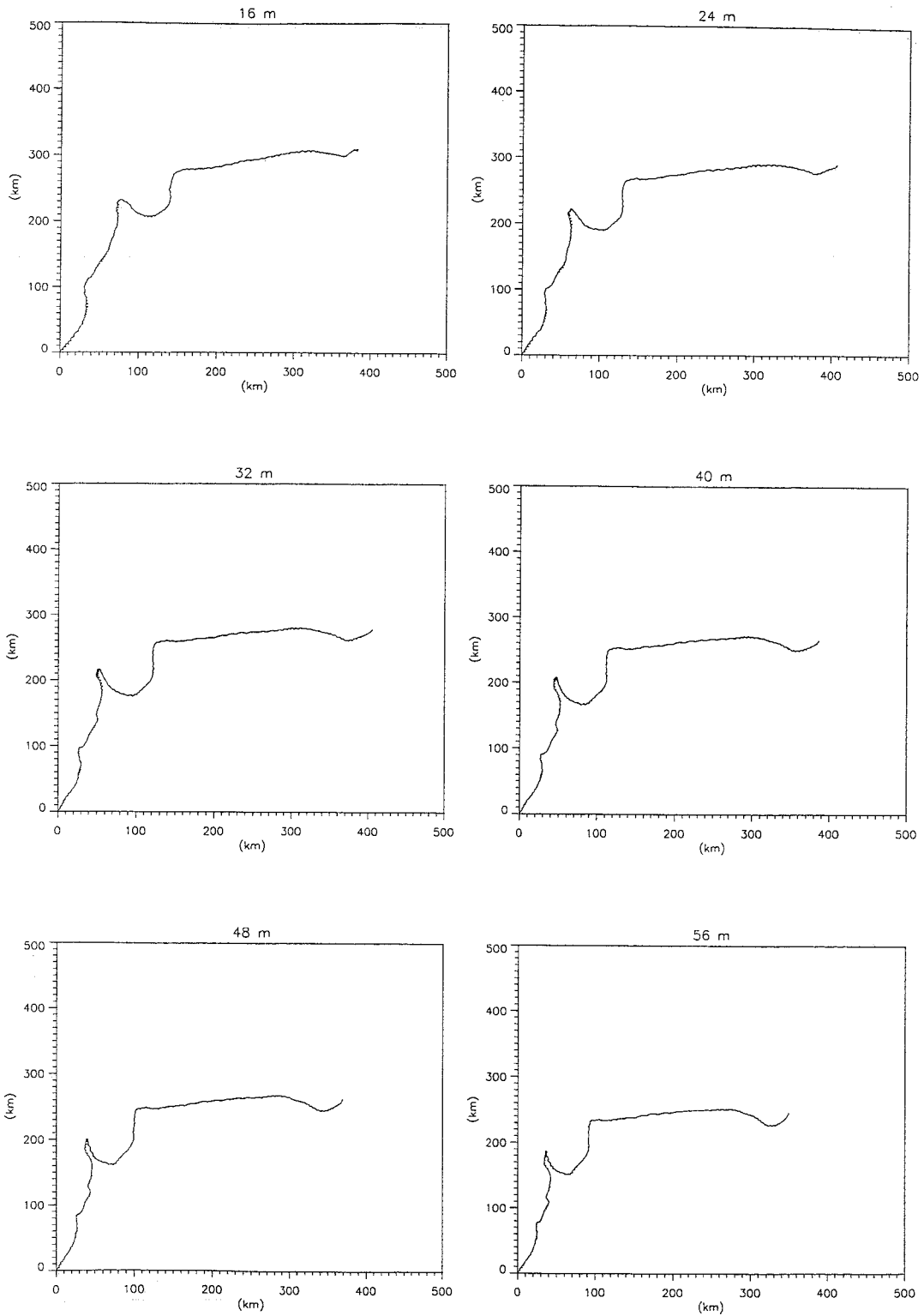


Figure 6.3.2: Progressive vectors plots at several depths recorded in Odon_3 data set. (Figs. 6.3.2-4)

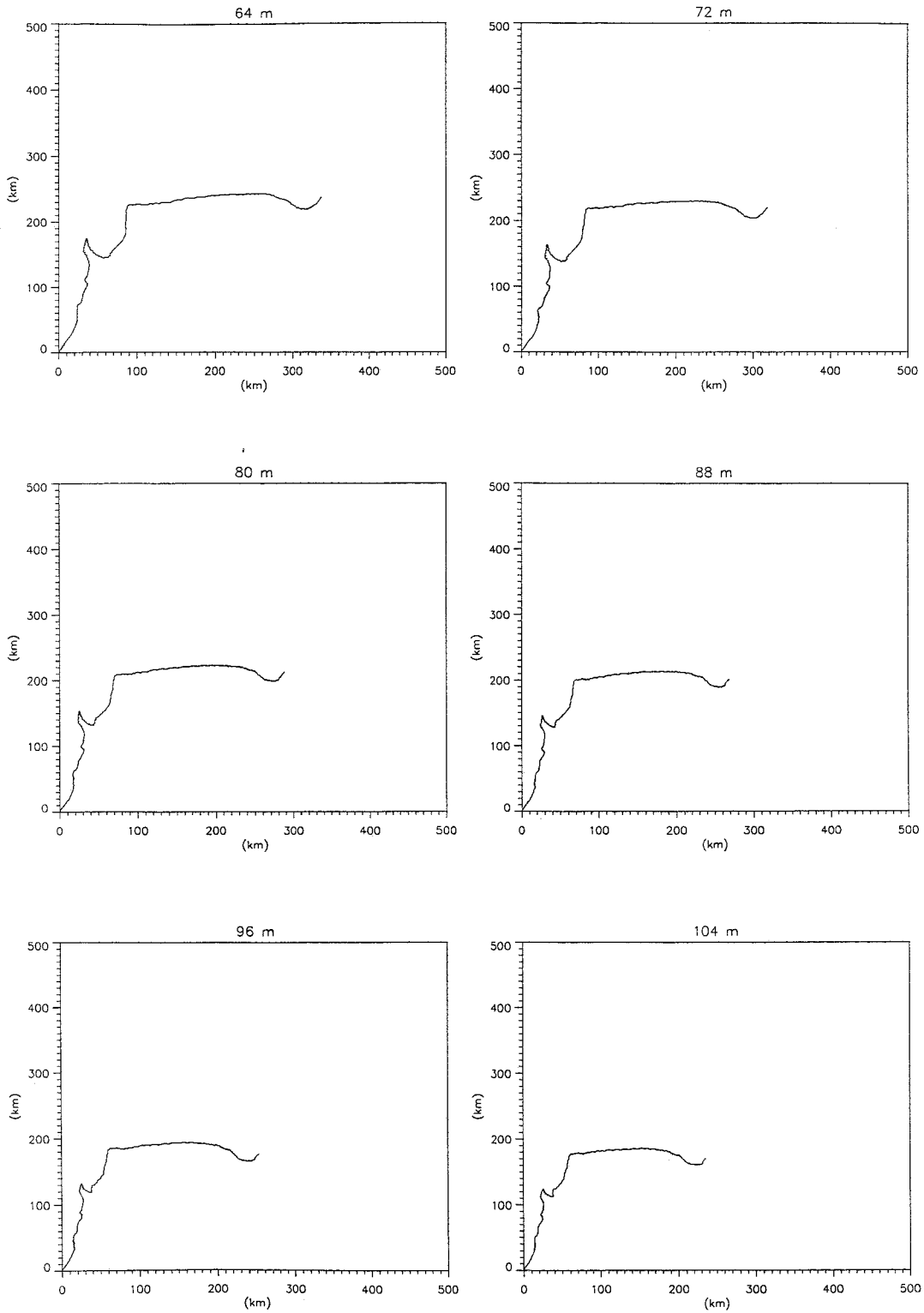


Fig.6.3.3: Odon_3. Progressive vectors (cont.)

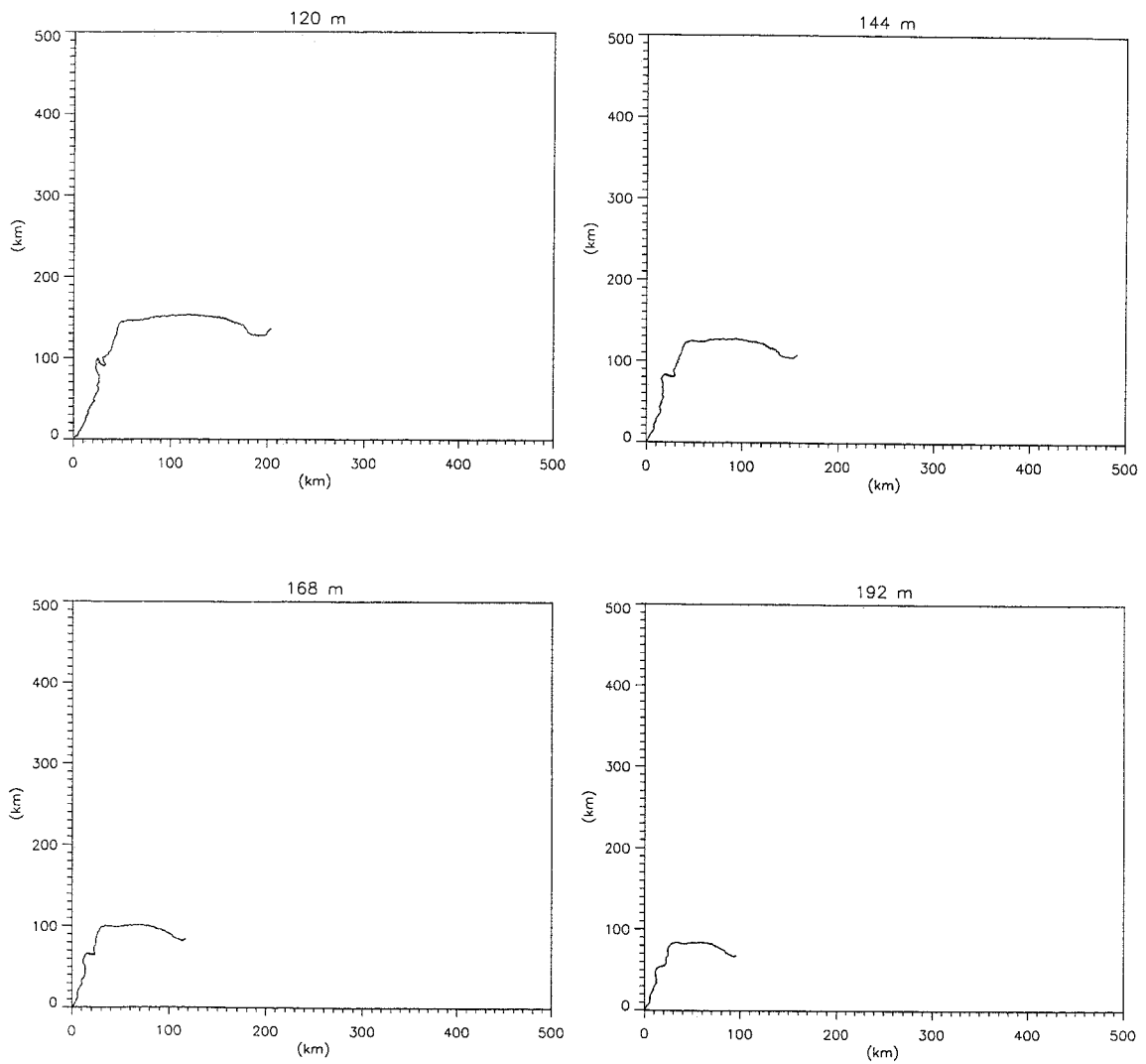


Fig.6.3.4: Odon_3. Progressive vectors (cont.)

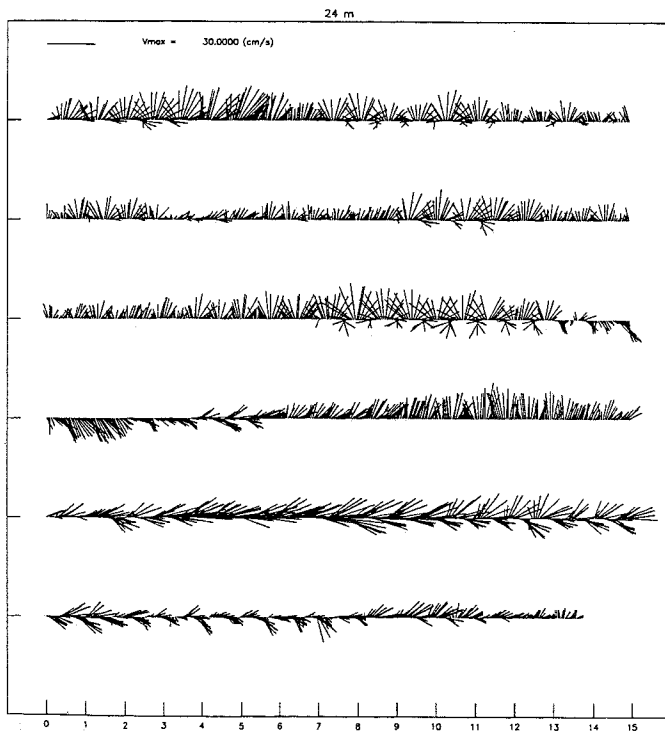
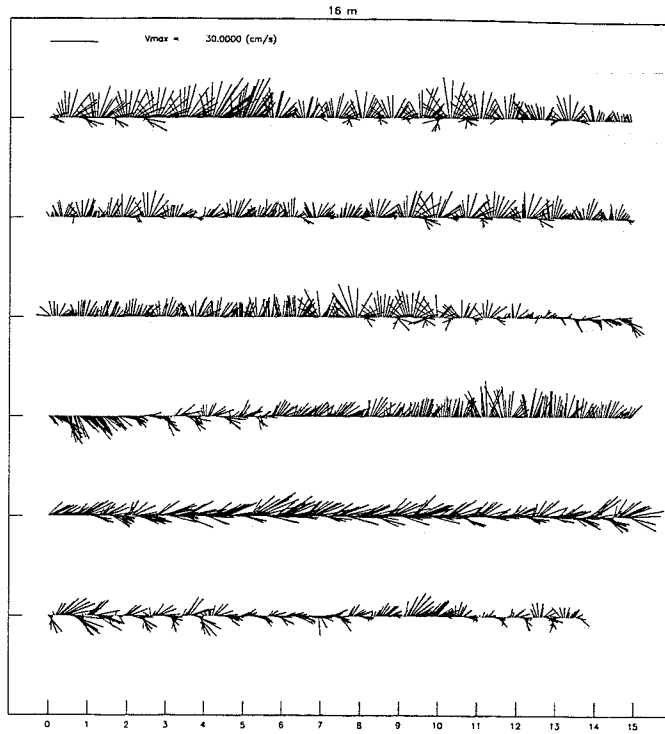


Figure 6.3.5: Stick plots at several depths recorded in Odon_3 data set. (Figs. 6.3.5-12)

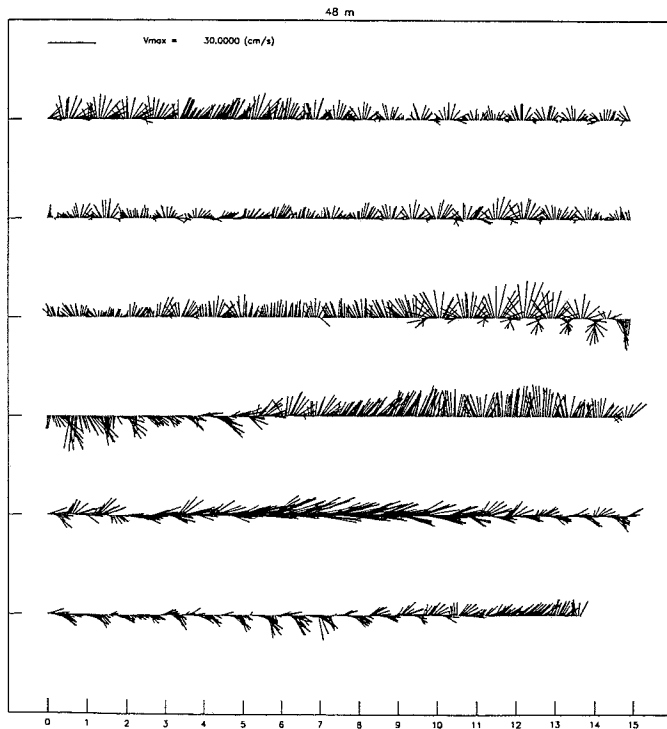
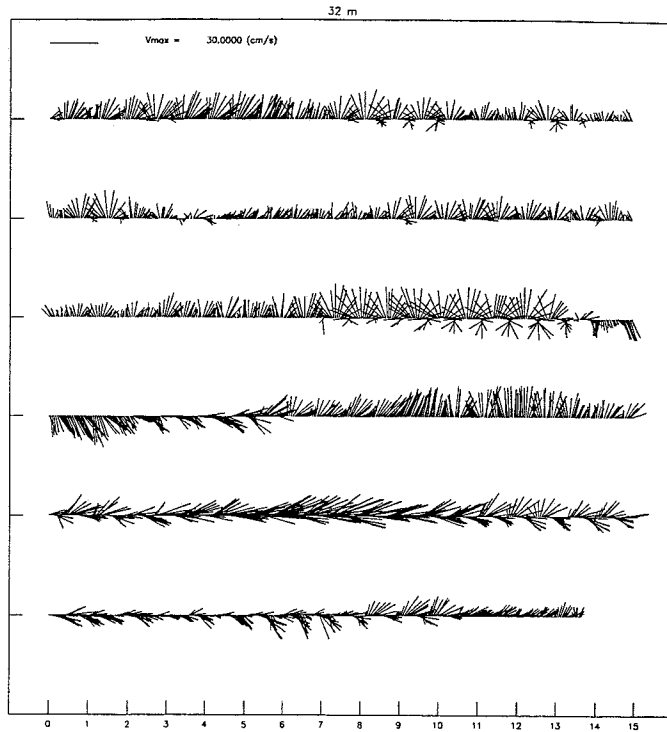


Fig.6.3.6: Odon_3: Stick plots (cont.)

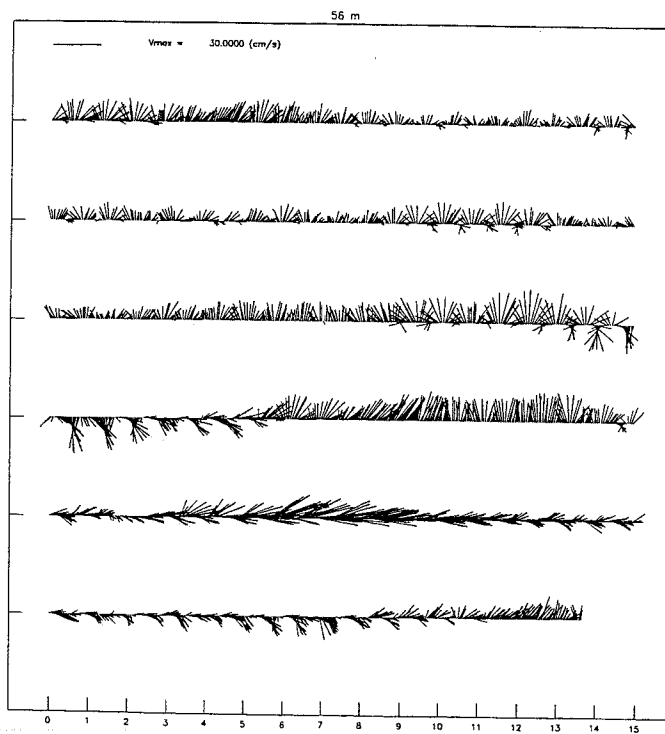
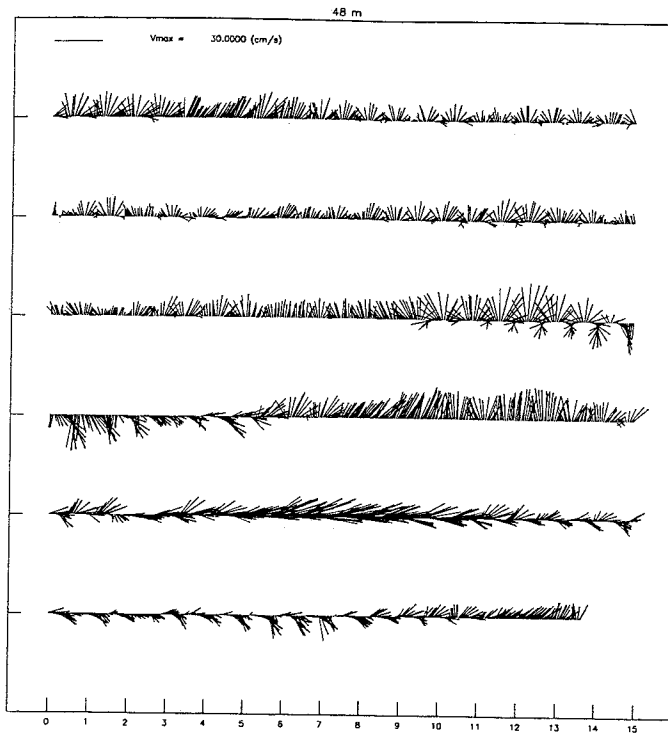


Fig.6.3.7: Odon_3: Stick plots (cont.)

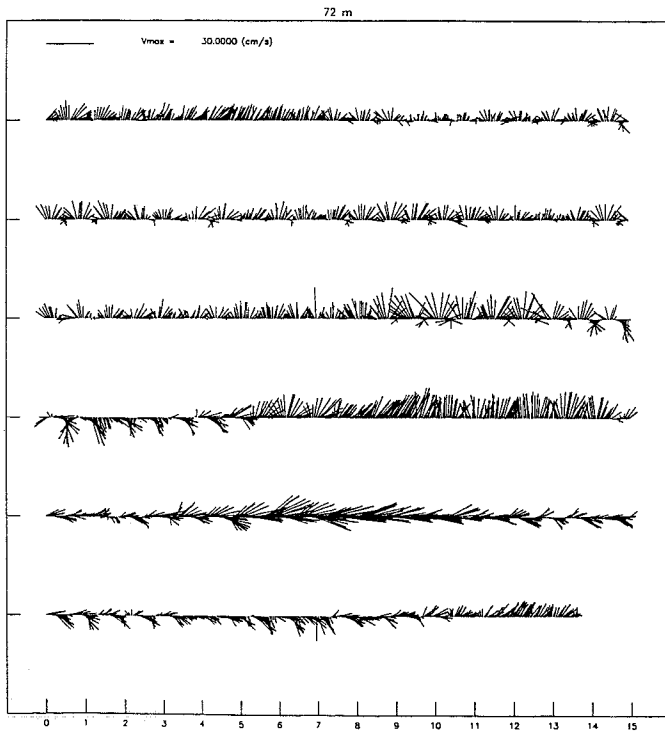
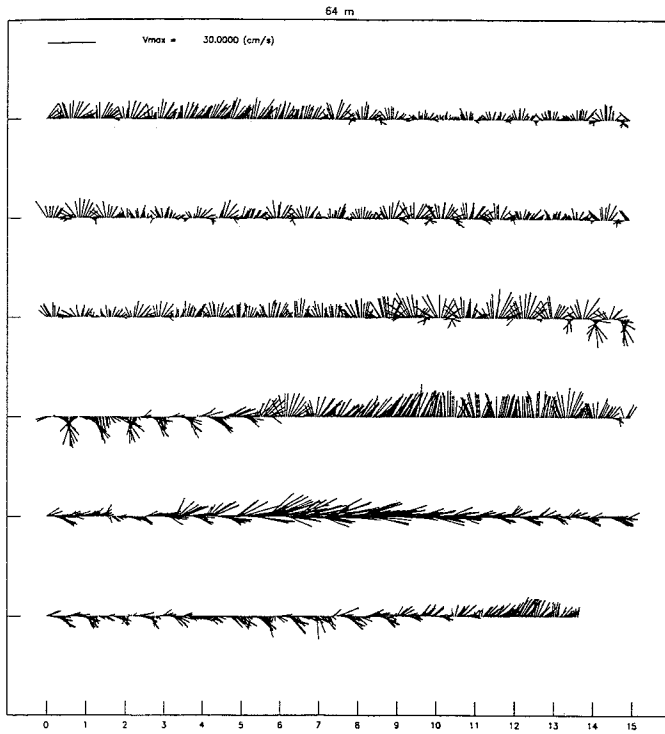


Fig.6.3.8: Odon_3: Stick plots (cont.)

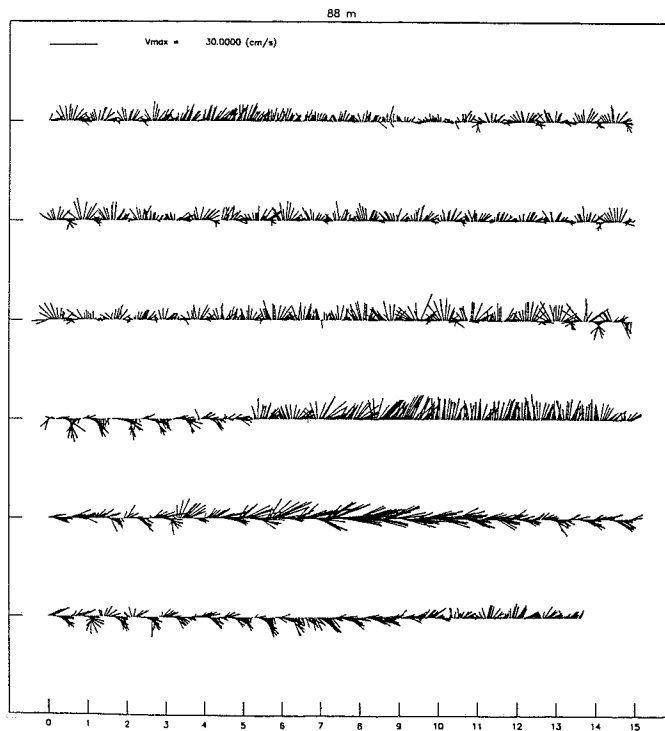
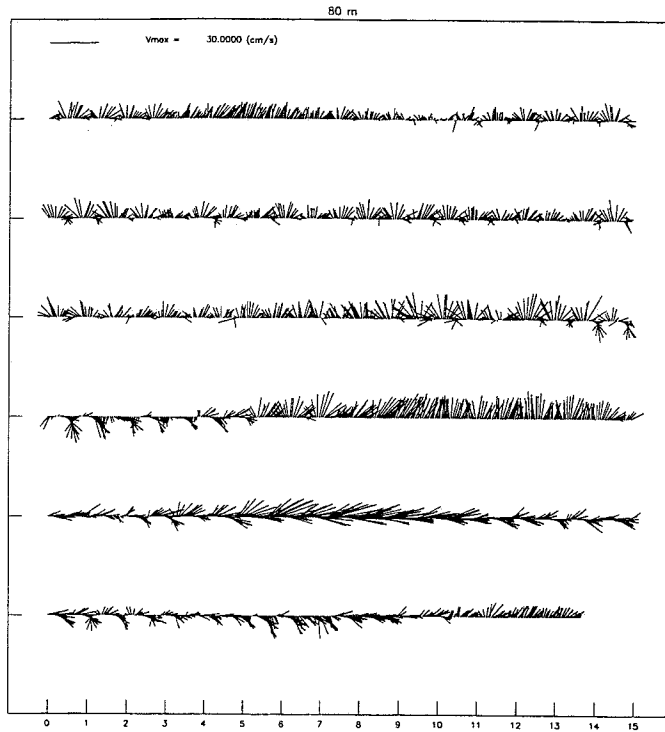


Fig.6.3.9: Odon_3: Stick plots (cont.)

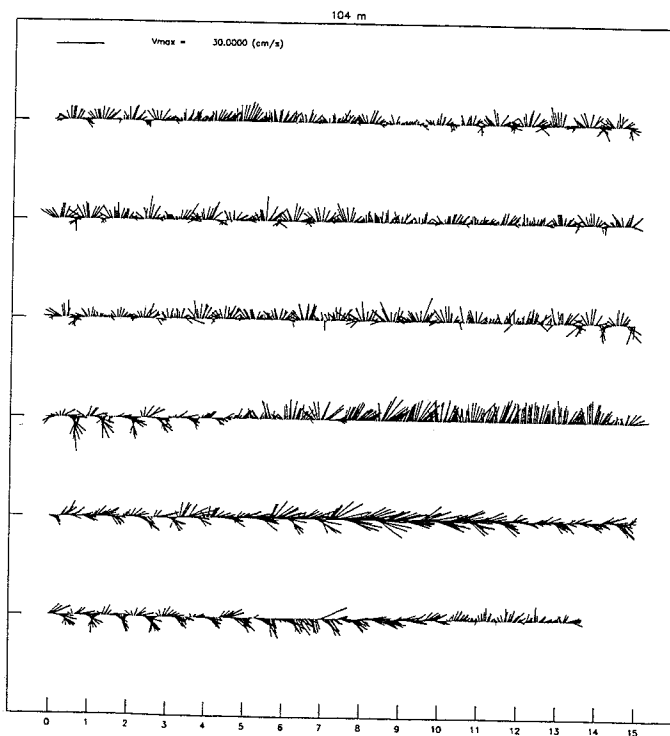
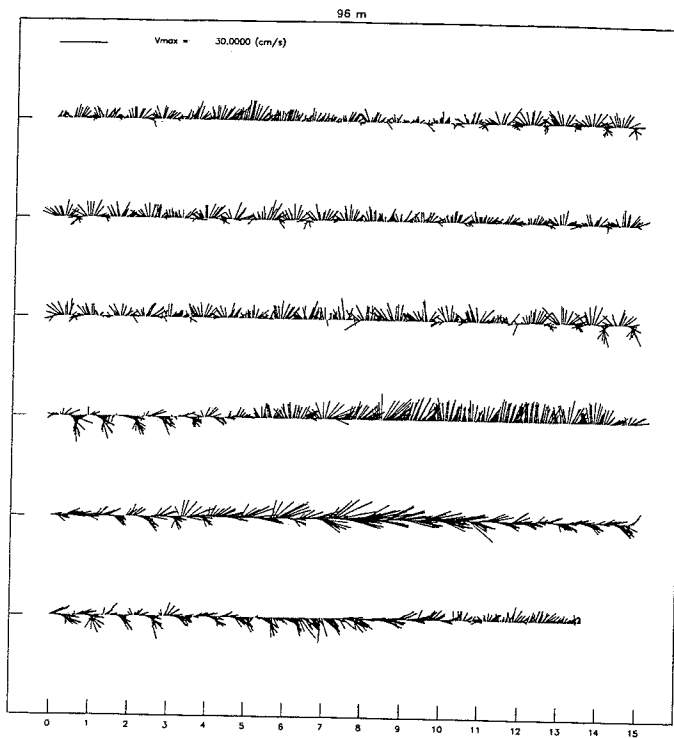


Fig.6.3.10: Odon_3: Stick plots (cont.)

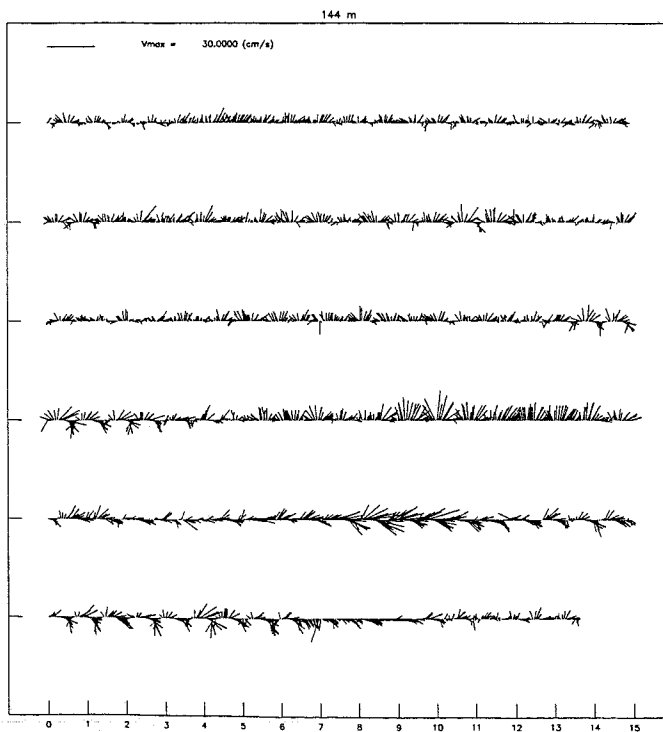
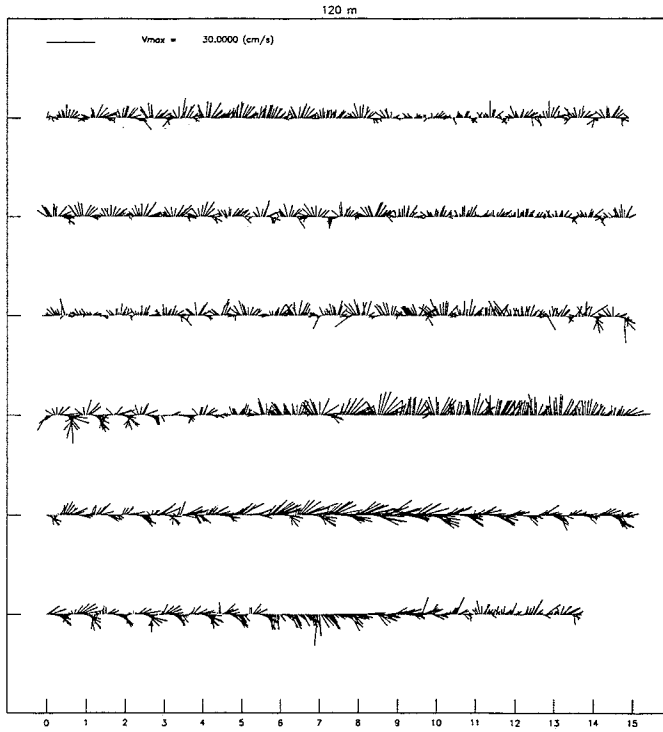


Fig.6.3.11: Odon_3: Stick plots (cont.)

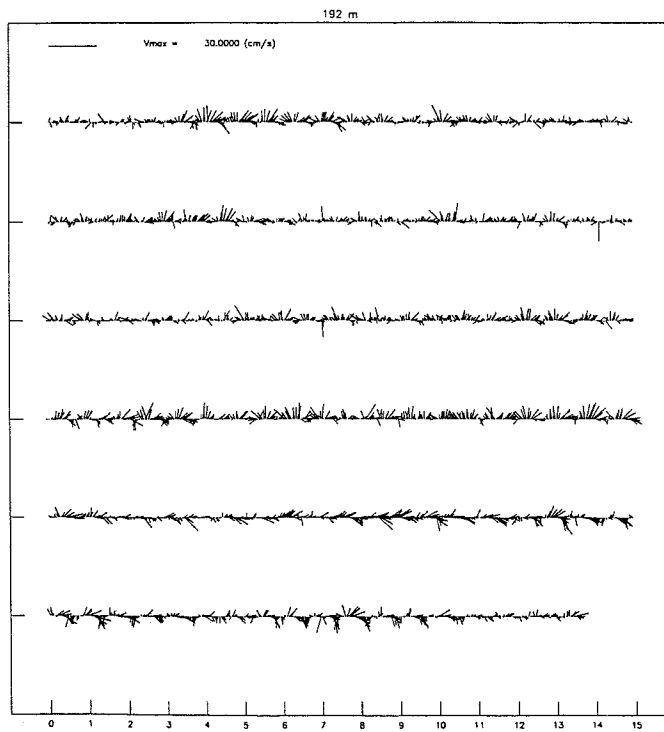
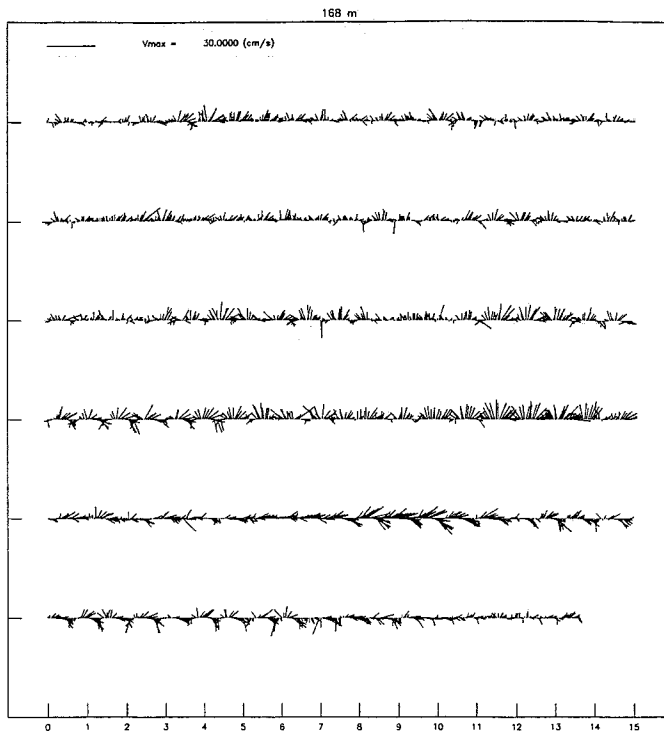


Fig.6.3.12: Odon_3: Stick plots (cont.)

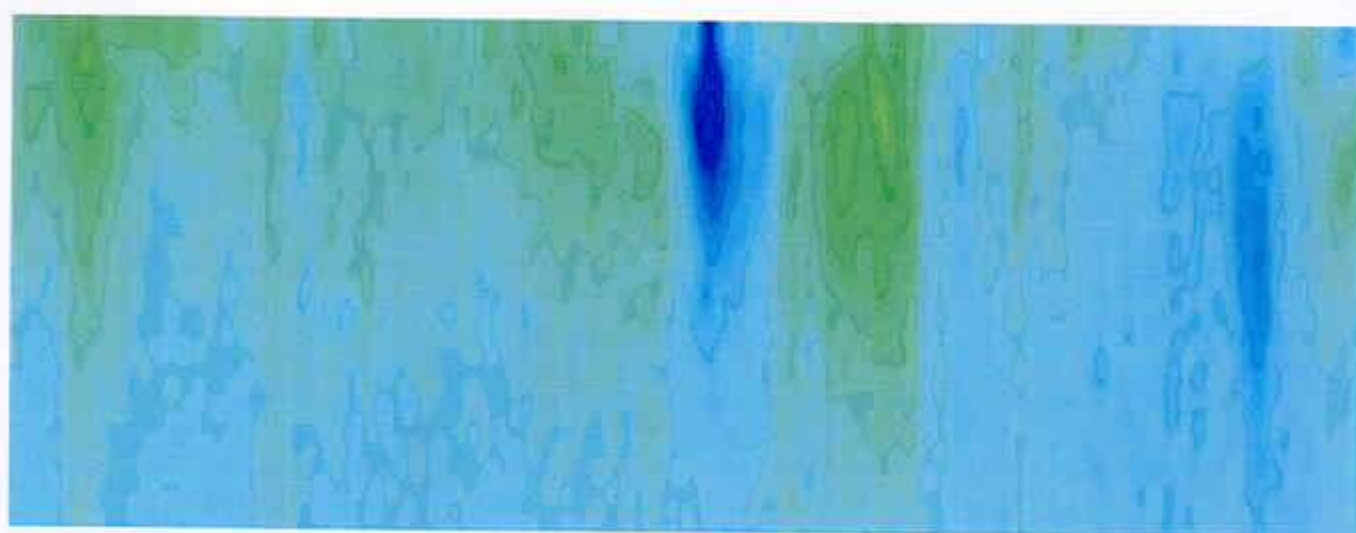


Figure 6.3.13: Filtered time series of U (upper) and V (lower) components in Odon_3. Time is julian days and the color scale goes between -35.0 (blue tones) to 35.0 (red tones) cm/s.

6.4 Data Set: Odon_4

For this deployment, good data were obtained during the period

14:15:21 of 08/10/97 (record 144) to 15:15:21 of 28/01/98 (record 2833)

These are the beginning and end records that correspond to scalar data as Temperature, heading, etc., while the pulished data file for vector data has been cut at record 1440 wich corresponds to 14:15:21 of 01/12/97. Throughout this section the bin-depth relationship (see section 5.1) is slightly modified (see an explanation in the footnote of section 5.2).

BIN	$ \vec{v} _{max}$	$\langle \vec{v} \rangle$	u_{max}	$\langle u \rangle$	σ_u	v_{max}	$\langle v \rangle$	σ_v
6	61.4	15.5	57.0	9.1	8.8	58.0	3.6	11.8
7	45.7	14.5	33.0	8.8	8.1	45.0	3.8	10.2
8	30.8	12.4	27.0	7.8	7.2	26.0	3.5	8.3
9	35.2	12.4	27.0	7.0	7.6	30.0	2.9	8.6
10	37.9	12.6	31.0	6.3	8.3	36.0	2.4	9.2
11	37.3	11.7	30.0	5.8	7.8	37.0	1.9	8.7
12	46.5	10.6	26.0	5.3	7.1	46.0	1.8	8.1
13	34.9	10.0	25.0	4.8	6.9	34.0	1.8	7.5
14	30.5	9.7	26.1	4.3	7.0	24.0	1.6	7.2
15	30.1	9.3	30.0	3.9	6.7	26.0	1.6	6.9
16	23.9	9.0	23.0	3.7	6.4	22.0	1.5	6.7
17	25.1	8.7	23.0	3.3	6.2	25.0	1.4	6.6
18	27.8	8.6	24.0	3.1	6.3	22.0	1.5	6.5
19	26.7	8.3	26.0	2.9	5.9	23.0	1.3	6.4
20	21.1	7.6	20.0	2.6	5.5	19.0	1.2	5.9
21	22.2	7.0	19.0	2.4	5.1	16.0	1.1	5.4
22	19.8	6.4	15.0	2.1	4.7	14.0	0.9	5.0
23	17.9	5.9	14.0	1.8	4.3	16.0	0.6	4.7
24	17.7	5.6	13.0	1.6	4.1	16.0	0.5	4.5
25	16.3	5.3	12.0	1.5	3.9	14.0	0.5	4.2
26	14.9	4.9	12.0	1.4	3.7	13.0	0.5	3.9
27	13.6	4.7	12.0	1.2	3.5	12.0	0.4	3.8
28	13.3	4.7	12.0	1.1	3.5	13.0	0.3	3.8
29	14.9	4.7	13.0	1.1	3.6	13.0	0.3	3.8
30	14.0	4.7	10.0	1.0	3.6	14.0	0.2	3.8
31	12.6	4.5	11.0	1.0	3.4	12.0	0.3	3.7
32	15.0	4.3	11.0	0.9	3.3	12.0	0.2	3.6

Table 6.4.4: Statistics of Odon_4 data set

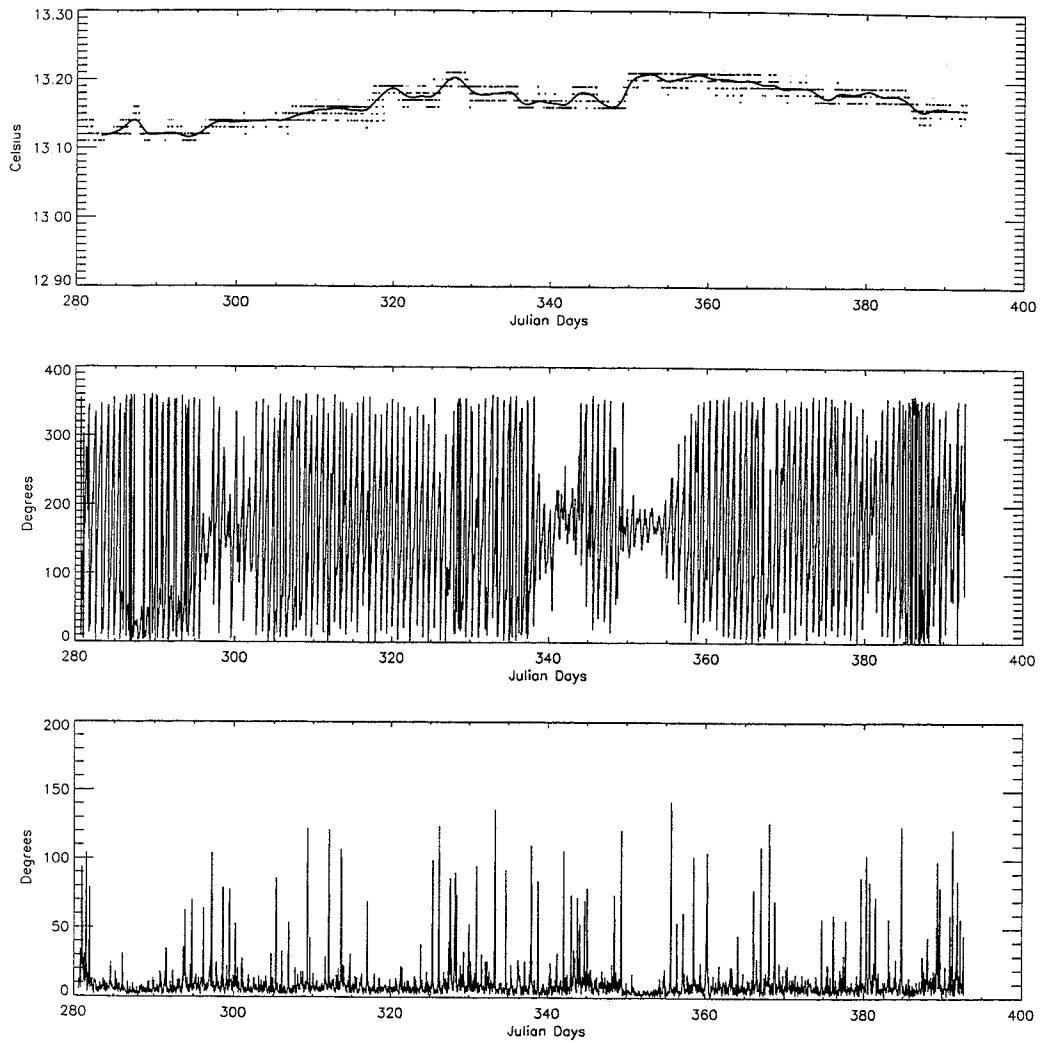


Figure 6.4.1: Temperature, Heading and Standard deviation of heading for Odon_4 data set.

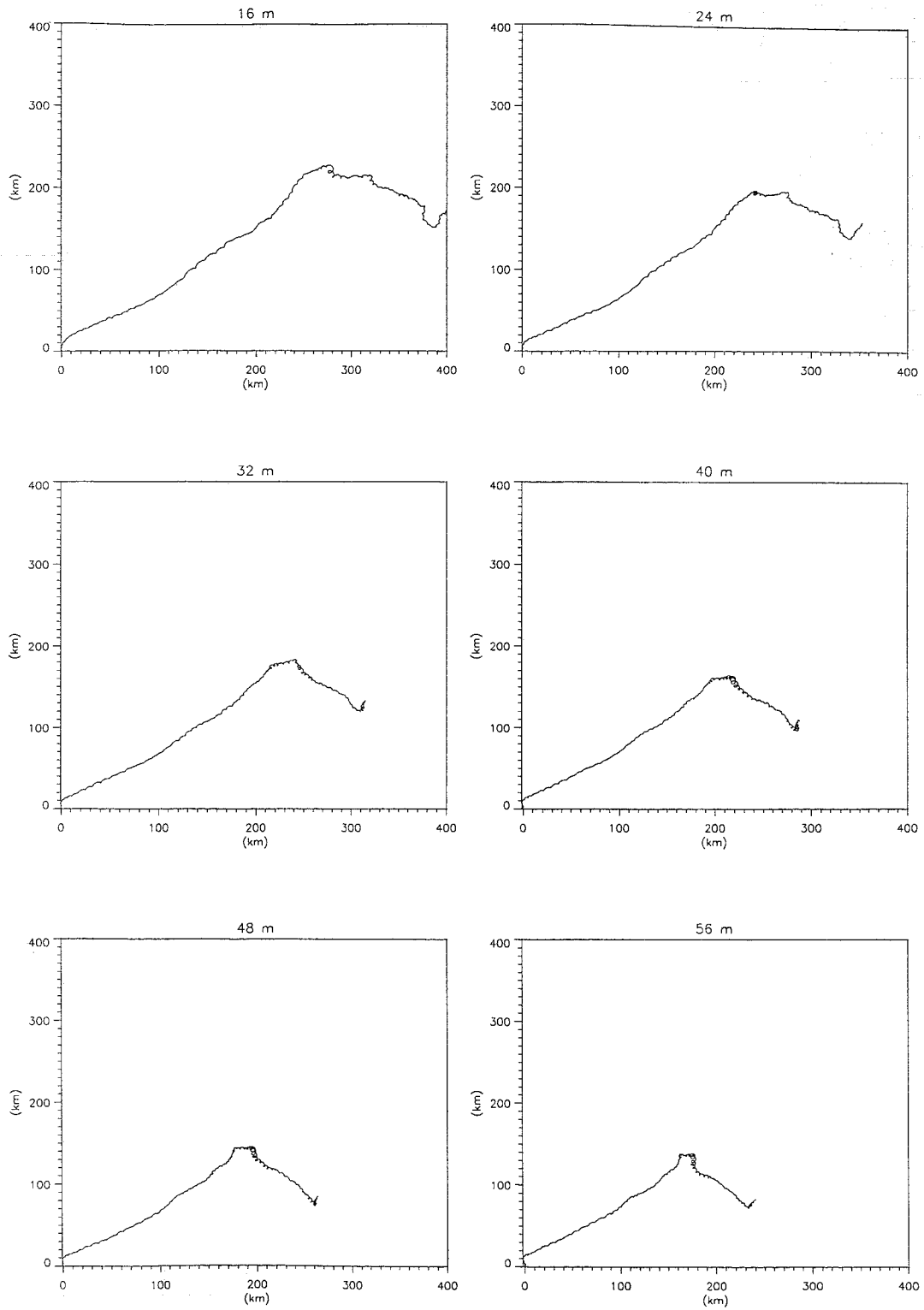


Figure 6.4.2: Progressive vectors plots at several depths recorded in Odon_4 data set. (Figs. 6.4.2-4)

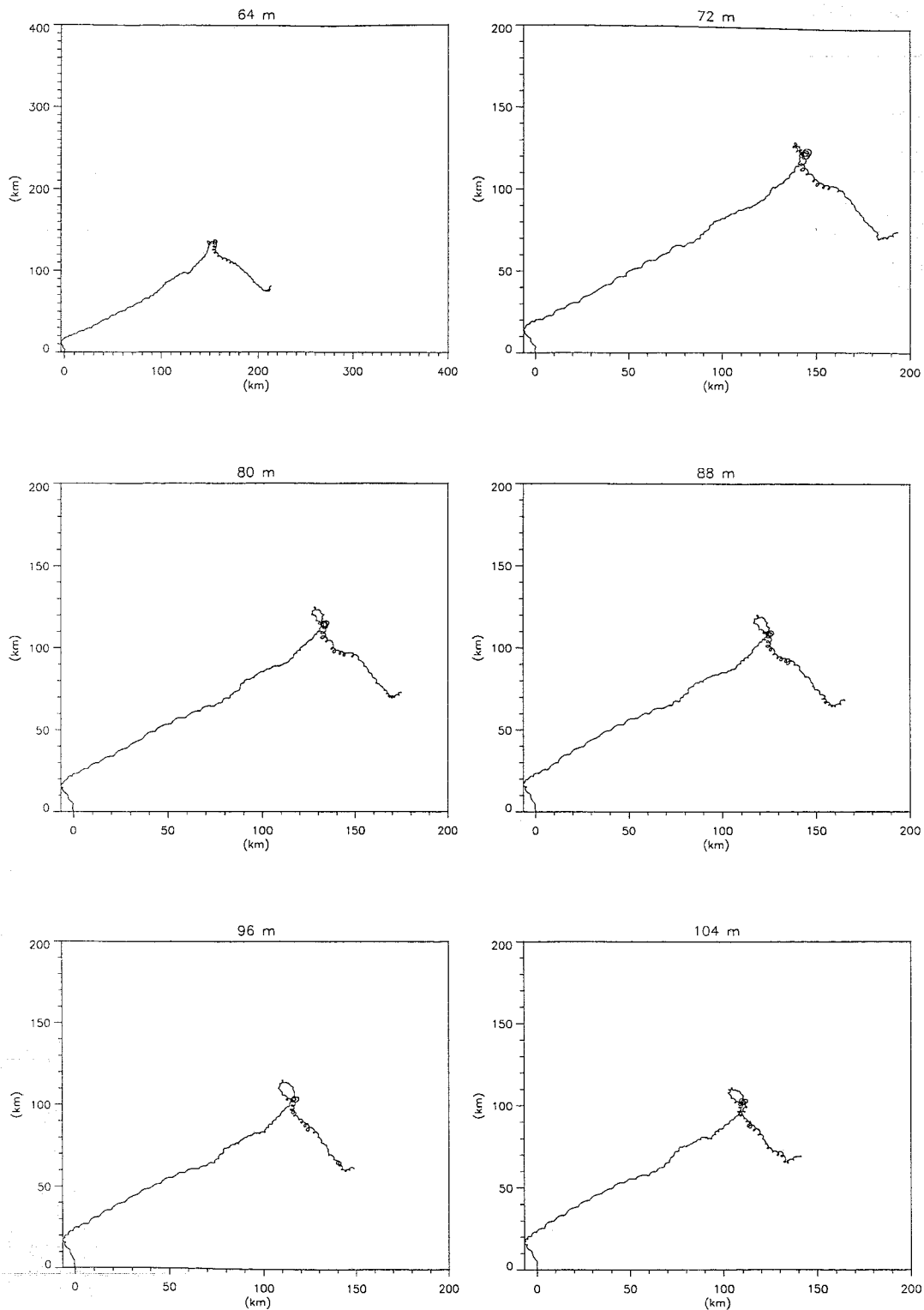


Fig.6.4.3: Odon.4. Progressive vectors (cont.)

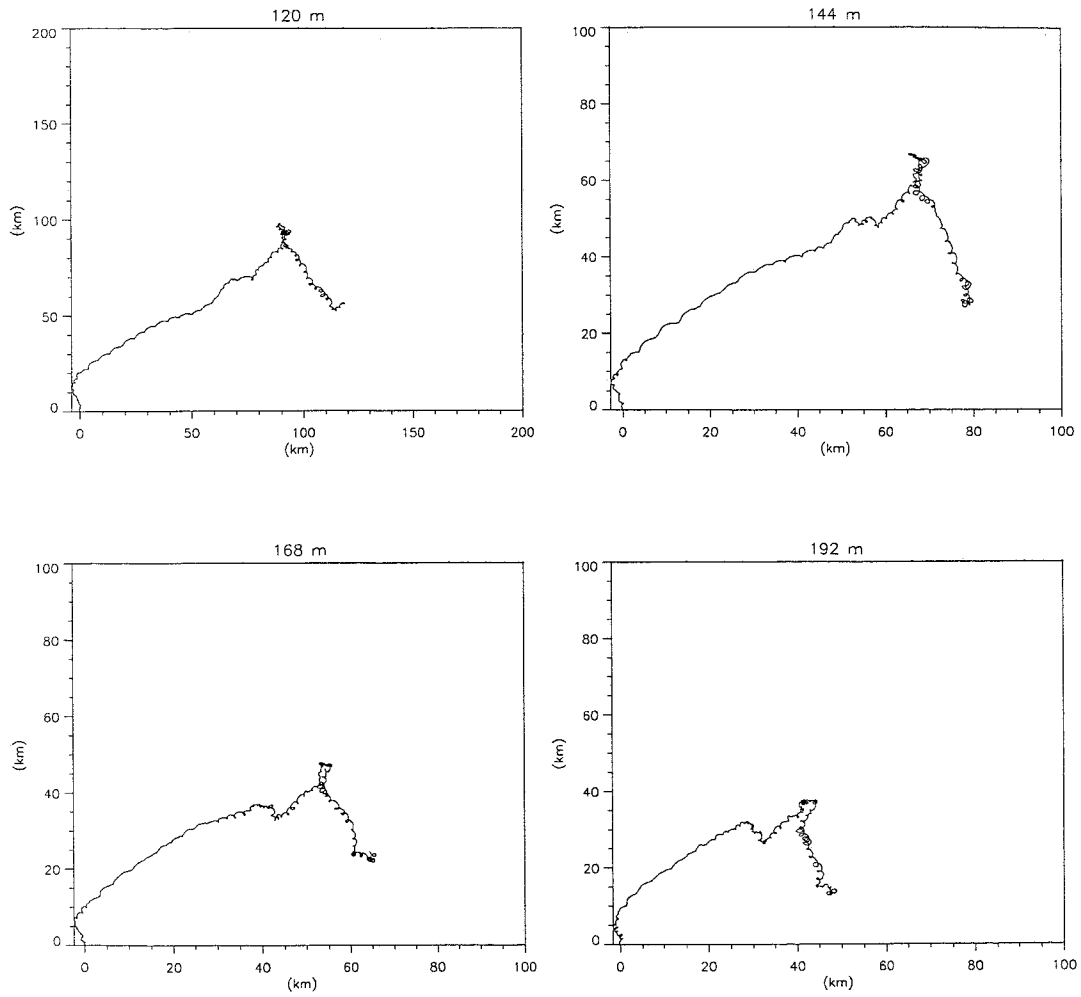


Fig.6.4.4: Odon_4. Progressive vectors (cont.)

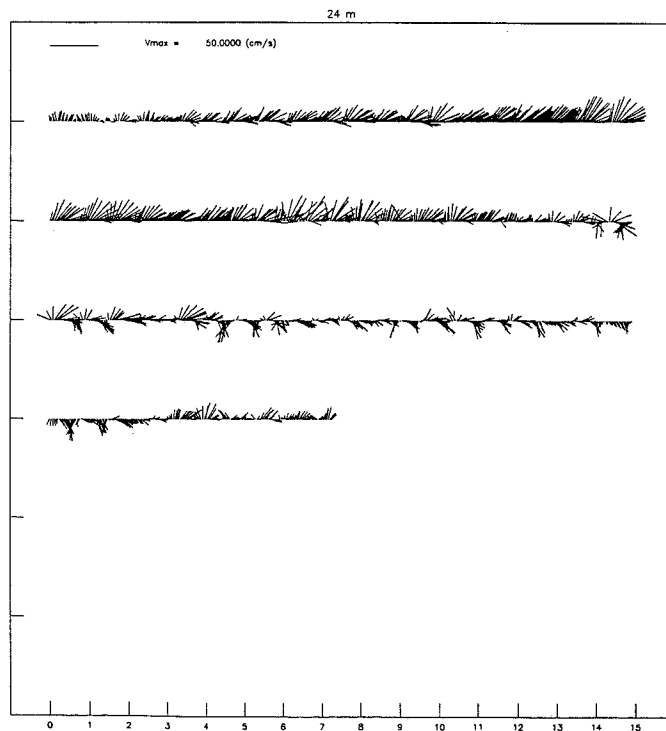
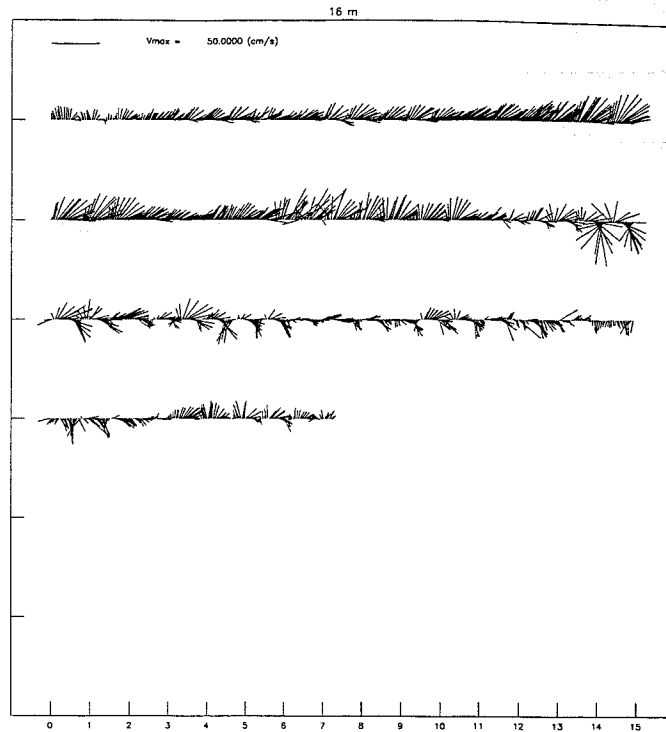


Figure 6.4.5: Stick plots at several depths recorded in Odon_4 data set. (Figs. 6.4.5-12)

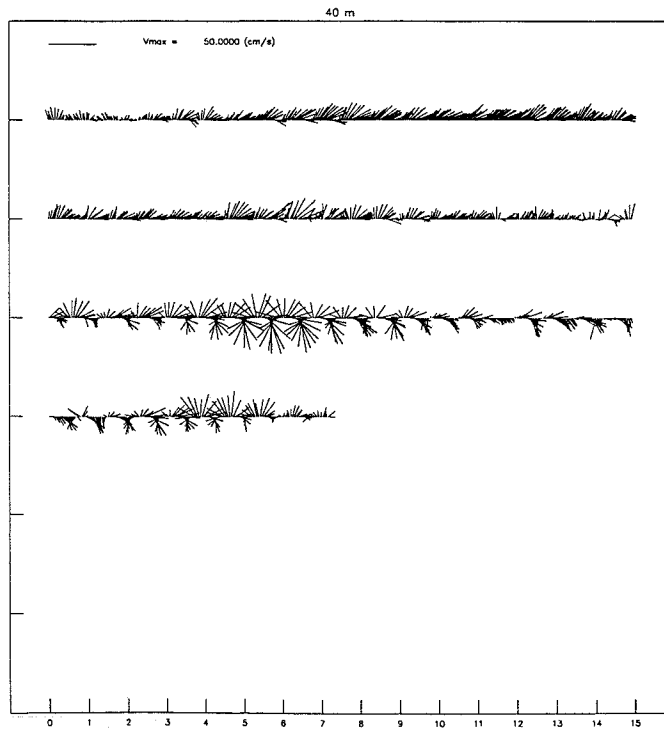
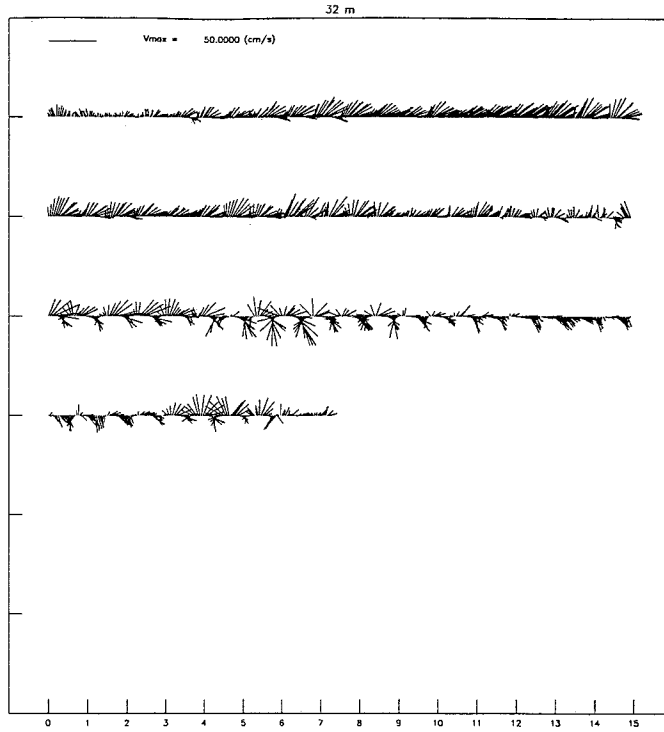


Fig.6.4.6: Odon_4: Stick plots (cont.)

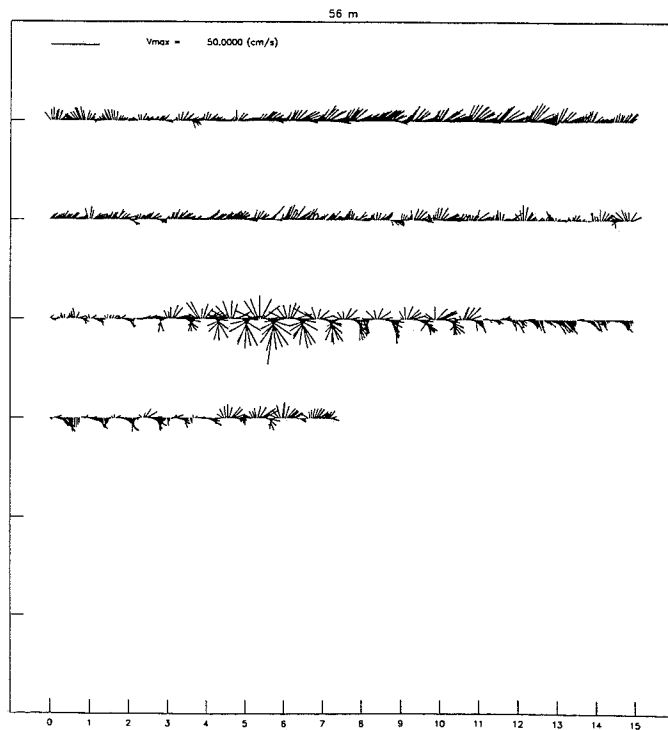
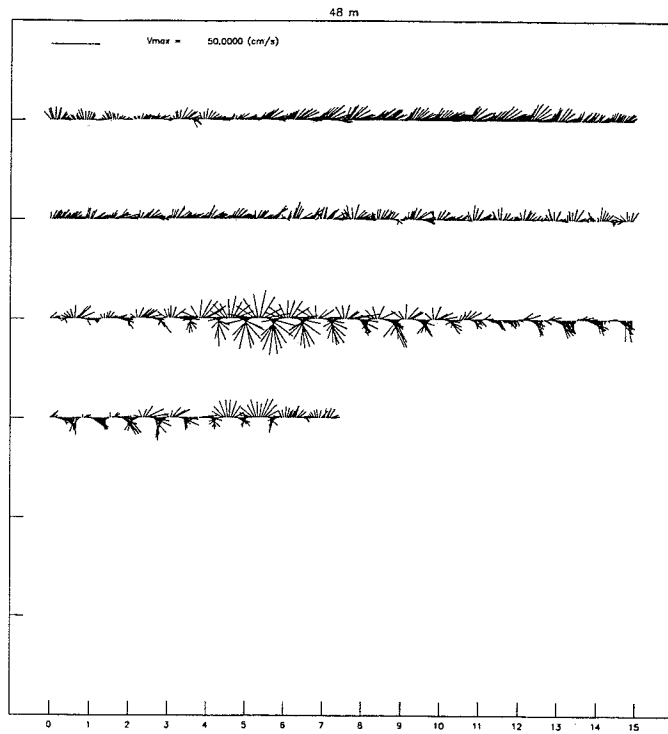


Fig.6.4.7: Odon_4: Stick plots (cont.)

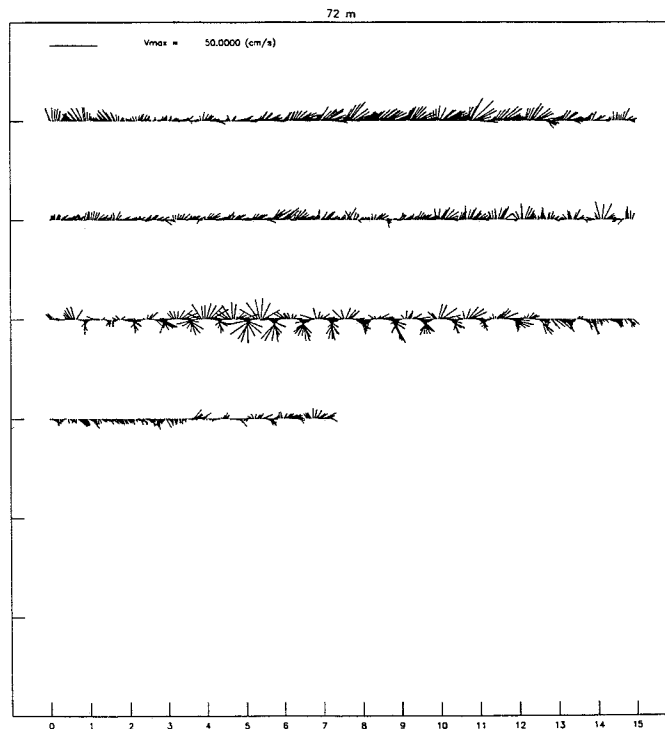
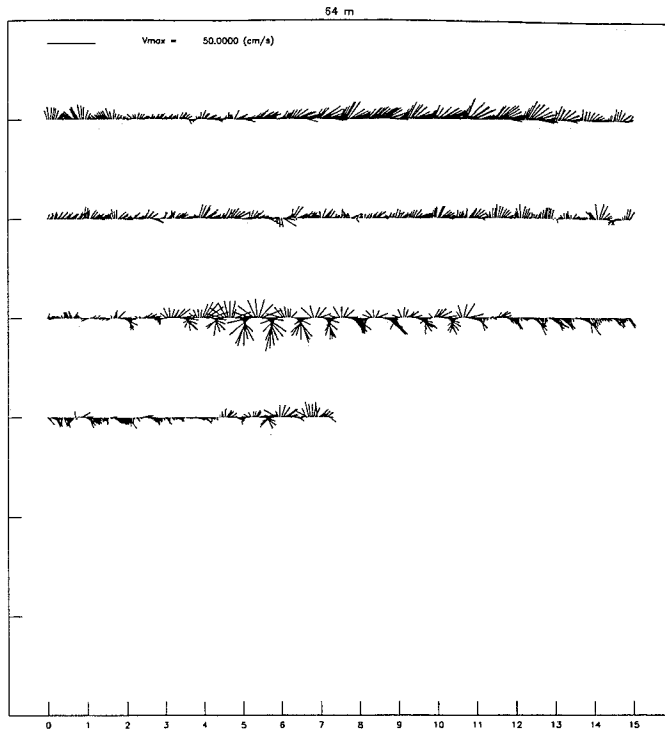


Fig.6.4.8: Odon_4: Stick plots (cont.)

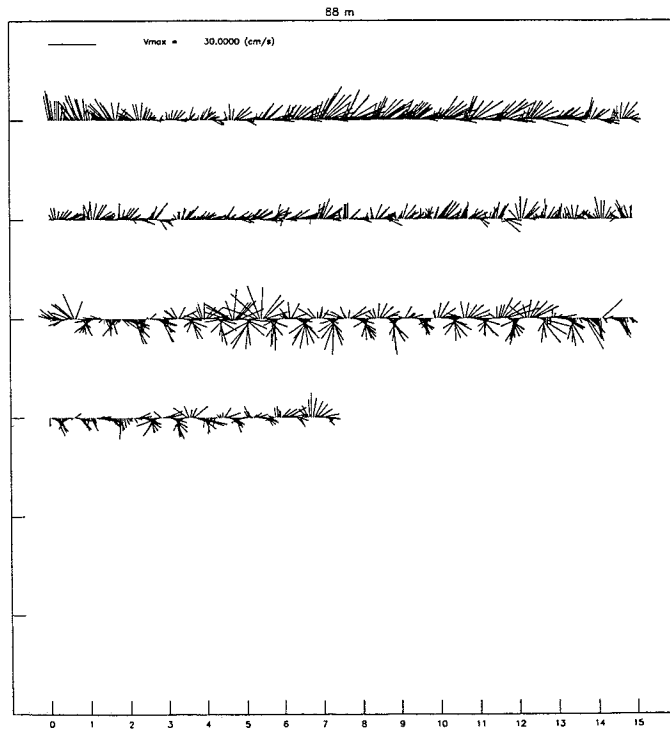
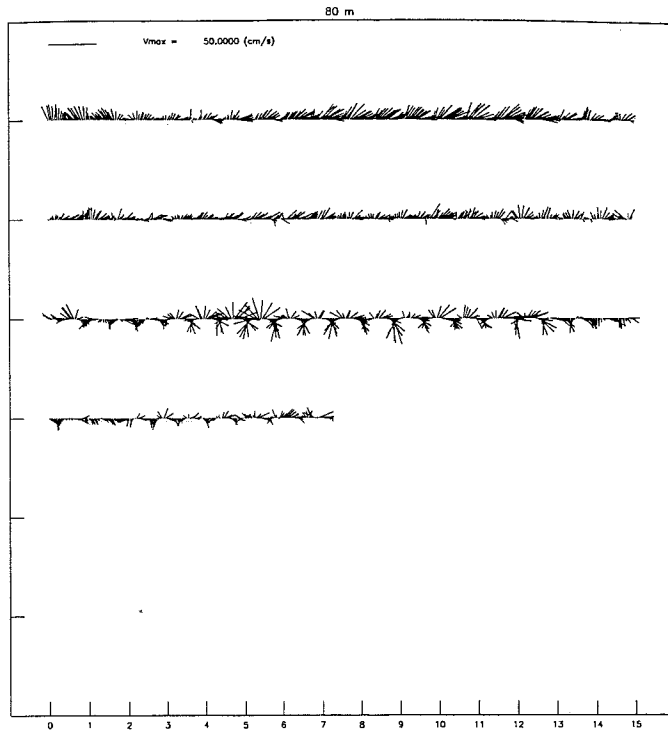


Fig.6.4.9: Odon_4: Stick plots (cont.)

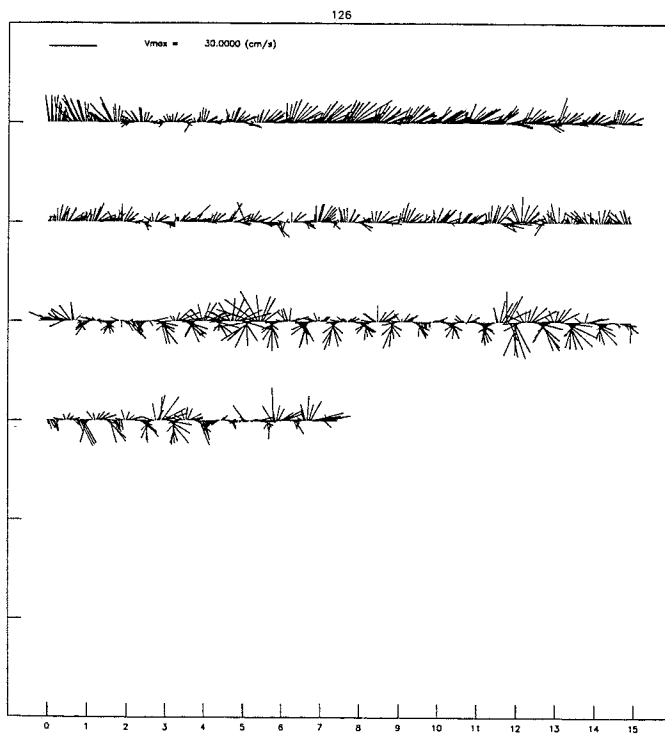
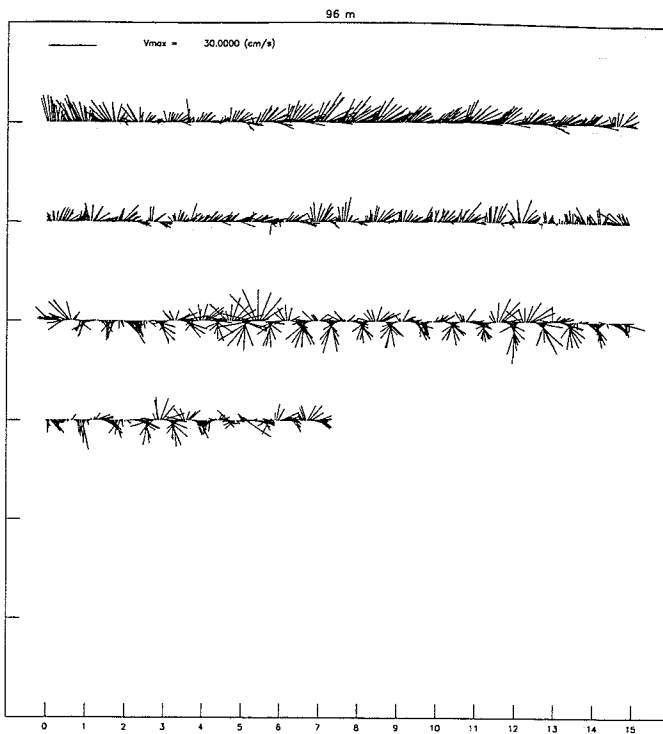


Fig.6.4.10: Odon_4: Stick plots (cont.)

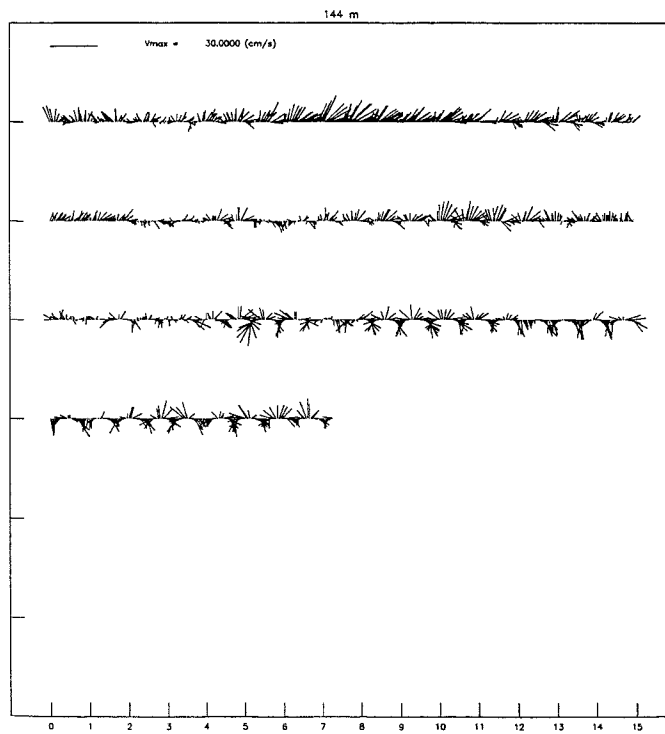
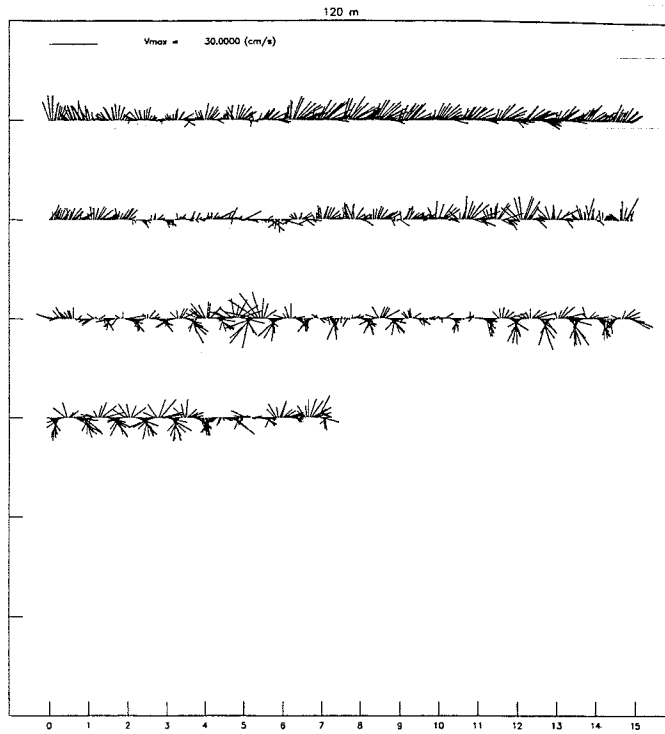


Fig.6.4.11: Odon_4: Stick plots (cont.)

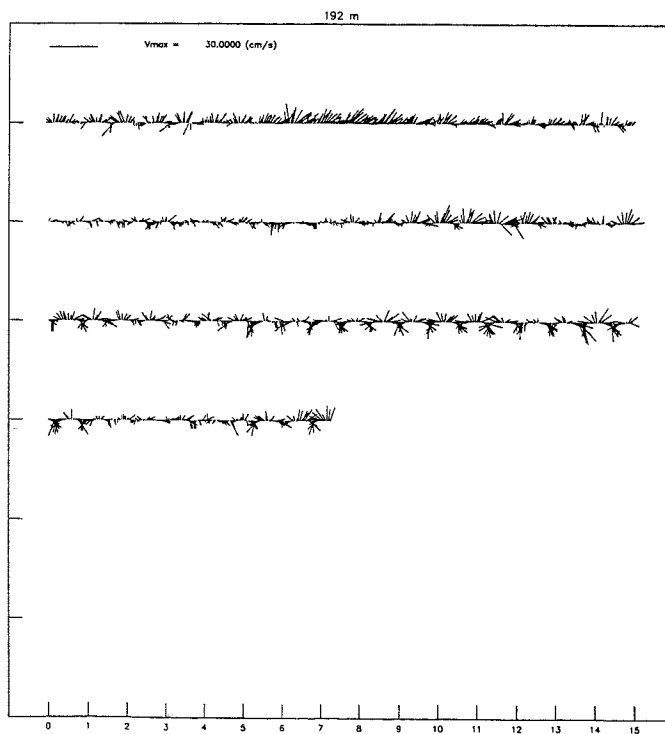
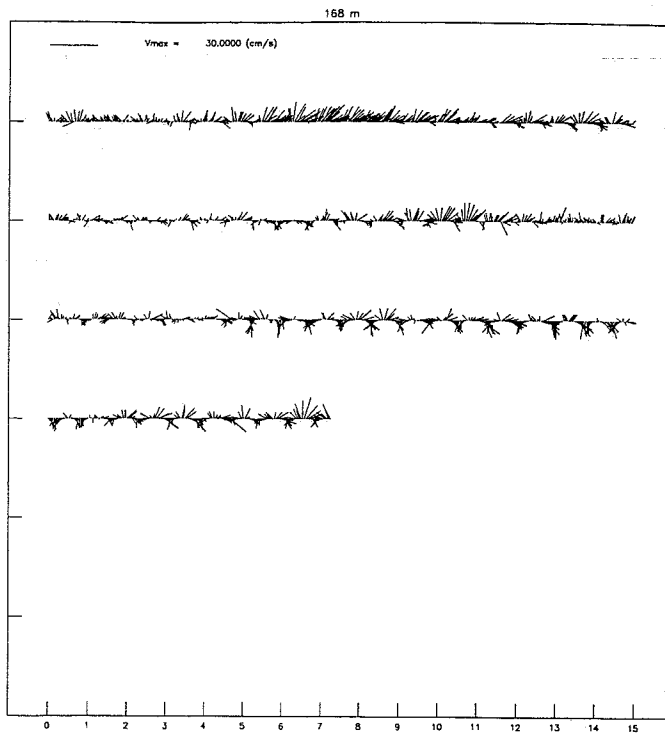


Fig.6.4.12: Odon_4: Stick plots (cont.)

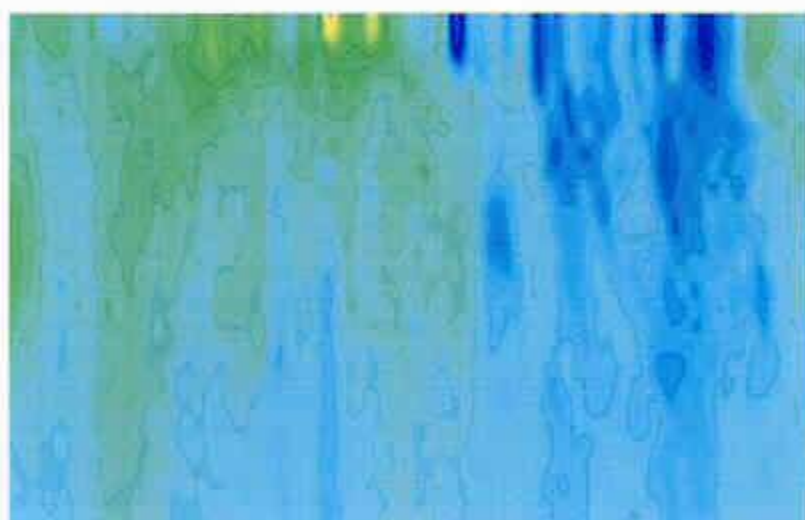


Figure 6.4.13: Filtered time series of U (upper) and V (lower) components in Odon_4. Time is Julian days and the color scale goes between -35.0 (blue tones) to 35.0 (red tones) cm/s.

Appendix I: Mooring Hydrodynamics

Simulations of the hydrodynamics of the ADCP mooring line using 'MOUSTASH':

- Case of a weak current profile ($V = 20$ cm/s down to 400 m and 10 cm/s below)

```

*****
*   ADCP - IBIZA CHANNEL - LOW CURRENT   *
*****

profondeur = 900.00 metres

profil de courant
=====

de 0.00 metres a 400.00 metres : vitesse = 0.200 m/s
de 400.00 metres a 900.00 metres : vitesse = 0.100 m/s

constitution du mouillage:
=====

il y a 7 elements

numero element longueur masse trainee friction elasticite
1 bouee spherique 1.20 m -420.000 kg 47.36 kg 47.36 kg 0.00e+00
2 chaine galva 12 10.00 m 2.800 kg 1.26 kg 0.08 kg 0.00e+00
3 kevlar 2 625.00 m 0.004 kg 0.50 kg 0.03 kg 0.53e-05
4 bouee cylindrique 0.70 m -60.000 kg 25.65 kg 1.61 kg 0.00e+00
5 largeur ORCA *2 0.72 m 37.000 kg 6.00 kg 1.40 kg 0.00e+00
6 chaine galva 12 10.00 m 2.800 kg 1.26 kg 0.08 kg 0.00e+00
7 lest 0.50 m 600.000 kg 0.00 kg 0.00 kg 0.00e+00

RESULTAT ANALYSE SUBSURFACE
*****
inmersion inclinaison tension rayon evitage longueur cumulee
element
250.67 m 0.0 degrees 0.00 kg 9.61 m 0.00 m
bouee spherique
251.87 m 0.3 degrees 420.00 kg 9.61 m 1.20 m
chaine galva 12
261.87 m 0.4 degrees 392.00 kg 9.55 m 11.20 m
kevlar 2 8
324.50 m 0.5 degrees 9.07 m
387.12 m 0.7 degrees 8.39 m
449.74 m 0.8 degrees 7.55 m
512.37 m 0.8 degrees 6.65 m
574.99 m 0.9 degrees 5.71 m
637.61 m 0.9 degrees 4.72 m
700.23 m 1.0 degrees 3.67 m
762.85 m 1.0 degrees 2.57 m
825.47 m 1.1 degrees 1.43 m
888.08 m 1.1 degrees 389.23 kg 0.23 m 637.49 m
bouee cylindre
888.78 m 1.0 degrees 449.22 kg 0.21 m 638.19m
largeur ORCA *2
889.50 m 1.1 degrees 412.22 kg 0.20 m 638.91 m
chaine galva 12
899.50 m 1.2 degrees 384.23 kg 0.00 m 648.91 m
lest
900.00 m 2.1 degrees 216.01 kg 0.00 m 649.41 m

extension verticale de la ligne = 649. m
poids du lest sur le fond = 216. kg
effort tangentiel au fond = 8. kg

```

- Case of an ocean 'storm' ($V = 40$ cm/s down to 400 m and 20 cm/s below)

```

*****
*   ADCP - IBIZA CHANNEL - HIGH CURRENT   *
*****

profondeur = 900.00 metres

      profil de courant
=====
de 0.00 metres a 400.00 metres : vitesse = 0.400 m/s
de 400.00 metres a 900.00 metres : vitesse = 0.200 m/s

      constitution du mouillage
=====
il y a 7 elements

numero  element      longueur      masse      trainee  friction  elasticite
1 bouee spherique    1.20 m      -420.000 kg  47.36 kg  47.36 kg  0.00e+00
2 chaine galva 12    10.00 m      2.800 kg    1.26 kg   0.08 kg   0.00e+00
3 klevlar 2          625.00 m     0.004 kg    0.50 kg   0.03 kg   0.53e-05
4 bouee cylindrique  0.70 m      -60.000 kg  25.65 kg  1.61 kg   0.00e+00
5 largeur ORCA *2    0.72 m      37.000 kg   6.00 kg   1.40 kg   0.00e+00
6 chaine galva 12    10.00 m      2.800 kg    1.26 kg   0.08 kg   0.00e+00
7 lest               0.50 m      600.000 kg  0.00 kg   0.00 kg   0.00e+00

      RESULTAT ANALYSE SUBSURFACE
      *****
inmersion  inclinaison  tension  rayon evitage  longueur cumulee
element
251.80 m   0.0 degrees  0.00 kg  38.37 m        0.00 m
bouee spherique
253.00 m   1.0 degrees  420.00 kg  38.35 m        1.20 m
chaine galva 12
263.00 m   1.4 degrees  392.00 kg  38.14 m        11.20 m
kevlar 2  8
325.60 m   2.1 degrees           36.21 m
388.17 m   2.9 degrees           33.47 m
450.71 m   3.2 degrees           30.12 m
513.24 m   3.4 degrees           26.56 m
575.75 m   3.5 degrees           22.79 m
638.25 m   3.7 degrees           18.82 m
700.74 m   3.9 degrees           14.65 m
763.22 m   4.1 degrees           10.27 m
825.68 m   4.3 degrees            5.69 m
888.12 m   4.5 degrees           0.91 m        637.49 m
bouee cylindre
888.82 m   4.0 degrees           0.85 m        638.19m
largeur ORCA *2
889.54 m   4.4 degrees           0.80 m        638.91 m
chaine galva 12
899.51 m   4.8 degrees           0.00 m        648.91 m
lest
900.01 m   8.4 degrees           0.00 m        649.41 m

extension verticale de la ligne = 648. m
poids du lest sur le fond      = 217. kg
effort tangentiel au fond      = 32. kg

```

Appendix II: Instrument Configuration

Command file used to set up the ADCP for deployment in July, 1997.

```
*****
*  COMMAND FILE FOR ADCP PARAMETER SETTINGS BEFORE DEPLOYMENT  *
*          JULY-1997 DEPLOYMENT                                *
*          (FILE : GDC_JUN.CMD)                                *
*****

WP00010 : number of pings averaged in each data ensemble = 10

WD11111110 : data typed collected will be velocity, correlation,
             echo intensity, percent good, status, sum of ensemble
             velocities, sum of (ensemble velocities)**2, numer of
             good pings.

WN033 : number of depths cells = 33

WS0800 : depth cell size = 8 m

WF0400 : blank after transmit = 4 m (standard value)

WM4 : profiling mode = 4 (default mode for most applications)

TP06 : 00.00 : time per ensemble = 1 h

EB+00100 : heading bias = 1 deg (for local magnetic variation)

ES38 : salinity value for speed calculation = 38 psu

ED3000 : depth of transducer for speed calculation = 300 m (actually 240 m
             would have been better)

EZ1011101 : sensor source : use all sensors data except depth and salinity

EX11111 : coordinate transformation : calculate earth coordinate using
             heading data, tilts (pitch and roll), allows 3-beam solutions if
             one beam is below the correlation treshold

CF11101 : flow control : automatic pinging and data storage in binary format
```

Appendix III: DATA files

- a. Report files: filename.rpt, ASCII data reports obtained from the factory BB-CONV.EXE program when converting raw data to ASCII.

- for 'vector' data (velocity, percent good, etc.)

REPORT FOR ASCII DATA CONVERSION

1. ADCP INFORMATION:

Frequency 150 kHz
Beam angle 20 deg
4 beam system
Down-looking orientation !!! NO, UPWARD-LOOKING
Convex beam pattern
Transducer head connected
CPU firmware 5.47

2. ADCP SETUP:

Number of bins 33
Bin length 8.0 m
Blank after transmit 4.0 m
Distance to first bin 13.6 m
Transmit length 9.0 m
Pings per ensemble 10
Time per ping 360.00 s
Profiling mode 4

3. ASCII FILE DATA FORMAT:

Line 1-33: Ensemble number, Binn range, Earth velocity E, N, V, Err,
Percent Good beam 1, 2, 3, 4, Intensity beam 1, 2, 3, 4,
Correlation beam 1, 2, 3, 4
line 34: Empty line

4. PROCESSING PARAMETERS:

Velocity units: cm/s
Velocity reference: ADCP
Depth units: m
Bins: From 1 to 33 skip 0 bin
Magnetic variation 0.00 deg
Do not mark data below bottom

END OF REPORT

- for scalar data (date, time, temperature, etc.)

REPORT FOR ASCII DATA CONVERSION

1. ADCP INFORMATION:

Frequency 150 kHz
Beam angle 20 deg
4 beam system
Down-looking orientation !!! NO, UPWARD-LOOKING
Convex beam pattern
Transducer head connected
CPU firmware 5.47

2. ADCP SETUP:

Number of bins 33
Bin length 8.0 m
Blank after transmit 4.0 m
Distance to first bin 13.6 m
Transmit length 9.0 m
Pings per ensemble 5
Time per ping 360.00 s
Profiling mode 4

3. ASCII FILE DATA FORMAT:

Line 1: Ensemble number, Recording date string, Recording time string,
Decimal Julian day, Temperature,
Heading, Pitch, Roll, Heading Std Dev, Pitch Std Dev, Roll Std Dev

4. PROCESSING PARAMETERS:

Velocity units: cm/s
Velocity reference: ADCP
Depth units: m
Bins: From 1 to 33 skip 0 bin
Magnetic variation 0.00 deg
Do not mark data below bottom

END OF REPORT

b. Data File: filename_00*.asc

774	270	9999	9999	9999	9999	0	0	100	0	36	39	45	38	26	23	26	23
774	262	9999	9999	9999	9999	0	0	100	0	44	44	53	44	26	33	22	27
774	254	9999	9999	9999	9999	0	0	100	0	62	59	72	60	25	22	25	47
774	246	9999	9999	9999	9999	0	0	100	0	124	104	129	108	67	39	61	43
774	238	-76	70	11	-76	40	0	40	20	152	153	155	158	73	98	68	84
774	230	9999	9999	9999	9999	0	0	100	0	119	135	127	134	54	33	52	54
774	222	10	0	1	5	40	0	0	60	91	94	96	92	73	78	72	74
774	214	9	6	2	7	0	0	0	100	50	55	59	52	119	122	119	116
774	206	6	10	1	3	0	0	0	100	48	53	57	50	120	119	118	118
774	198	9	11	1	5	0	0	0	100	49	53	57	50	120	120	119	117
774	190	13	11	0	5	0	0	0	100	49	53	57	51	116	118	120	118
774	182	14	6	0	1	0	0	0	100	52	55	61	55	120	124	123	122
774	174	13	4	0	2	0	0	0	100	58	60	67	59	123	124	125	128
774	166	11	5	0	2	0	0	0	100	63	65	70	64	124	125	129	127
774	158	11	6	0	1	0	0	0	100	65	67	72	66	125	120	125	129
774	150	10	5	0	0	0	0	0	100	65	68	74	67	124	127	125	124

c. Data File: filename.asc

14	97/01/31	14:18:17	30.59603	13.08	133	0	0	47	0	0
15	97/01/31	14:48:17	30.61687	13.07	106	0	1	4	0	0
16	97/01/31	15:18:17	30.63770	13.07	107	-1	1	3	0	0
17	97/01/31	15:48:17	30.65853	13.07	118	-1	1	3	0	0
18	97/01/31	16:18:17	30.67937	13.07	100	-1	1	4	0	0
19	97/01/31	16:48:17	30.70020	13.07	99	-1	1	2	0	0
20	97/01/31	17:18:17	30.72103	13.07	90	-1	1	3	0	0
21	97/01/31	17:48:17	30.74187	13.07	82	-1	1	4	0	0
22	97/01/31	18:18:17	30.76270	13.07	74	-1	1	4	0	0
23	97/01/31	18:48:17	30.78353	13.07	66	-1	1	8	0	0
24	97/01/31	19:18:17	30.80437	13.07	51	-1	1	2	0	0
25	97/01/31	19:48:17	30.82520	13.07	66	-1	1	3	0	0
26	97/01/31	20:18:17	30.84603	13.07	70	-1	1	4	0	0
27	97/01/31	20:48:17	30.86687	13.07	90	-1	1	5	0	0

d. Data File: filename_000.rms

14	270	99.9	99.9	99.9	99.9	0	0	0	0
14	262	99.9	99.9	99.9	99.9	0	0	0	0
14	254	99.9	99.9	99.9	99.9	0	0	0	0
14	246	99.9	99.9	99.9	99.9	0	0	0	0
14	238	0.0	0.0	0.0	0.0	2	2	2	4
14	230	99.9	99.9	99.9	99.9	0	0	0	0
14	222	1.6	2.2	4.1	4.1	5	5	5	5
14	214	1.4	3.8	1.4	3.7	5	5	5	5
14	206	1.8	4.9	3.5	3.1	5	5	5	5
14	198	2.0	4.7	1.2	1.8	5	5	5	5
14	190	0.9	3.8	2.2	2.9	5	5	5	5
14	182	1.5	4.5	1.2	3.8	5	5	5	5
14	174	1.8	4.8	1.4	1.9	5	5	5	5
14	166	1.8	3.8	2.1	1.5	5	5	5	5

Appendix IV: RDI mail

From: Darryl Symonds
Sent: Thursday, June 05, 1997 7:38 PM
To: rdifs2
Subject: RE: For Darryl...

Dear Jean Michel,

I have looked at the data and the reason that your system stops collecting data at the 230 meter mark is because this is where the surface is. The echo intensity data goes up when our signal hits the surface. The signal then will fall off again as the signal is being bounced away from the surface. If you look at the 2 examples you sent to me you can see that the echo intensity rises at the 222 meter mark. This is where our side lobes are starting to strike the surface. The next bin (230 meters) is the peak of the echo intensity and is when the main lobe strikes the surface. The bin after that (238 meters) is where the pulse is leaving the surface.

Since our systems have side lobes, the data must be cut off at 6% + 1 bin from the surface (or bottom depending on direction of mounting). If I use the numbers I see then it would appear that the surface is 238 meters away from the ADCP. Therefore, you should be cutting your data off at 6% (223 meter) + 1 bin (214 meters). This would mean that your last valid bin should be 206 meters. However, the data you have it appears that the bin at 222 meters looks just fine. All bins above this (or in this case the last 6 to 7 bins or 48-56 meters) should be thrown out as they are biased by side lobe contamination and are beyond the surface.

I hope that this clarifies the last bins of data for you.

Best regards,

Darryl

Appendix V: IDL procedures

Here you can find IDL command lines and routines to work interactively with the ADCP data. In the future, some of these procedures will be implemented in a GUI tool actually under development by S. Delecraz (e-mail: delecraz@univ-perp.fr) at CEFREM⁵.

- How to start. You prompt IDL and run the ADCP function that asks for a listing file (*filename.lis*) containing a list of data files to be read. Note that the ADCP function makes a call to the NLINES routine⁶. ADCP fills an array of data (*a*).

```
mk::user 3> idl
IDL Version 5.0.2 (IRIX mipseb). Research Systems, Inc.
  Installation number: 10481-0.
  Licensed for use by: Ciencias del Mar
  For basic information, enter "IDLInfo" at the IDL> prompt.
IDL> a=adcp()
% Compiled module: ADCP.
% Compiled module: NLINES.
Total...          2972.00 perfiles
Reading... /canales1/odi_fil.dat with 2972 perfiles
Perfil...        2971 de          2972.00 perfiles
IDL>
```

- Interactive session to filter data using FILTER procedure. FILTER is a general GUI tool to filter time series. First we read data into an array (*a*) and we create an array (*b*) to temporarily store *u* and *v* components for all bins. Then we call FILTER with the */all* keyword to directly process the whole data set once the filter function has been chosen. Finally, the input array is filled with filtered values (*out*). For further information contact E. del Rio (e-mail: edelrio@icm.csic.es) at the Institut de Ciències del Mar.

```
IDL> a=adcp()
% Compiled module: ADCP.
% Compiled module: NLINES.
Total...          2086.00 perfiles
Reading... canales2/limpio.dat with 2086 perfiles
Perfil...        2085 de          2086.00 perfiles
IDL> b=fltarr(n_elements(a(0,0,*)),66)
IDL> for bin=0,32 do begin $
IDL>   b(*,2*bin)=a(2,bin,*) & b(*,2*bin+1)= a(3,bin,*) & endfor
IDL> filter,b,out,/all & b=0.0
IDL> for bin=0,32 do begin $
IDL>   a(2,bin,*)=out(*,2*bin) & a(3,bin,*)=out(*,2*bin+1) & endfor
IDL>
```

⁵CEFREM: Centre de Formation et de Recherche sur L'Environnement Marin. University of Perpignan.

⁶NLINES.PRO: IDL routine written by F.K. Knight. It returns the number of lines in a file.

- A simple example of the powerful capabilities of IDL to deal with array operations. Here, you find records physically irrelevant by fixing indexes where velocity is greater than a threshold.

```
bu=where(a(2,bin,*) gt 100) & bv=where(a(3,bin,*) gt 100)
```

- Example of how to generate interactively the complex plots of filtered data (see figs. 6.1.21 and 6.2-4.13)

```
jdays=61.9 & pix=fix(80.0*jdays/9.0)
x=fltarr(n_elements(a(2,10,*)),26) & y=x
for i=0,25 do begin x(*,25-i)=a(2,i+6,*) & y(*,25-i)=a(3,i+6,*) & endfor
;
window,0,retain=2,xsize=pix,ysize=300
window,1,retain=2,xsize=pix,ysize=300
sx= bytscl( $
    smooth(congrid(x,pix,300,/interp,cubic=-0.5),6), $
    min=-35.0,max=35.0,top=166)
sy= bytscl( $
    smooth(congrid(y,pix,300,/interp,cubic=-0.5),6), $
    min=-35.0,max=35.0,top=166)
;
wset,0 & tv, sx & wset,1 & tv, sy
```

- **CORRECT**: IDL function that searches for spikes in the error velocity column following the criterium described in section 5.3 and corrects them by linear interpolation. You need to be sure that anomalous values are not grouped in intervals of consecutive bad values.

```
FUNCTION CORRECT,c,in,fin
;
; C ==> matriz de datos
; in ==> bin inicial (0 < in < 32)
; fin ==> bin final (0 < fin < 32 and in < fin)
;
for i=in,fin do begin
    m=moment(c(5,i,*),sdev=ss) & bb=where(abs(c(5,i,*)-m(0)) ge 3.0*ss)
    if bb(0) ne -1 then begin
        for j=0,n_elements(bb)-1 do begin
            c(2,i,bb(j))=0.5*(c(2,i,bb(j)-1)+c(2,i,bb(j)+1))
            c(3,i,bb(j))=0.5*(c(3,i,bb(j)-1)+c(3,i,bb(j)+1))
        endfor
    endif
endfor
return,c
END
```

- ADCP: IDL function that reads ASCII data from the output of BB CONV.EXE.

```

FUNCTION ADCP
;
f='' & filein=' ' & path=' '
;
; Filelist = es el fichero *.lis con la lista de ficheros de datos
; Path = es el path donde reside el *.lis y los ficheros de datos
;
filelist=dialog_pickfile(get_path=path)
openr,1,filelist
  readf,1,filein
  while not eof(1) do begin
    readf,1,f & filein=[filein,f]
  endwhile
close,1
filein=path+filein
if n_elements(filein) gt 0 then nfiles=n_elements(filein) else nfiles=1
;
ntl=intarr(nfiles)
  for I=0,nfiles-1 do ntl(i)=nlines(filein(i))/34
nt=total(ntl)
b=fltarr(18,33,nt) ; Matriz de datos
;
jj=-1
print,'Total... ',nt,' perfiles'
for I=0,nfiles-1 do begin
  a=fltarr(18,33) ; Matriz de lectura
  openr,2,filein(i)
  print,'Reading... ',filein(i),' with',ntl(i),' perfiles'
  for j=0,ntl(i)-1 do begin
    jj=jj+1
    readf,2,a & b(*,*,jj)=a
  endfor
  close,2
endfor
;
RETURN,B
END

```

References

- [1] **Alvarez A., Tintoré J., Holloway G., Eby M. and J.M. Beckers** (1994): The effect of the topographic stress on the Western Mediterranean circulation. *Journal of Geophysical Research*, 99, 16053-16064.
- [2] **Castellón A., J. Font and E. García** (1990): The Liguro-Provenal-Balearic Current observed by Doppler profiling in the Balearic Sea. *Scientia Marina*, 54 (3), 269-276.
- [3] **Font J., J. Salat and J. Tintoré** (1988): Permanent features of the circulation in the Catalan Sea. *Oceanologica Acta*, S-9, 51-57.
- [4] **Font J.** (1990): A comparison of seasonal winds with currents on the continental slope of the Catalan Sea (Northwestern Mediterranean). *Journal of Geophysical Research*, 95, 1537-1546.
- [5] **Font J., J. Salat and A. Julià** (1990): Marine circulation along the Ebro continental margin. *Marine Geology*, 95, 165-177.
- [6] **García-Ladona E., A. Castellón, J. Font and J. Tintoré** (1996): The Balearic current and volume transports in the Balearic basin. *Oceanologica Acta*, 19 (5), 489-497.
- [7] **García-Lafuente J., J.L. López-Jurado, N. Cano, M. Vargas and J. Aguiar** (1995): Water masses circulation through the Ibiza channel. *Oceanologica Acta*, 18 (2), 245-254.
- [8] **López-García M.J., C. Millot, J. Font and E. García-Ladona** (1994): Surface circulation variability in the Balearic Basin. *Journal of Geophysical Research*, 99, 3285- 3296.
- [9] **López-Jurado J.L., J. García-Lafuente and N.Cano** (1995): Hydrographic conditions of the Ibiza channel during November 1990, March 1991 and July 1992. *Oceanologica Acta*, 18 (2), 235-243.
- [10] **Pinot J.M., J. Tintoré and D. Gomis** (1994): Quasi-synoptic mesoscale variability in the Balearic Sea. *Deep-Sea Research*, 41(5-6), 897-914.
- [11] **Pinot J.M., J. Tintoré and D. Gomis** (1995): Multivariate analysis of the surface circulation in the Balearic Sea. *Progress in Oceanography*, 36, 343-376.
- [12] **Salat J.** (1995): The interaction between the Catalan and Balearic currents in the southern Catalan Sea. *Oceanologica Acta*, 18 (2), 227-234.
- [13] **Akaike** (1973). Maximum likelihood identification of Gaussian autoregressive moving average models. *Biometrika*, 60, 255-265.
- [14] **Akaike** (1974). A new look at the statistical model identification. *I.E.E.E Trans. Automatic Control*. AC-19, 716-722.
- [15] **Priestley M.B.** (1981). *Spectral Analysis and Time Series*. Academic Press.
- [16] **Thompson R.** (1983). Low-Pass filters to suppress inertial and tidal frequencies. *Journal of Physical Oceanography*. Vol. 13, 6, 1077-1083.

List of Figures

1.1	CANALES_97 experiment	5
2.1	Schematic view of the mooring line including the ADCP.	7
5.1	Time coverage during CANALES_97 experiment	10
5.2	Example of a complete temperature record (Odon_4 data set)	12
5.3	Example of spikes in velocity records	14
5.4	Vertical extent of spikes	15
5.5	Example of spike correction	16
5.6	AIC's function	18
6.1.1	Odon_1: Temperature and Heading	21
6.1.2	Odon_1: Progressive vectors (Figs. 6.1.2-4)	22
6.1.5	Odon_1: Stick plots (Figs. 6.1.5-20)	25
6.1.21	Odon_1: Filtered time series	41
6.2.1	Odon_2: Temperature and Heading	43
6.2.2	Odon_2: Progressive vectors (Figs. 6.2.2-4)	44
6.2.5	Odon_2: Stick plots (Figs. 6.2.5-12)	47
6.2.13	Odon_2: Filtered time series	55
6.3.1	Odon_3: Temperature and Heading	57
6.3.2	Odon_3: Progressive vectors (Figs. 6.3.2-4)	58
6.3.5	Odon_3: Stick plots (Figs. 6.3.5-12)	61
6.3.13	Odon_3: Filtered time series	69
6.4.1	Odon_4: Temperature and Heading	71
6.4.2	Odon_4: Progressive vectors (Figs. 6.4.2-4)	72
6.4.5	Odon_4: Stick plots (Figs. 6.4.5-12)	75
6.4.13	Odon_4: Filtered time series	83